Engineering of electrochromic materials as activatable probes for molecular imaging and photodynamic therapy

Luyan Wu[†], Yidan Sun[†], Keisuke Sugimoto[‡], Zhiliang Luo[†], Yusuke Ishigaki[‡], Kanyi Pu[§], Takanori Suzuki [‡,*], Hong-Yuan Chen[†], Deju Ye[†,ǁ,*]

[†] State Key Laboratory of Analytical Chemistry for Life Science, School of Chemistry and Chemical Engineering, Nanjing University, Nanjing, 210023, China

[‡] Department of Chemistry, Faculty of Science, Hokkaido University, N10 W8, North-ward, Sapporo 060-0810, Japan

[§] School of Chemical and Biomedical Engineering Nanyang Technological University, 637457, Singapore

[ǁ] Research Center for Environmental Nanotechnology (ReCent), Nanjing University, Nanjing, 210023, China

Table of Contents

Figure S1. Characterization of the reaction between $\mathbf{1}^{2+}$ and different reducing agents (reductant) *in vitro*. (a) Proposed conversion of EM $\mathbf{1}^{2+}$ to diene **2** upon reduction by a reductant. (b) HPLC traces and (c) Absorption spectra of $\mathbf{1}^{2+}$, **2**, and $\mathbf{1}^{2+}$ (8 μg/mL) following incubation with indicated reductants (Cys, Hcy, VC, 1 mM; GSH, DTT, 5 mM; NaHS, 100 μM) in PBS buffer (pH 7.4，1% DMSO) at 37 ºC overnight. (d) Normalized time-dependent decline of UV-Vis absorption (546 nm) of $\mathbf{1}^{2+}(BF_4^-)_2$ (8 μg/mL) following incubation with indicated agents (Cys, Hcy, VC, 1 mM; GSH, DTT, 5 mM; NaHS, 100 μM) in PBS buffer (pH 7.4) at room temperature (r.t.). (e) Normalized time-dependent decline of UV-Vis absorption (546 nm) of $\mathbf{1}^{2+}(BF_4^-)_2$ (8 μg/mL) following incubation with varying concentration of NaHS in PBS buffer (pH 7.4) at r.t. (f) Plot of the pseudo-first-order rate (k_{obs}) versus H_2S concentration (40-100 μM) afford the second-order reaction rate ($k_2 = 304 \pm 8\ M^{-1}\ s^{-1}$) between $\mathbf{1}^{2+}$ and NaHS at r.t.. The k_{obs} was determined by fitting the absorption intensity with single exponential function of $y = y_0 + A \times \exp(R_0 \times t)$, where $k_{obs} = -R_0$, and the k_2 value was obtained from the slope of the linear plot between k_{obs} and H_2S concentration ($R^2 = 0.996$). (g-j) The exponential fit curves of $\mathbf{1}^{2+}(BF_4^-)_2$ (8 μg/mL) following incubation with 40 (g), 50 (h), 70 (i), and 100 μM (j) NaHS in PBS buffer (pH 7.4) at r.t. Values are mean ± SD (n = 3).

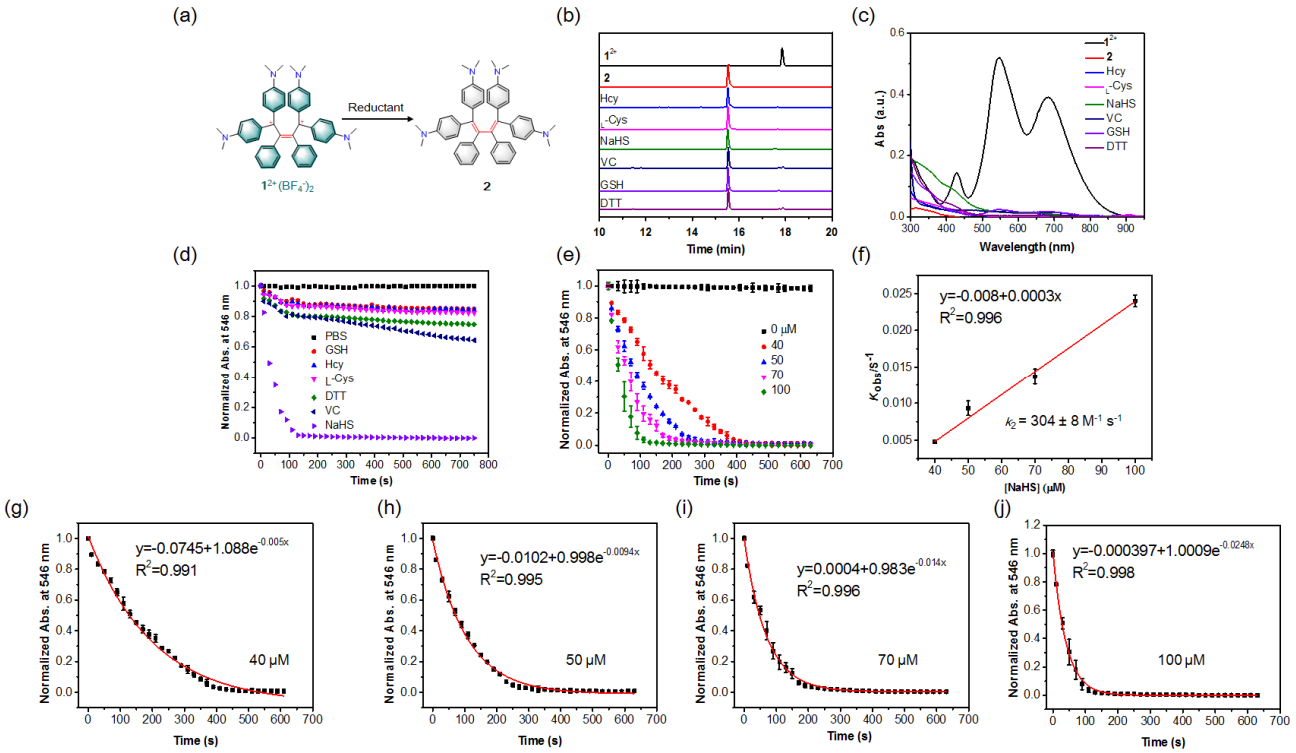

Figure S2. Characterization of $\mathbf{1}^{2+}$-NPs and the selectivity of $\mathbf{1}^{2+}$-NPs toward H_2S *in vitro*. (a) Schematic illustration of the preparation of $\mathbf{1}^{2+}$-NPs through DSPE-PEG_{2000}-assisted nanoprecipitation process. Owing to the hydrophobic π-electron structure of EM $\mathbf{1}^{2+}$, it can be easily encapsulated to form micellar nanoparticles. (b) Absorption spectra of free $\mathbf{1}^{2+}$ and $\mathbf{1}^{2+}$-NPs in PBS buffer (pH 7.4). (c) TEM image and (d) DLS analysis of $\mathbf{1}^{2+}$-NPs in PBS buffer (pH 7.4). Scale bar: 200 nm. (e) Absorption spectra and photograph (inset) of $\mathbf{1}^{2+}$-NPs before (-) and after (+) reaction with 350 μM NaHS in PBS buffer (pH 7.4) for 10 min. (f) Normalized time-dependent decline of absorption of $\mathbf{1}^{2+}$-NPs (8 μg/mL) following incubation with indicated reductants (Cys, Hcy, VC, 1 mM; GSH, DTT, 5 mM; NaHS, 300 μM) in PBS buffer (pH 7.4) at r.t.. (g) Normalized time-dependent decline of absorption of $\mathbf{1}^{2+}$-NPs (8 μg/mL) following incubation with varying concentration of NaHS in PBS buffer (pH 7.4) at r.t.. (h) Plot of the pseudo-first-order rate (k_{obs}) versus H_2S concentration (100-300 μM) afford the apparant second-order reaction rate k_2 between $\mathbf{1}^{2+}$-NPs and NaHS. The k_{obs} was determined by fitting the absorption intensity with single exponential function of $y = y_0 + A \times \exp(R_0 \times t)$, where $k_{obs} = -R_0$, and the apparent k_2 value was obtained from the slope of the linear plot between k_{obs} and H_2S concentration ($R^2 = 0.992$). The apparent k_2 for $\mathbf{1}^{2+}$-NPs was found to be 96.6 ± 3.3 M^{-1} s^{-1}, which was ~3-fold lower than that for the homogeneously dispersed $\mathbf{1}^{2+}$. (i-l) The exponential fit curves of $\mathbf{1}^{2+}$-NPs (8 μg/mL $\mathbf{1}^{2+}(BF_4^-)_2$) following incubation with 100 (i), 150 (j), 200 (k), and 300 μM (l) NaHS in PBS buffer (pH 7.4) at r.t. Values are mean ± SD (n = 3). We postulated that the reduce reaction rate between $\mathbf{1}^{2+}$-NPs and NaHS could be due to two possible reasons: 1) it may have to take some time for the H_2S molecules to across the phospholipid layer on $\mathbf{1}^{2+}$-NPs and diffuse into the nanoparticles; 2) as the environment within $\mathbf{1}^{2+}$-NPs was stickier and more hydrophobic compared to the exterior aqueous buffer, EM$\mathbf{1}^{2+}$ molecules may be not homogeneously dispersed, but packed closely as aggregates within $\mathbf{1}^{2+}$-NPs. This will increase the steric hindrance for H_2S molecules to reduce EM$\mathbf{1}^{2+}$ presenting in the interior of the aggregates, which will also prolong the reaction.

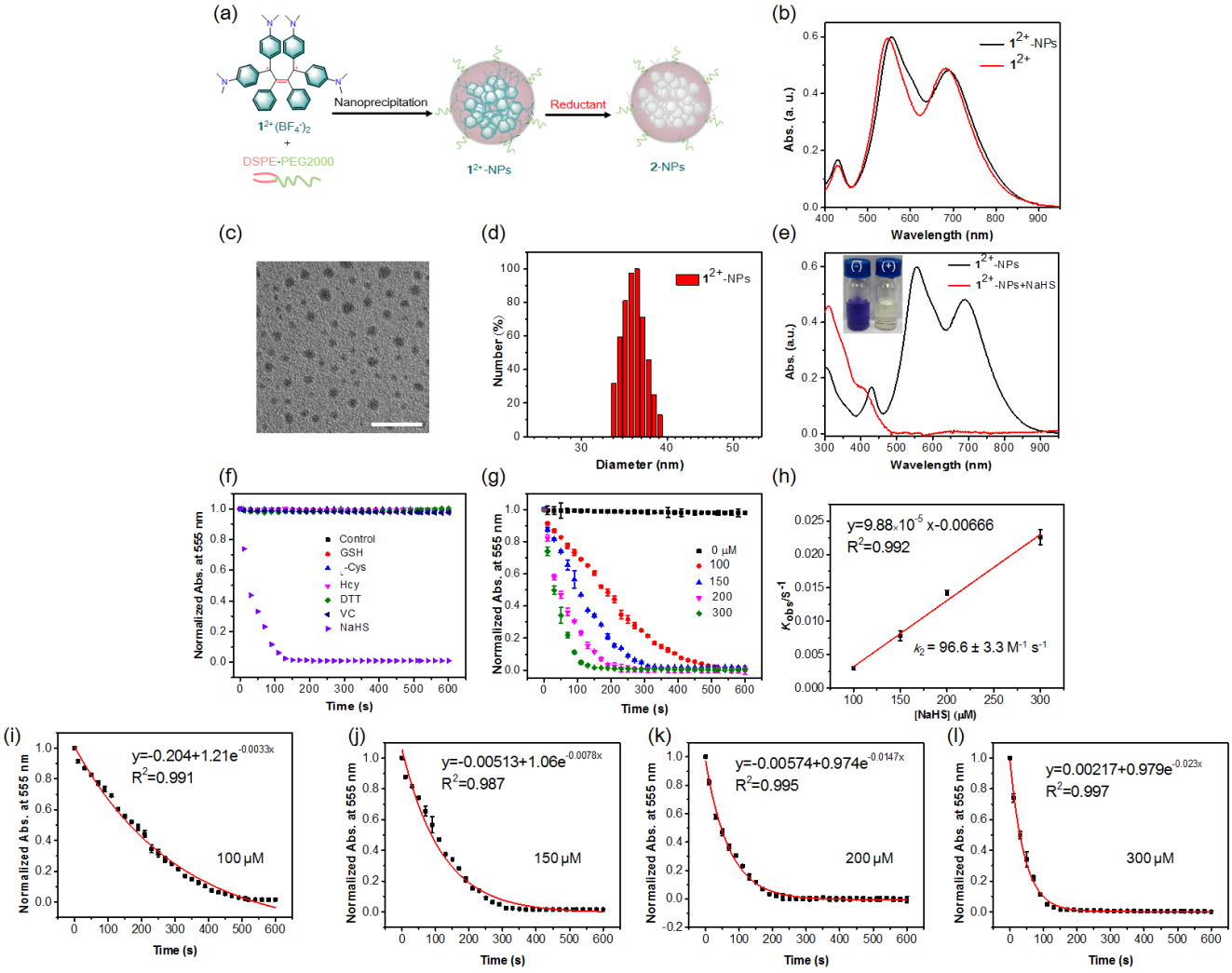
(a)
Nanoprecipitation
Reductant
DSPE-PEG2000
2-NPs
(b)
Abs. (a. u.)
Wavelength (nm)
(c)
(d)
Number (%)
Diameter (nm)
(e)
Abs. (a.u.)
Wavelength (nm)
(f)
Control
GSH
Cys
Hcy
DTT
VC
NaHS
Normalized Abs. at 555 nm
Time (s)
(g)
0 μM
100
150
200
300
Normalized Abs. at 555 nm
Time (s)
(h)
y=9.88x10^-5 x-0.00666
R^2=0.992
k2 = 96.6 ± 3.3 M^-1 s^-1
[NaHS] (μM)
(i)
y=-0.204+1.21e^-0.0033x
R^2=0.991
100 μM
(j)
y=-0.00513+1.06e^-0.0078x
R^2=0.987
150 μM
(k)
y=-0.00574+0.974e^-0.0147x
R^2=0.995
200 μM
(l)
y=0.00217+0.979e^-0.023x
R^2=0.997
300 μM

Figure S3. Evaluation of the stability of $\mathbf{1}^{2+}$ and $\mathbf{1}^{2+}$-NPs *in vitro*. (a) Normalized absorption spectra of $\mathbf{1}^{2+}$ (8 μg/mL) following incubation in PBS buffer (pH 7.4) at r.t. for 14 days. (b) Normalized absorption spectra of $\mathbf{1}^{2+}$-NPs (8 μg/mL)following incubation in PBS buffer (pH 7.4) at r.t. for 14 days. (c) Normalized absorption spectra of $\mathbf{1}^{2+}$-NPs (8 μg/mL) before and after five consecutive irradiation with 808 nm laser (1 W/cm^2) for 5 min each, with an interval of 5 min between each irradiation.

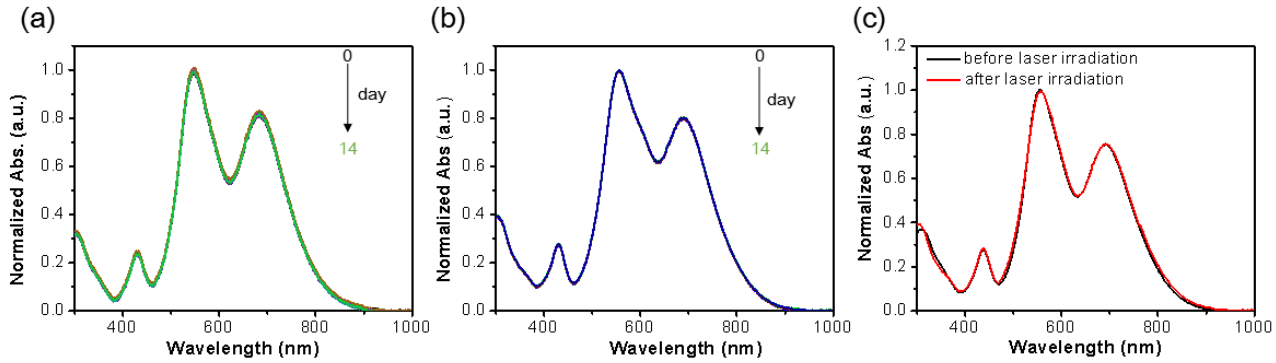

Figure S4. Optimization of doping ratio between $\mathbf{1}^{2+}(BF_4^-)_2$ and PCPDTBT within $\mathbf{1}^{2+}$-SNP830. (a) UV-Vis spectra of the filtrates collected from the ultrafiltration of $\mathbf{1}^{2+}$-SNP830. $\mathbf{1}^{2+}$-SNP830 was prepared by encapsulating PCPDTBT (28 μg/mL) with varying amount of $\mathbf{1}^{2+}(BF_4^-)_2$ (0, 2, 7, 14, 36, 48, 56 μg/mL) with DSPE-PEG$_{2000}$. The resulting nanoparticles were filtrated via ultrafiltration (3500 rpm, 15 min), washed with D.I. water for three time (8 mL ×3). The filtrates were combined, and analyzed by UV-Vis. The results showed that nearly all EM $\mathbf{1}^{2+}$ were encapsulated into the nanoparticles when the amount of EM $\mathbf{1}^{2+}$ was lower than 48 μg/mL, while there was only 91.3% of EM $\mathbf{1}^{2+}$ was loaded when 56 μg/mL EM $\mathbf{1}^{2+}$ was added. (b) Fluorescence spectra of SPN830 (28 μg/mL PCPDTBT) doping with different amount of $\mathbf{1}^{2+}(BF_4^-)_2$ (0, 2, 7, 14, 36, 48, 56 μg/mL). λ_{em} = 650 nm. (c) Comparison of the fluorescence intensity of SPN830 at 830 nm containing different amount of $\mathbf{1}^{2+}(BF_4^-)_2$. The results showed the optimum ratio of 28/48 = 0.58 (by mass) between PCPDTBT and $\mathbf{1}^{2+}(BF_4^-)_2$ within $\mathbf{1}^{2+}$-SNP830, affording ~15-fold flurescence quenched.

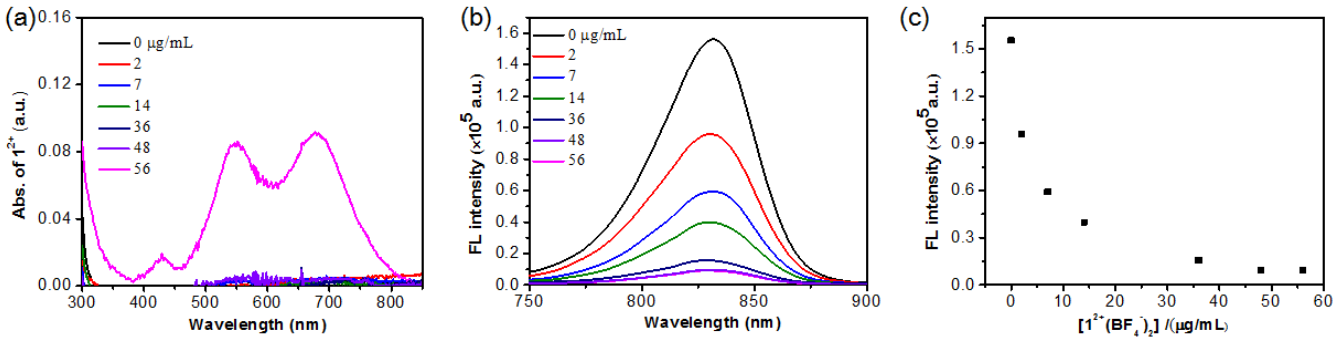

Figure S5. Characterization of $\mathbf{1}^{2+}$-SNP830, $\mathbf{1}^{2+}$-SNP700 and $\mathbf{1}^{2+}$-SNP580. (a) Comparison of the UV–Vis absorption spectra of $\mathbf{1}^{2+}$-SNP830 (black), $\mathbf{1}^{2+}$ (blue) and SPN830 (red) in PBS buffer (pH 7.4). (b) Comparison of the UV–Vis absorption spectra of $\mathbf{1}^{2+}$-SNP700 (black), $\mathbf{1}^{2+}$ (blue) and SPN700 (red) in PBS buffer (pH 7.4). (c) Comparison of the UV–Vis absorption spectra of $\mathbf{1}^{2+}$-SNP580 (black), $\mathbf{1}^{2+}$ (blue) and SPN580 (red) in PBS buffer (pH 7.4). (d) Comparison of the fluorescence spectra between $\mathbf{1}^{2+}$-SNP830 (black) and SPN830 (red) shows ~15-fold quenched fluorescence in $\mathbf{1}^{2+}$-SNP830. (e) Comparison of the fluorescence spectra between $\mathbf{1}^{2+}$-SNP700 (black) and SPN700 (red) shows ~60-fold quenched fluorescence in $\mathbf{1}^{2+}$-SNP700. (f) Comparison of the fluorescence spectra between $\mathbf{1}^{2+}$-SNP580 (black) and SPN580 (red) show ~25-fold quenched fluorescence in $\mathbf{1}^{2+}$-SNP580.

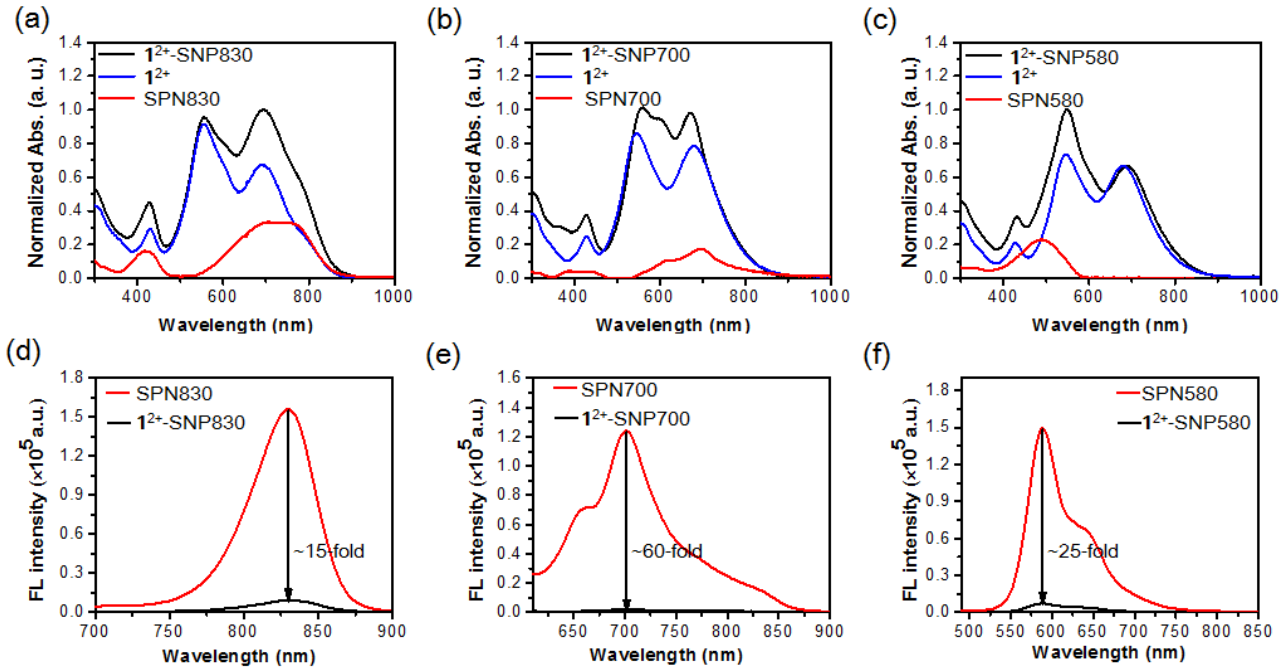

Figure S6. Nanocharacterization of $\mathbf{1}^{2+}$-SNP700 and $\mathbf{1}^{2+}$-SNP580. (a) DLS, TEM and AFM analysis of $\mathbf{1}^{2+}$-SNP700. (b) DLS, TEM and AFM analysis of $\mathbf{1}^{2+}$-SNP580. Scale bar is 200 nm.

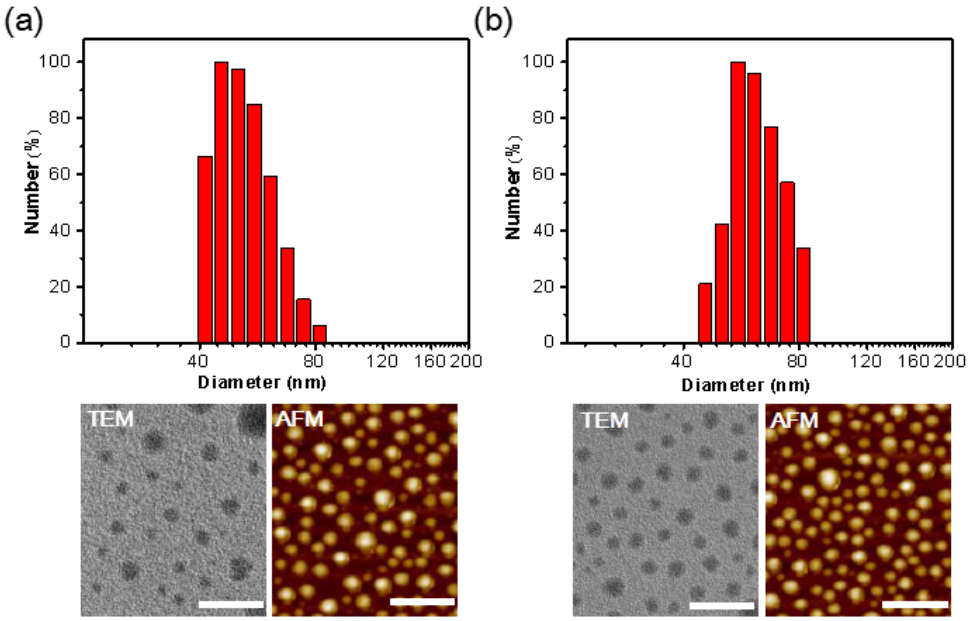

Figure S7. Evaluation of the stability of $\mathbf{1}^{2+}$-SNP830. (a) Comparison of the hydrodynamic size of $\mathbf{1}^{2+}$-SNP830 following incubation in PBS buffer (pH 7.4) for 7 days. (b) Comparison of the hydrodynamic size of $\mathbf{1}^{2+}$-SNP830 following incubation in aqueous buffer under different pH for 24 h. (c) Comparison of the fluorescence spectra and (d) fluorescence intensity of $\mathbf{1}^{2+}$-SNP830 and $\mathbf{1}^{2+}$-SNP830 with 350 μM NaHS following incubation in PBS buffer (pH 7.4) at r.t. for 7 days. The results showed that $\mathbf{1}^{2+}$-SNP830 was very stable under physiological conditions. Error bars indicated the standard deviations of three repeated measurements.

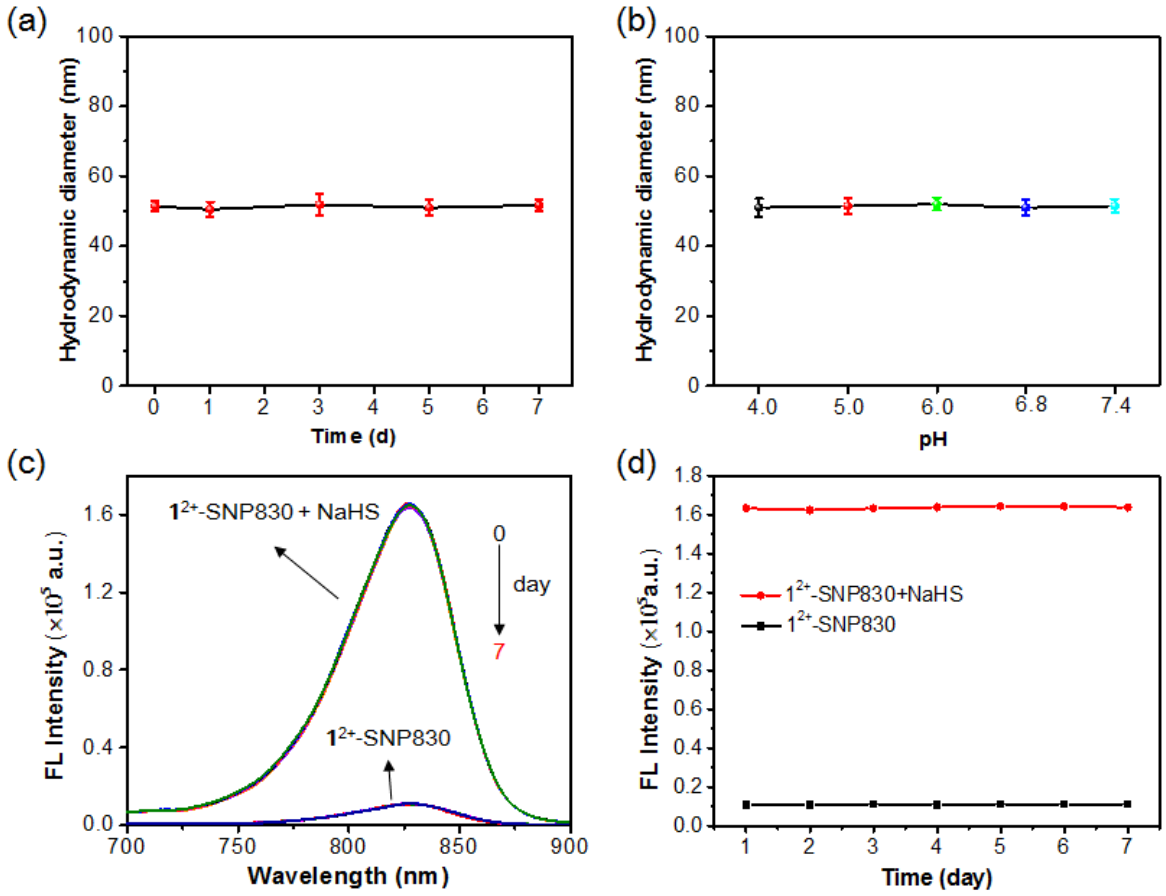

Figure S8. Evaluation of the apparant reaction kinetics between $\mathbf{1}^{2+}$-SNP830 and H_2S. (a) Normalized time-dependent fluorescence intensity (λ_{em} = 830 nm) of $\mathbf{1}^{2+}$-SNP830 (4.6/8 μg/mL PCPDTBT/$\mathbf{1}^{2+}(BF_4^-)_2$) following incubation with varying concentration of NaHS in PBS buffer (pH 7.4) at r.t.. (b-e) The exponential fit curves of $\mathbf{1}^{2+}$-SNP830 following incubation with 100 (b), 150 (c), 200 (d), and 400 μM (e) NaHS in PBS buffer (pH 7.4) at r.t. (f) Plot of the pseudo-first-order rate (k_{obs}) versus H_2S concentration (100-400 μM) afford the apparant second-order reaction rate (k_2 = 91.6 M^{-1} s^{-1}) between $\mathbf{1}^{2+}$-SNP830 and NaHS. The k_{obs} was determined by fitting the FL intensity with single exponential function of $y = y_0 + A' \times \exp(R_0 \times t)$, where $k_{obs} = -R_0$, and the k_2 value was obtained from the slope of the linear plot between k_{obs} and H_2S concentration (R^2 = 0.999).

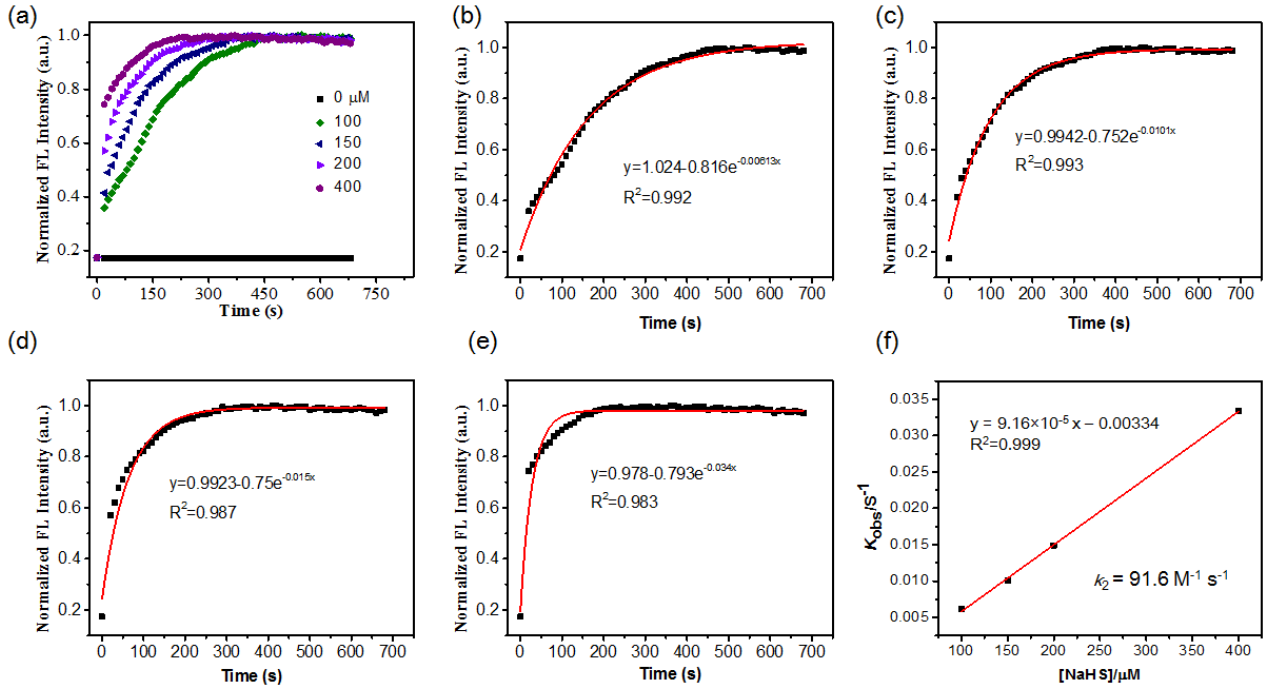

Figure S9. Determination of the detection limit for H_2S. (a) Fluorescence spectra of $\mathbf{1}^{2+}$-SNP830 (28/48 μg/mL PCPDTBT/$\mathbf{1}^{2+}(BF_4^-)_2$) upon incubation with varying concentration NaHS (0, 0.5, 1.0, 1.8, 5.0, 7.5, 10, 15, 20, 30, 40, 55, 70, 90 μM) in PBS buffer (pH 7.4) at 37 ºC for 10 min. (b) The linear relationship between the fluorescence intensity at 830 nm and the concentration of NaHS from 1.0 – 90 μM. The limit of detection (LOD) was calculated based on the blank + 3σ method (the concentration at which the fluorescence equals that of [blank + 3σ]) according to a linear regression fit of the data. The LOD was determined to be ~0.70 μM. Values are mean ± SD (n = 3).

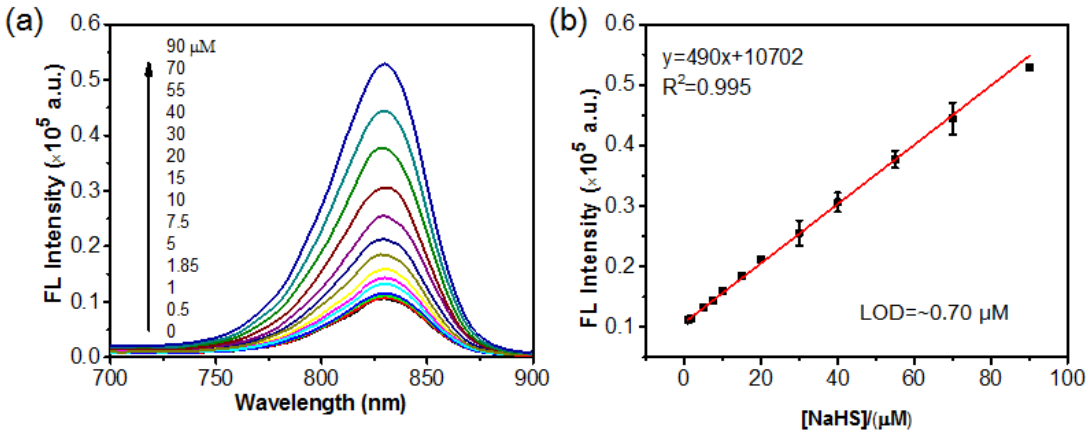

Figure S10. Investigation of the response of $\mathbf{1}^{2+}$-SNP830 toward H_2S under different pH. (a) Fluorescence spectra of $\mathbf{1}^{2+}$-SNP830 (28/48 μg/mL PCPDTBT/$\mathbf{1}^{2+}(BF_4^-)_2$) before (Ctrl) and after incubation with NaHS (350 μM) under indicated pH at r.t. for 10 min. (b) Comparison of the H_2S-induced fluorescence enhancement (F/F_0) of $\mathbf{1}^{2+}$-SNP830 at 830 nm at indicated pH. Error bars indicated the standard deviaions (n = 3). The results showed that $\mathbf{1}^{2+}$-SNP830 could be similarly activated by H_2S at pH ranging from 4.0-9.0.

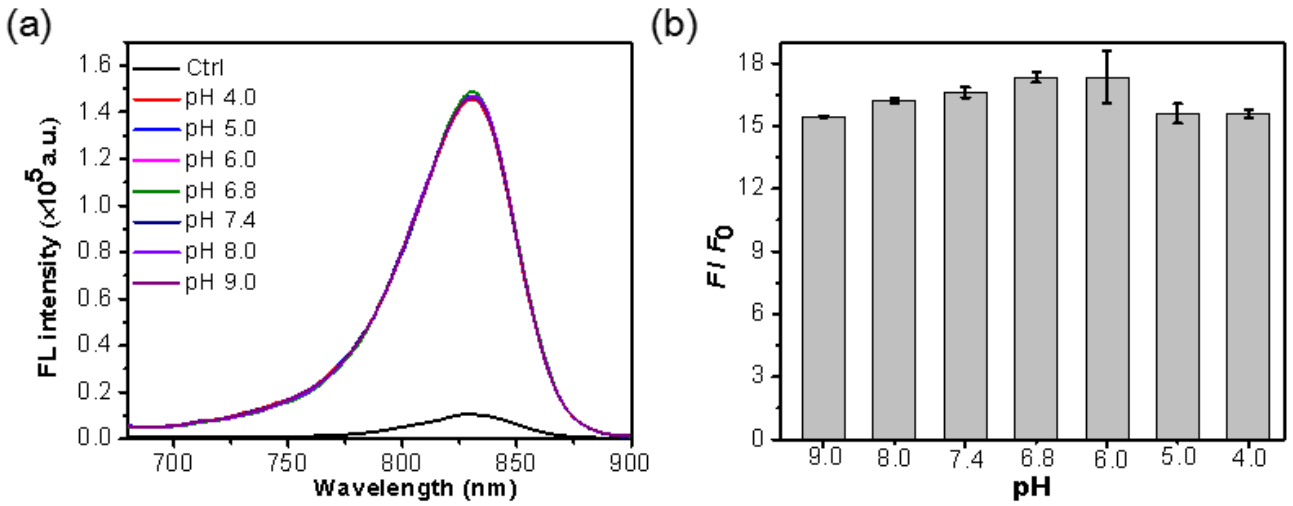

Figure S11. Evaluation of the activation of $\mathbf{1}^{2+}$-SNP700 by H_2S *in vitro*. (a) UV−Vis absorption spectra of $\mathbf{1}^{2+}$-SNP700 (8 μg/mL PFDPP, 14 μg/mL $\mathbf{1}^{2+}(BF_4^-)_2$) upon incubation with NaHS (100 μM) in PBS buffer (pH 7.4) at r.t. for 0 to 600 s. Inset: photograph of $\mathbf{1}^{2+}$-SNP700 before (-) and after (+) reaction with 100 μM NaHS at r.t. for 10 min. (b) Time-dependent fluorescence spectra of $\mathbf{1}^{2+}$-SNP700 upon incubation with NaHS in PBS buffer (pH 7.4) for 0 to 600 s. (c) Fluorescence spectra of $\mathbf{1}^{2+}$-SNP700 upon incubation with different concentration NaHS (0, 5, 10, 30, 50, 90, 125, 160, 190, 220, 240, 260, 350, 500 μM) in PBS buffer at 37 ºC for 10 min. (d) Fluorescence spectra of $\mathbf{1}^{2+}$-SNP700 upon incubation with NaHS at concentration ranging from 0.05 – 20 μM. (e) The linear relationship between the fluorescence intensity at 700 nm and the concentration of NaHS from 0.1 – 20 μM. The limit of detection (LOD) was calculated based on the blank + 3σ method (the concentration at which the fluorescence equals that of [blank + 3σ]) according to a linear regression fit of the data. The LOD was determined to be ~79 nM. The fluorescence spectra were acquired with excitation at 580 nm. Each data point was the mean of three measurements, and the error bars represented the standard deviation.

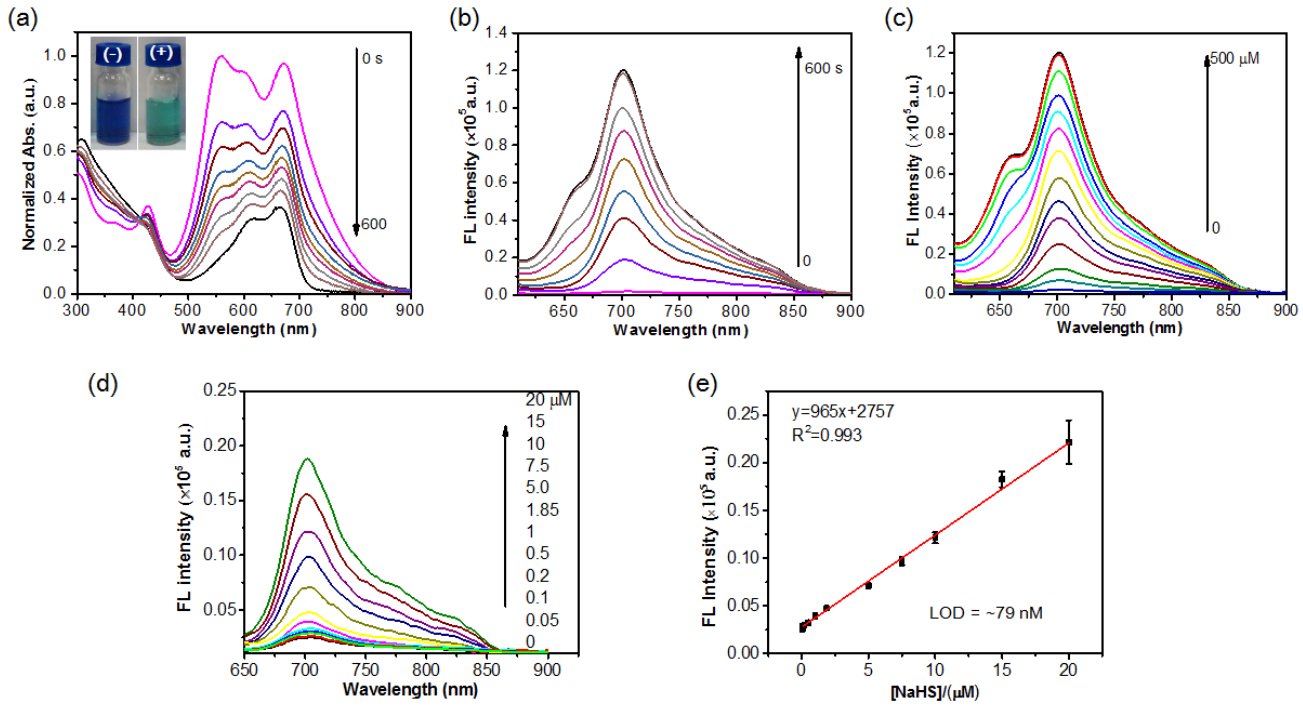

Figure S12. Evaluation of the activation of $\mathbf{1}^{2+}$-SNP580 by H_2S *in vitro*. (a) UV−Vis absorption spectra of $\mathbf{1}^{2+}$-SNP580 (8 μg/mL MEH-PPV, 14 μg/mL $\mathbf{1}^{2+}(BF_4^-)_2$) upon incubation with NaHS (100 μM) in PBS buffer (pH 7.4) for 0 to 600 s. Inset: photograph of $\mathbf{1}^{2+}$-SNP580 before (-) and after (+) reaction with 100 μM NaHS at r.t. for 10 min. (b) Time-dependent fluorescence spectra of $\mathbf{1}^{2+}$-SNP580 upon incubation with NaHS in PBS buffer (pH 7.4) for 0 to 600 s. (c) Fluorescence spectra of $\mathbf{1}^{2+}$-SNP580 upon incubation with different concentration of NaHS (0, 5, 10, 30, 50, 90, 125, 160, 190, 220, 240, 260, 350, 500 μM) in PBS buffer at 37 ºC for 10 min. (d) Fluorescence spectra of $\mathbf{1}^{2+}$-SNP580 upon incubation with NaHS at concentration ranging from 0.1 – 15 μM. (e) The linear relationship between the fluorescence intensity at 700 nm and the concentration of NaHS from 0.2 – 15 μM. The limit of detection (LOD) was calculated based on the blank + 3σ method (the concentration at which the fluorescence equals that of [blank + 3σ]) according to a linear regression fit of the data. The LOD was determined to be ~0.14 μM. The fluorescence spectra were acquired with excitation at 460 nm. Each data point was the mean of three measurements, and the error bars represented the standard deviation.

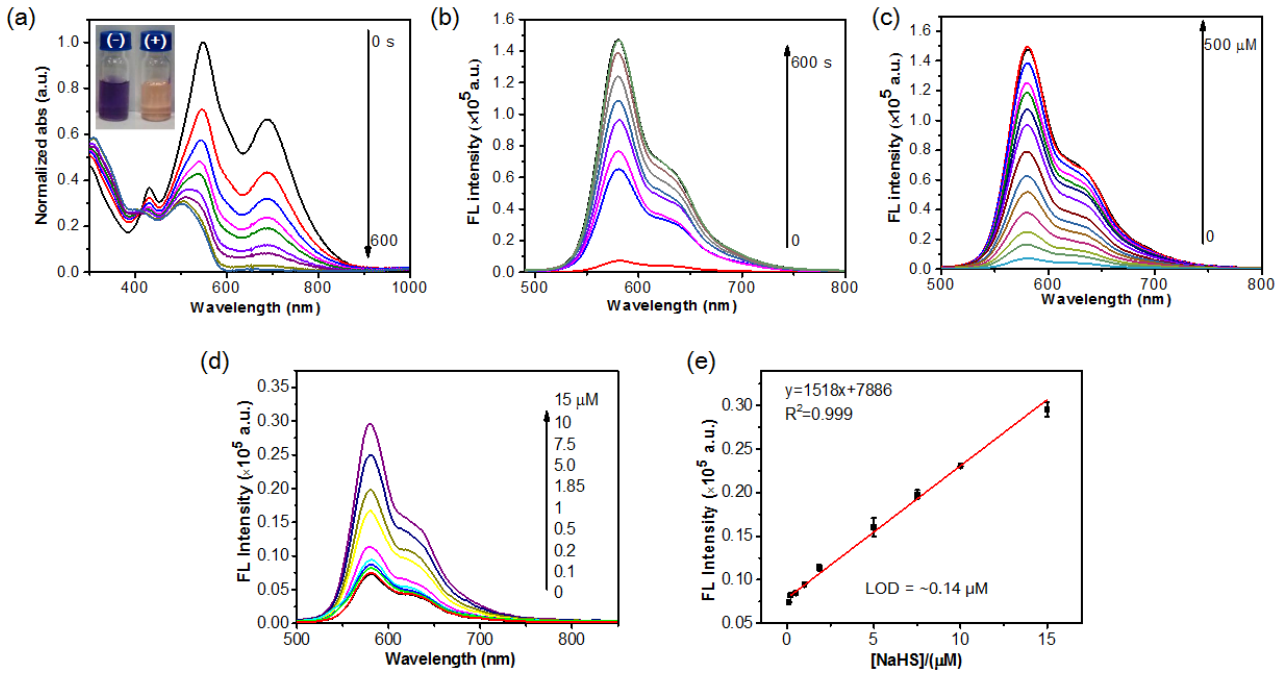

Figure S13. (a) Fluorescence spectra and (b) fluorescence intensity of **2**-SNP830 upon incubation with $ZnCl_2$ (300 μM) or PAG (50 mg/L) for 30 min. Values are mean ± SD (n = 3). These result suggested that the fluorescence of **2**-SNP830 could not be directly quenched by $ZnCl_2$ or PAG.

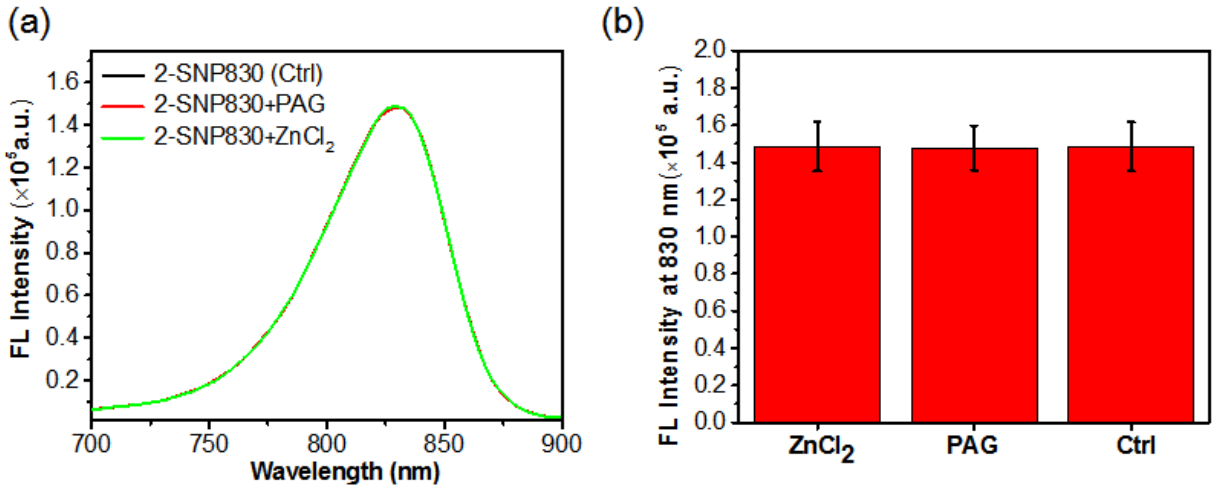

Figure S14. Investigation of the stability and response of $\mathbf{1}^{2+}$-SNP830 in biologically relevant conditions. (a) Comparison the hydrodynamic size of $\mathbf{1}^{2+}$-SNP830 upon incubation in PBS (black), PBS containing 10% mouse serum (blue), or RPMI 1640 cell culture medium (red) at r.t. for 2 days. (b) Comparison of the fluorescence intensity of $\mathbf{1}^{2+}$-SNP830 following incubation with or without 350 μM NaHS in D.I. water, PBS buffer (pH 7.4) or RPMI 1640 medium. The results showed that the hydrodynami size of $\mathbf{1}^{2+}$-SNP830 was stable, and $\mathbf{1}^{2+}$-SNP830 was capable of reducing by H_2S in these conditions. Values are mean ± SD (n = 3).

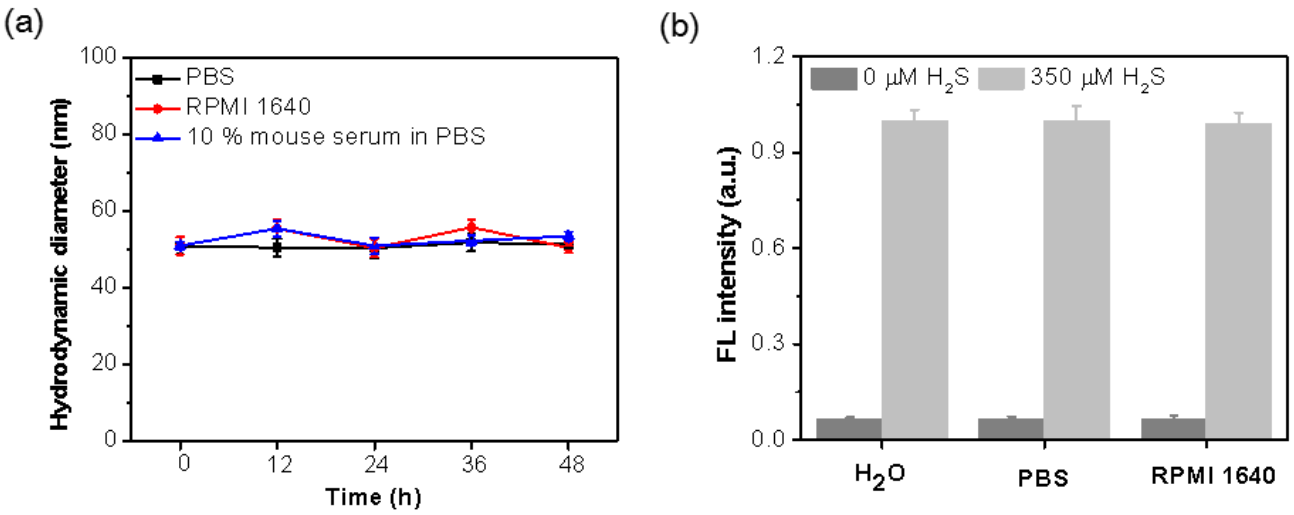

Figure S15. Evaluation of the cytotoxicity of $\mathbf{1}^{2+}$-SNP830 and $\mathbf{1}^{2+}$-SNP580 against RAW264.7 macrophages. Cells were incubated with indicated concentration of nanoparticles for 24 h, and the cytotoxicity was test by MTT assay. Error bars represent standard deviations of three measurements.

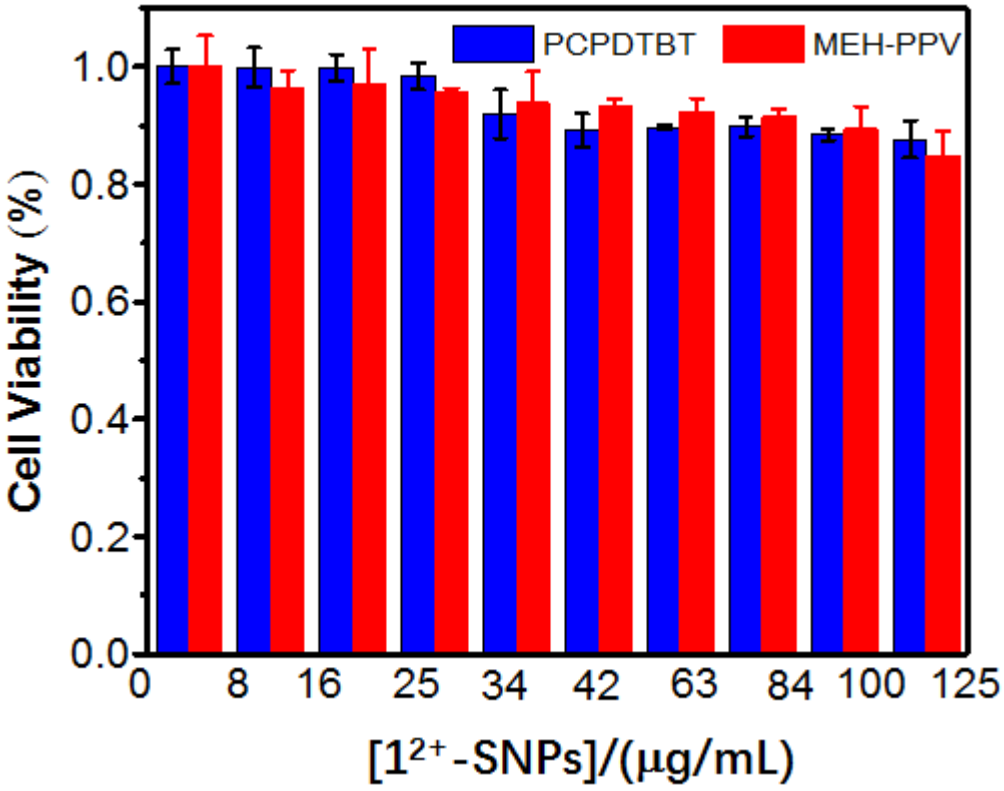

Figure S16. Visualization of exogenous H_2S in RAW264.7 cells with $\mathbf{1}^{2+}$-SNP580 (28 μg/mL MEH-PPV, 48 μg/mL $\mathbf{1}^{2+}(BF_4^-)_2$). RAW264.7 cells were incubated with $\mathbf{1}^{2+}$-SNP580 for 3 h, and then incubated with NaHS (1 mM) for 1 h. The fluorescence images were acquired with a Cy3 filter with exposure time of 0.2 s. Scale bar: 20 μm.

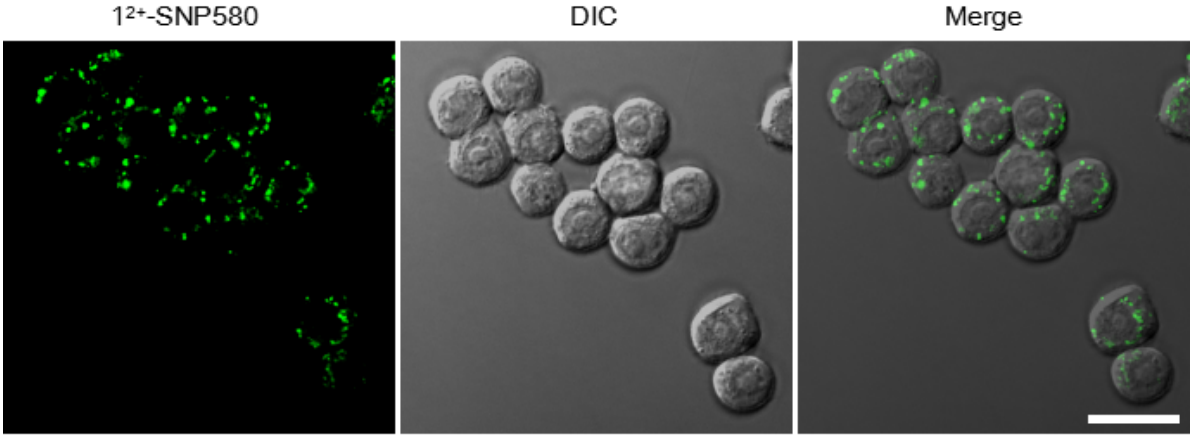

Figure S17. Visualization of endogenous H_2S in RAW264.7 cells stimulated with L-Cys. (a) Cell images (Left) and the average fluorescence intensity (Right) of RAW264.7 cells upon treatment with different concentration of L-Cys. Cells were incubated with 0, 100, 200 and 500 μM L-Cys for 1 h, washed, and then further incubated with $\mathbf{1}^{2+}$-SNP830 (28 μg/mL PCPDTBT, 48 μg/mL $\mathbf{1}^{2+}(BF_4^-)_2$) for 3 h. (b) Cell images (Left) and the average fluorescence intensity (Right) of RAW264.7 cells upon treatment with L-Cys (200 μM) for different time. Cells were incubated with 200 μM L-Cys for 0, 0.5, 1 and 2 h , washed, and then further incubated with $\mathbf{1}^{2+}$-SNP830 for 3 h. The fluorescence images were acquired with a Cy5.5 filter with an exposure time of 1 s. The fluorescence regions in cells in the visual field of each image were selected for the ROI measurement in ImageJ (NIH), and the average fluorescence intensity in each image was quantified. Values are mean ± SD from three repeated experiments. Scale bars: 20 μm.

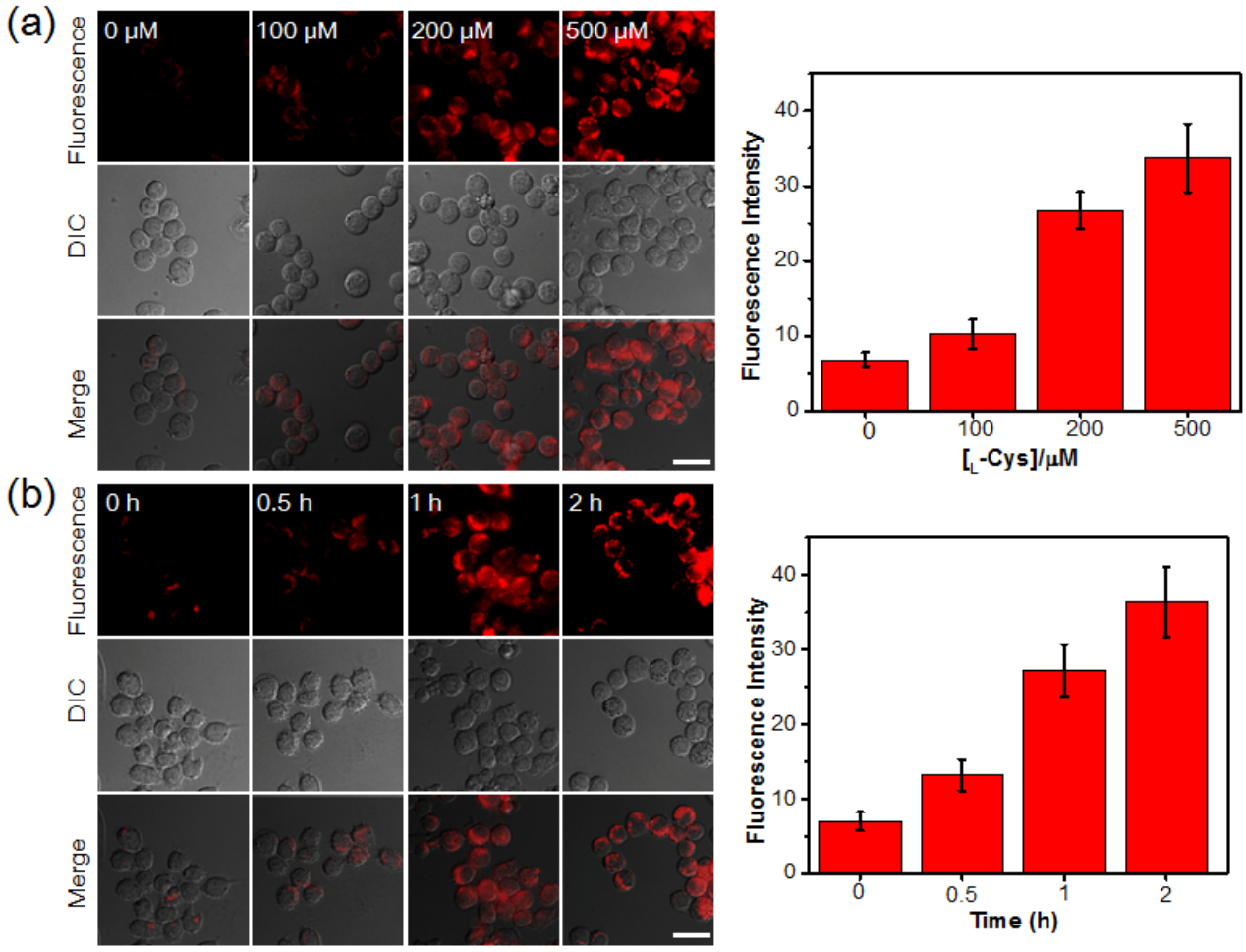

Figure S18. Investigation of the CSE expression in RAW264.7 cells stimulated with LPS. (a) Western Blot analysis of different CSE expression in RAW264.7 cells upon treatment with 0, 0.2, 0.5 and 1.0 μg/mL LPS for 6 h. (b) Comparison of the relative CSE protein levels based on the Western blot results. The CSE protein level in each band was quantified using Gel-Pro32 and qualified against the band of GAPDH. The CSE levels were normalized to the one in untreated cells (0 μg/mL). (c) Quantitative real-time RT-PCR analysis showed the relative CSE mRNA levels upon treatment with 0, 0.2, 0.5 and 1.0 μg/mL LPS for 6 h. Error bars indicated standard deviation from three experiments. These results revealed that LPS significantly increased CSE expression in RAW264.7 cells.

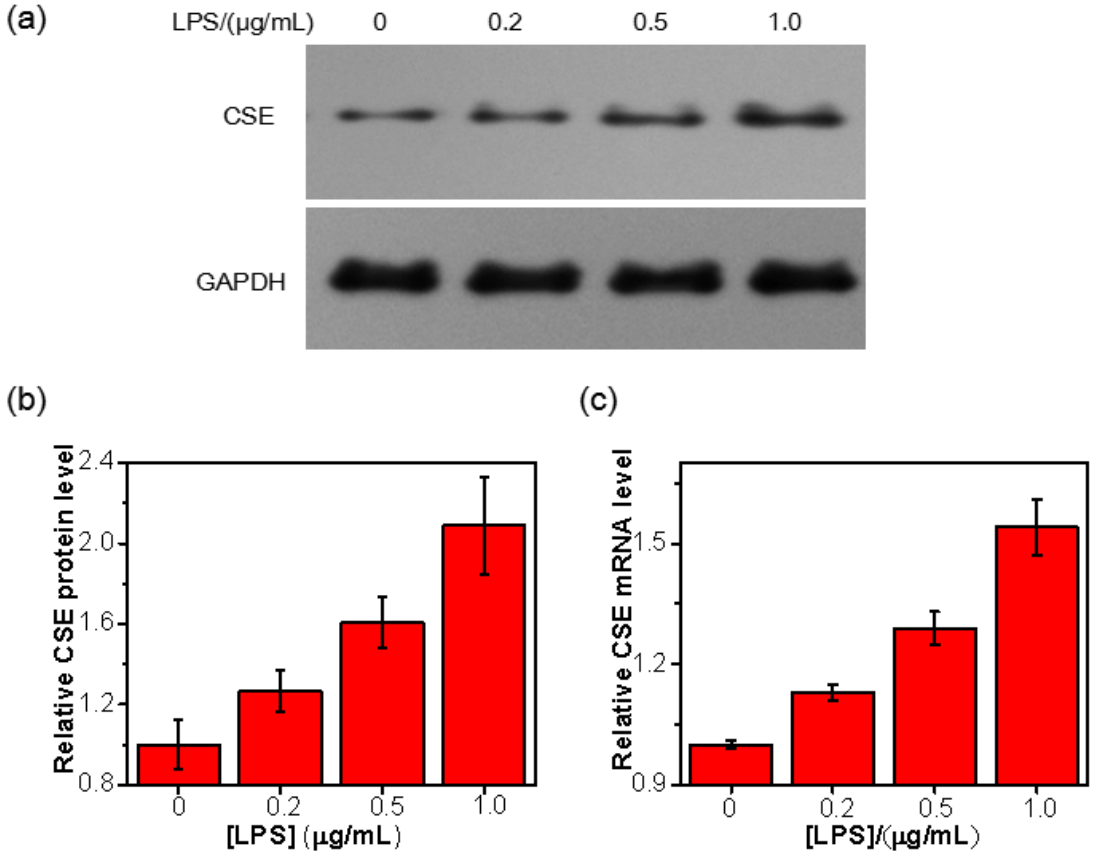

Figure S19. Measurement of H_2S levels in RAW264.7 cell lysates using MB method. (a) Illustration of the mechanism of MB method for the detection of H_2S. (b) UV-Vis absorption spectra of MB generated from the reaction of *N,N*-dimethyl-p-phenylenediamine-dihydrochloride, $Fe_2(SO_4)_3$ $Zn(OAc)_2$ and varying concentration of NaHS. (c) Plot of the absorption intensity of MB at 665 nm versus the concentration of NaHS. (d) UV-Vis absorption spectra of MB generated from the reaction of *N,N*-dimethyl-p-phenylenediamine-dihydrochloride, $Fe_2(SO_4)_3$ $Zn(OAc)_2$ and RAW264.7 cell lysates treated with different conditions. I: Control; II: $ZnCl_2$; III: NaHS; IV: $_L$-Cys; V: PAG + $_L$-Cys; VI: LPS + $_L$-Cys; VII: LPS + PAG + $_L$-Cys. (e) The calculated H_2S concentration in RAW264.7 cell lysates treated with conditions in d. Values are mean ± SD (n = 3). * $P < 0.05$; ** $P < 0.01$; *** $P < 0.001$. (f) Chemical structure and mechanism of a previously reported H_2S-activatable fluorescent probe. (g) Fluorescence images of RAW264.7 cells incubated with the reported H_2S-activatable probe or probe plus $ZnCl_2$. RAW264.7 cells were untreated (control) or pretreated with $ZnCl_2$ (300 μM, 10 min), and then incubated with H_2S-activatable probe (2 μM) for 0.5 h. Scale bar: 20 μm. (h) Normalized fluorescence intensity of RAW264.7 cells treated with the indicated conditions in g. Values are mean ± SD from three repeated experiments. * $P < 0.05$.

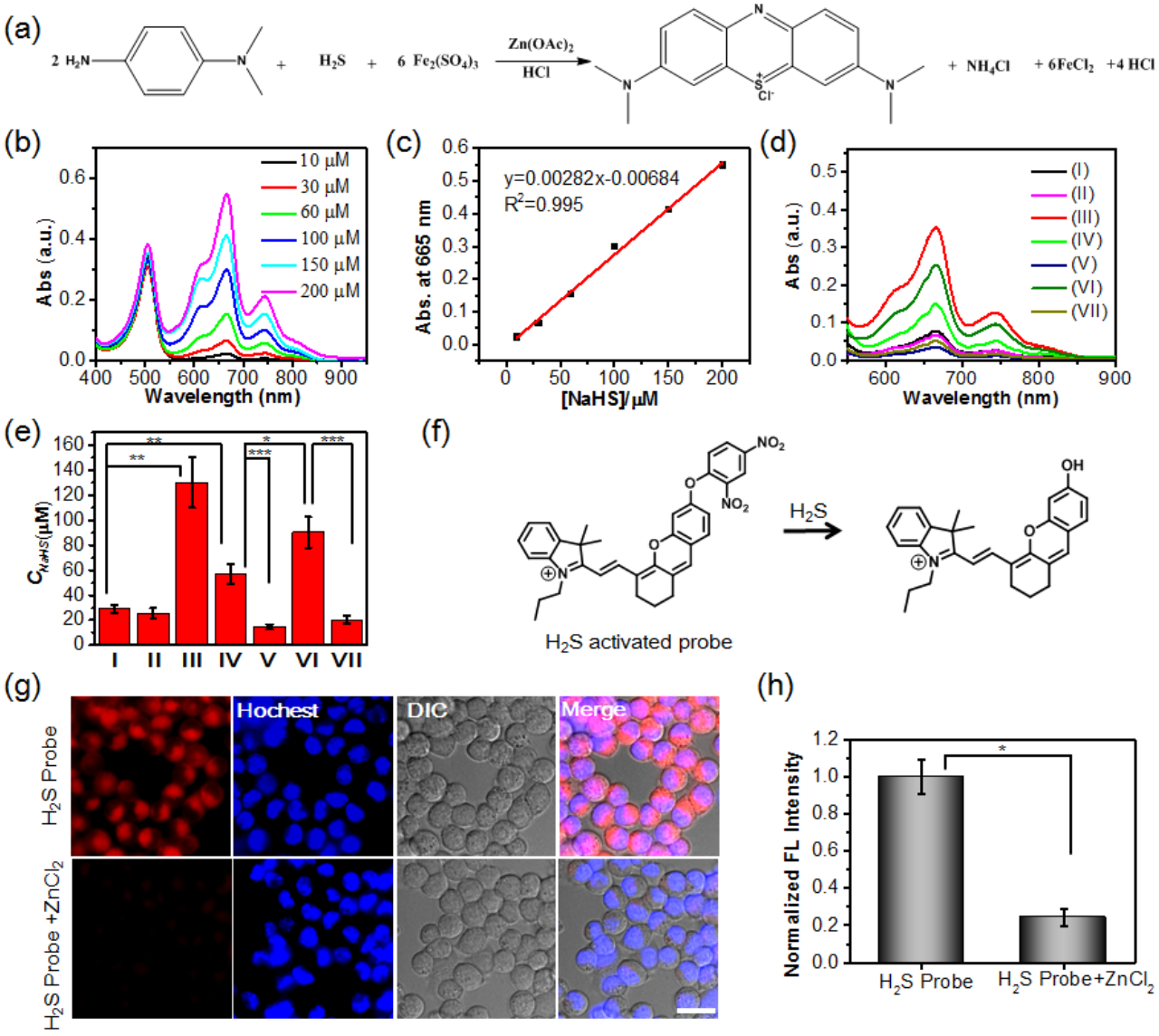

Figure S20. Non-invasive imaging of exogenous H_2S in living mice. (a) Representative time-dependent fluorescence imaging of exogenous H_2S with $\mathbf{1}^{2+}$-SNP830 (78.4 μg PCPDTBT, 134 μg $\mathbf{1}^{2+}(BF_4^-)_2$, 100 μL). $\mathbf{1}^{2+}$-SNP830 was i.p. injected into mice, followed by injection with NaHS (1 mM, 200 μL) or saline (0.9%, 200 μL). The images were acquired at 0, 2, 6, 10, 15, 20 and 60 min after injection of NaHS or saline (Ex: 780 nm; Em: 845 nm). (b) Quantitative analysis of the average fluorescence intensity in the i.p. cavity and (c) signal-to-background ratio (SBR) of mice following indicated treatment for 0–60 min. Black circles indicate the locations of background selected in mice. Values are mean ± SD (n = 3, * P < 0.05, ** P < 0.01, *** P <0.001).

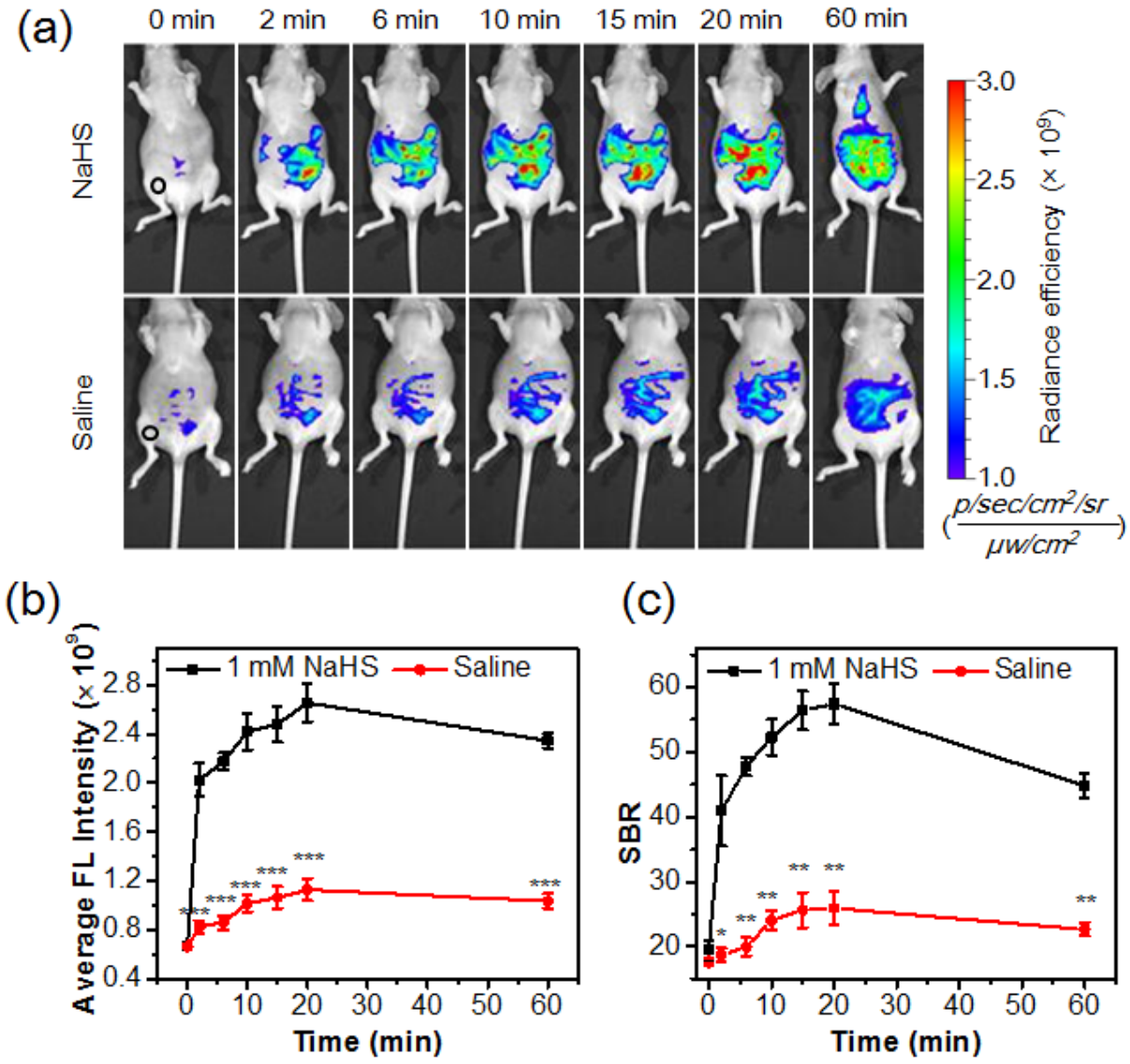

Figure S21. Longitudial average fluroescence (FL) intensity of livers in saline, L-Cys or PAG-treated mice following i.v. injection of $\mathbf{1}^{2+}$-SNP830 (78.4/134 μg PCPDTBT/$\mathbf{1}^{2+}(BF_4^-)_2$, 100 μL). Values are mean ± SD (n = 3, ** $P < 0.01$).

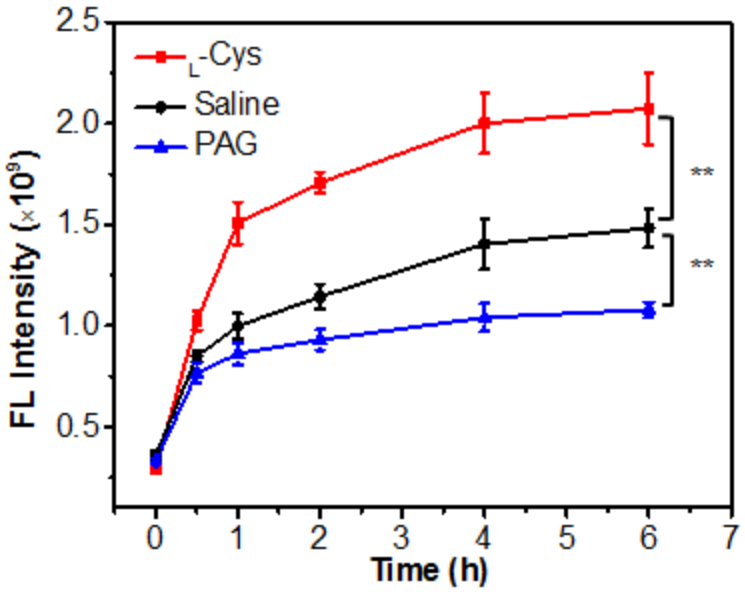

Figure S22. Evaluation of the biodistribution of $\mathbf{1}^{2+}$-SNP830 *ex vivo*. (a) Representative ex vivo fluorescence images of main organs resected from mice at 6 h post i.v. injection of $\mathbf{1}^{2+}$-SNP830 (78.4 μg PCPDTBT, 134 μg $\mathbf{1}^{2+}(BF_4^-)_2$, 100 μL). (b) Representative ex vivo images of main organs resected from mice at 6 h post i.v. injection of $\mathbf{1}^{2+}$-SNP830 (78.4 μg PCPDTBT, 134 μg $\mathbf{1}^{2+}(BF_4^-)_2$, 100 μL) and i.p. injection of L-Cys (1 mM, 100 μL). The results showed that the livers hold the brigthest fluorescence in both L-Cys-untreated and –treated mice.

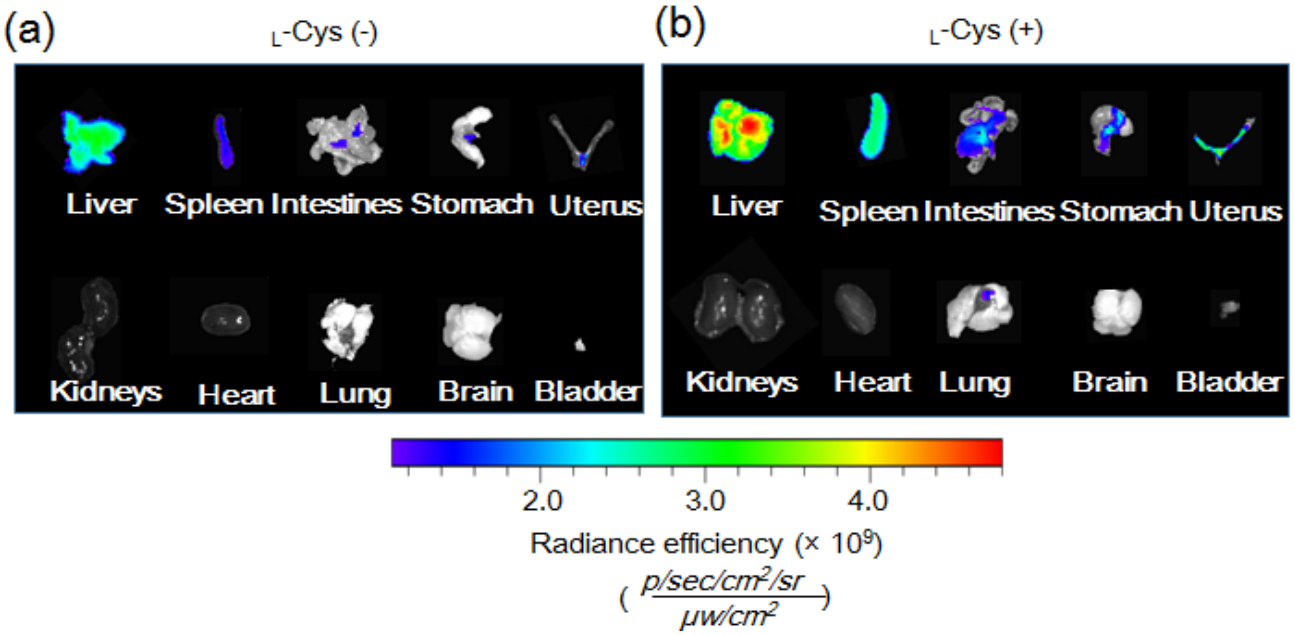

Figure S23. The average FL intensity of livers in mice following i.p. injection of varying doses of LPS (0, 5, 10, 20 mg/kg, or 10 mg/kg LPS + 5 mg/kg PAG) and $_L$-Cys (5 nmol/kg), and then i.v. injection of $\mathbf{1}^{2+}$-SNP830 (78.4/134 μg PCPDTBT/$\mathbf{1}^{2+}(BF_4^-)_2$, 100 μL). Values are mean ± SD (n = 3, * P < 0.05, ** P < 0.01).

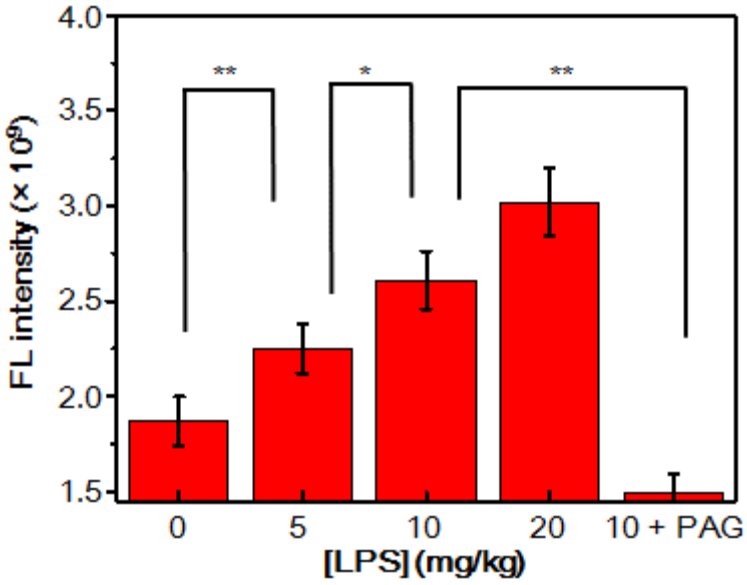

Figure S24. Fluorescence images of liver tissue slices resected from mice 6 h after indicated treatments. Mice with different treatment were i.v. injected with $\mathbf{1}^{2+}$-SNP830 (78.4 μg PCPDTBT, 134 μg $\mathbf{1}^{2+}(BF_4^-)_2$, 100 μL). After 6 h, mice were sacrificed, and the livers were resected from mice, frozen in OTC, and cut into 10 μm-thickness slices. After staining with DAPI, the images were acquired with Cy5.5 and DAPI filters, respectively. Scale bar: 20 μm.

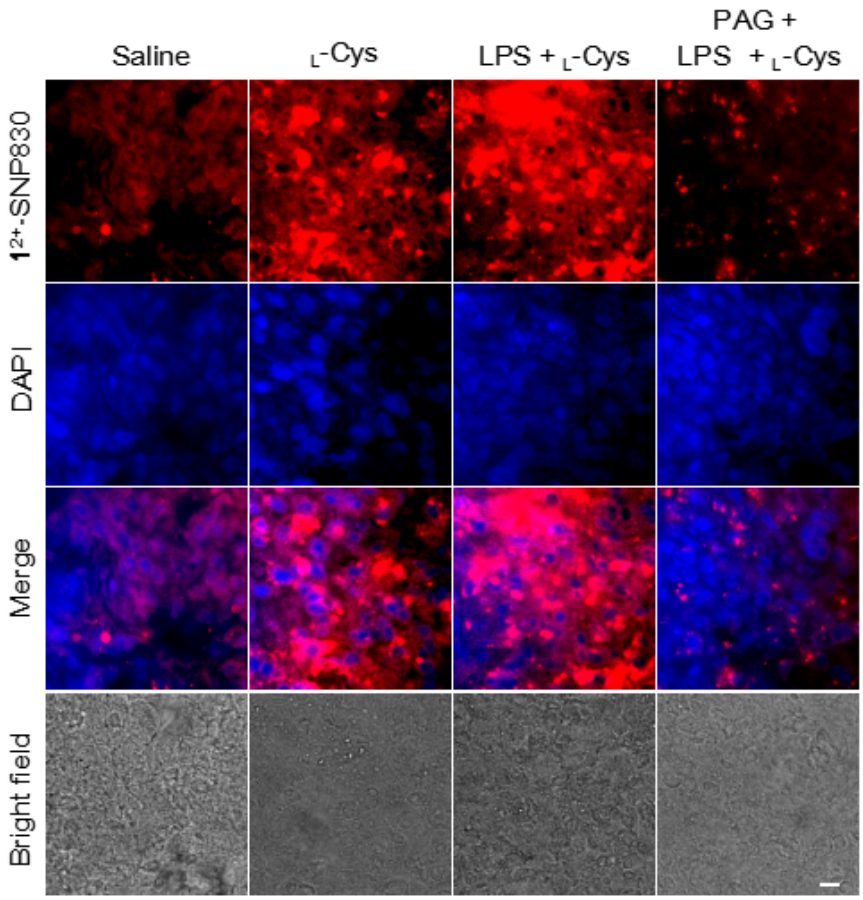

Figure S25. Investigation of the CSE expression in the livers following treatment with LPS. (a) Comparison of the relative CSE protein levels based on the Western Blot results in Fig. 4f. The CSE protein level in each band was quantified using Gel-Pro32 and qualified against the band of GAPDH. The CSE levels were normalized to the one in untreated mice (0 mg/kg LPS). (b) Quantitative real-time RT-PCR analysis showed the relative CSE mRNA levels in liver tissues upon treatment with 0, 5, 10 and 20 mg/kg LPS for 6 h. Error bars indicate standard deviation from three independent experiments. * $P < 0.05$.

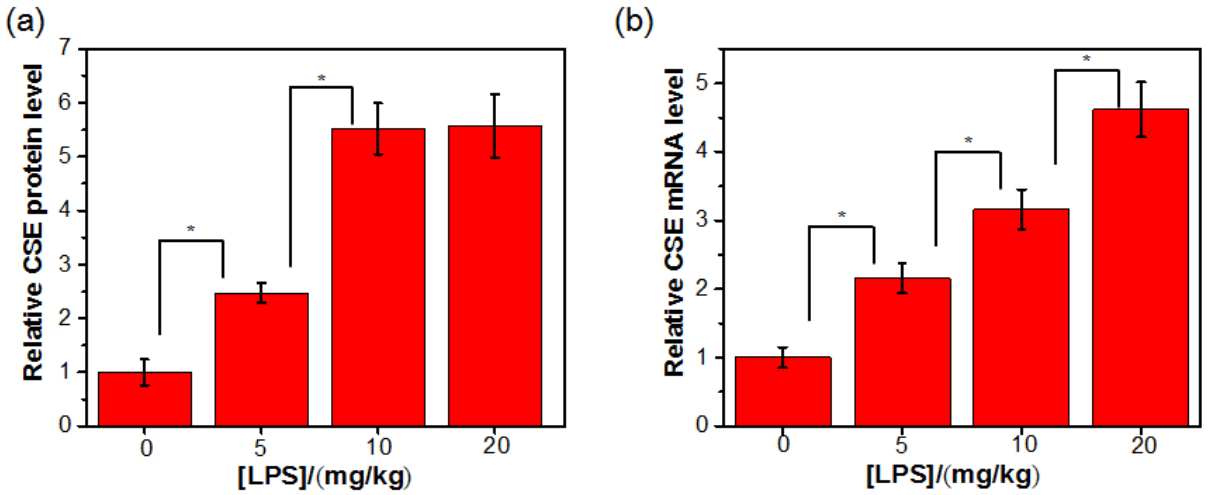

Figure S26. Characterization of tumor-targeting and H_2S-activatable probe $\mathbf{1}^{2+}$-SNP830-FA *in vitro*. (a) The hydrodynamic diameter, (b) TEM, and (c) AFM of $\mathbf{1}^{2+}$-SNP830-FA. (d) Zeta potentials of $\mathbf{1}^{2+}$-SNP830 and $\mathbf{1}^{2+}$-SNP830-FA in D.I. water showed that $\mathbf{1}^{2+}$-SNP830-FA was more negative compared to that of $\mathbf{1}^{2+}$-SNP830 due to the presence of FA on the surface. (e) UV−Vis absorption spectra of $\mathbf{1}^{2+}$-SNP830 and $\mathbf{1}^{2+}$-SNP830-FA showed the presence of typical UV-Vis absorption of FA (~295 nm, indicated by arrow) in $\mathbf{1}^{2+}$-SNP830-FA. (f) FL spectra of $\mathbf{1}^{2+}$-SNP830-FA before and after activation by NaHS. The results showed that $\mathbf{1}^{2+}$-SNP830-FA could be similarly activated by H_2S, resulting in ~15-fold fluorescence enhancement.

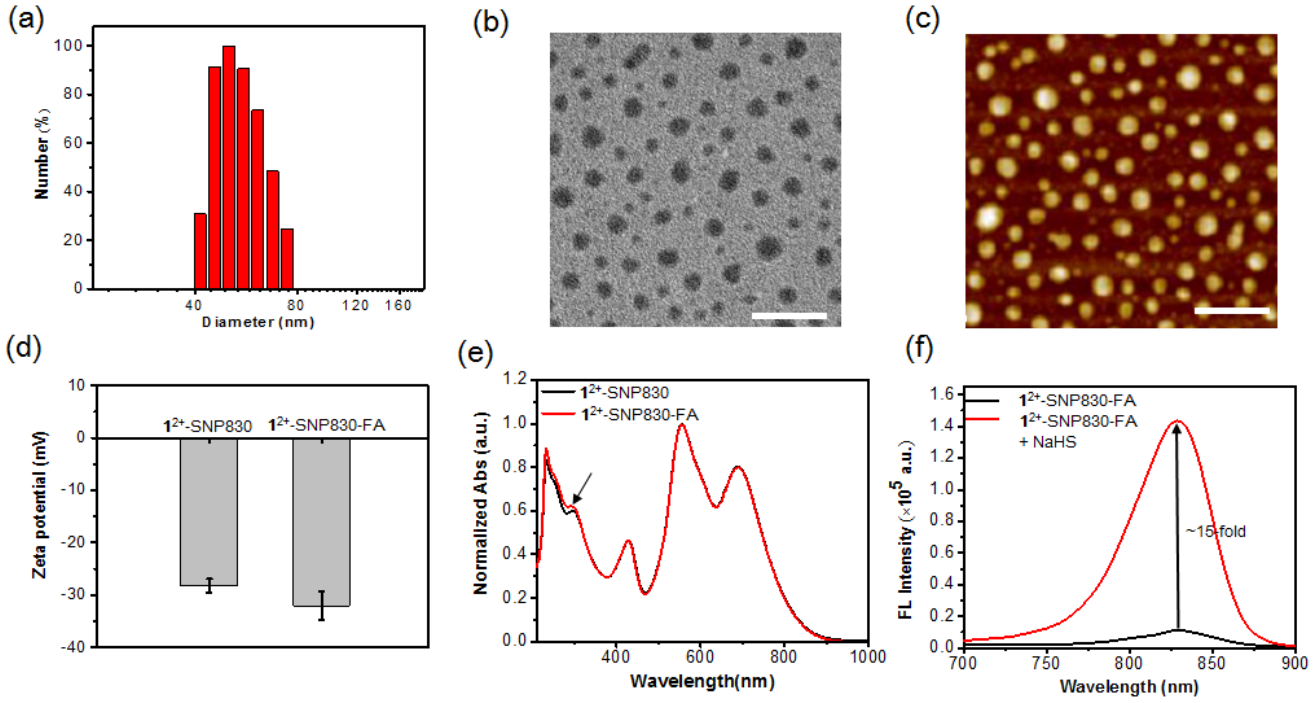

Figure S27. Evaluation of the cytotoxicity of $\mathbf{1}^{2+}$-SNP830-FA against different cells. KB, HCT116, HT29 or HEK293 cells were incubated with varying concentration of $\mathbf{1}^{2+}$-SNP830-FA for 24 h, and the cell viability was measured using MTT assay. Error bars represent standard deviations of three separate measurements. These results showed that $\mathbf{1}^{2+}$-SNP830-FA exhibits high biocompatibility against these four cells.

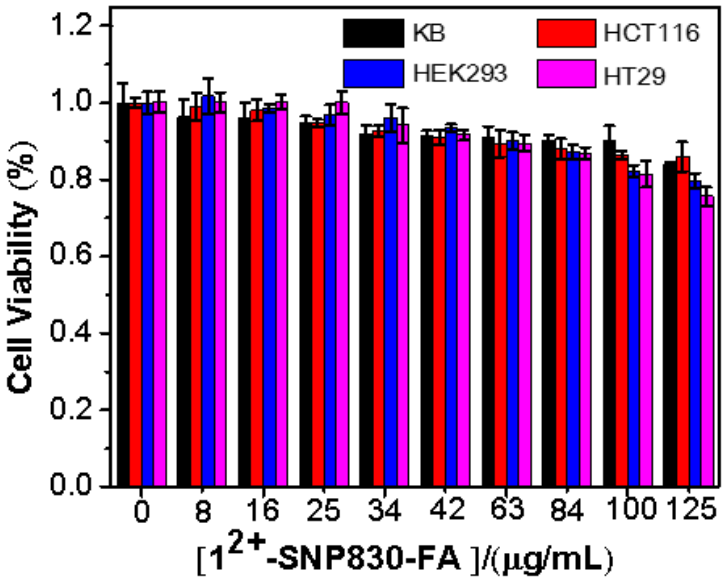

Figure S28. Imaging of endogenous H_2S in KB tumor cells. Fluorescence images of KB cells after incubation with $\mathbf{1}^{2+}$-SNP830-FA, $\mathbf{1}^{2+}$-SNP830 or $\mathbf{1}^{2+}$-SNP830-FA (28 μg/mL PCPDTBT, 48 μg/mL $\mathbf{1}^{2+}(BF_4^-)_2$) together with 1 mM free FA for 1 h (exposure time: 0.5 s). Scale bar: 20 μm. The cell imaging results demonstrated that the uptake of $\mathbf{1}^{2+}$-SNP830-FA into KB cells was folate receptor-dependent.

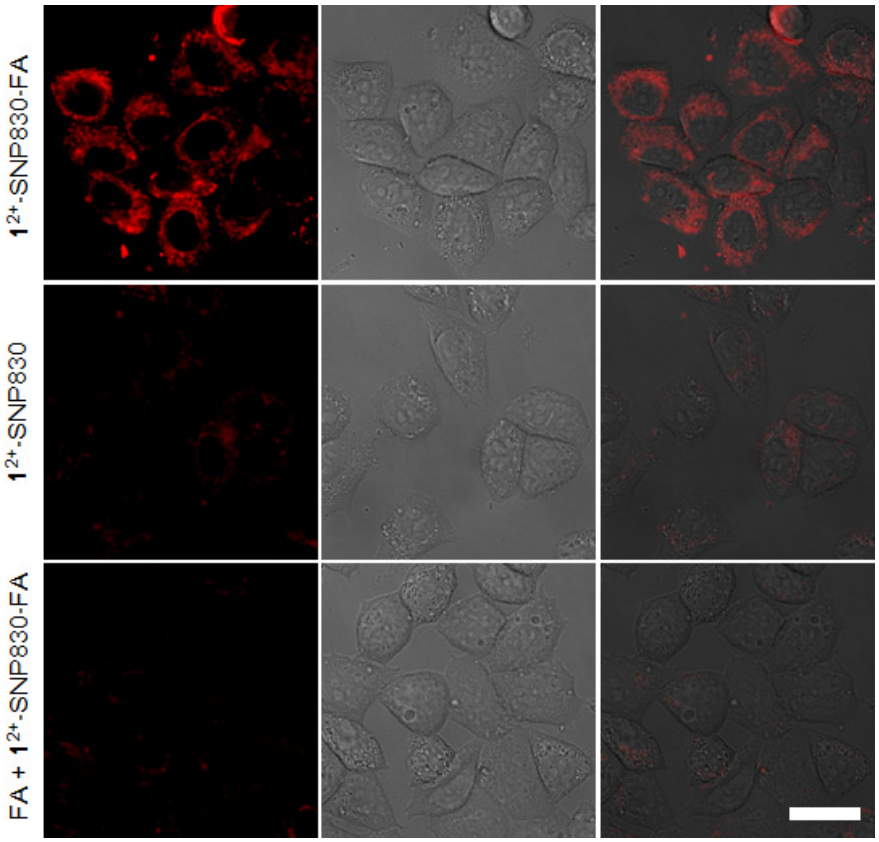

Figure S29. Colocalization studies of $\mathbf{1}^{2+}$-SNP830-FA in KB cells. (a) Fluorescence images showed that the red (pseudo color) fluorescence from $\mathbf{1}^{2+}$-SNP830-FA overlapped well with the green (pseudo color) fluorescence from Lyso-Tracker, indicating thta $\mathbf{1}^{2+}$-SNP830-FA was distributed maily in the lysosomes of KB cells. Cells were incubated with $\mathbf{1}^{2+}$-SNP830-FA (28 μg/mL PCPDTBT, 48 μg/mL $\mathbf{1}^{2+}(BF_4^-)_2$, Red) for 1 h, and stained with 1.0 μM Lyso-Tracker (green) and 2.0 μM Hoechst 34333 (blue) for 20 min. (b) Intensity profile of linear region of interest (ROI 1) across the KB cell costained with Lyso-Tracker and $\mathbf{1}^{2+}$-SNP830-FA. Scale bar: 20 μm.

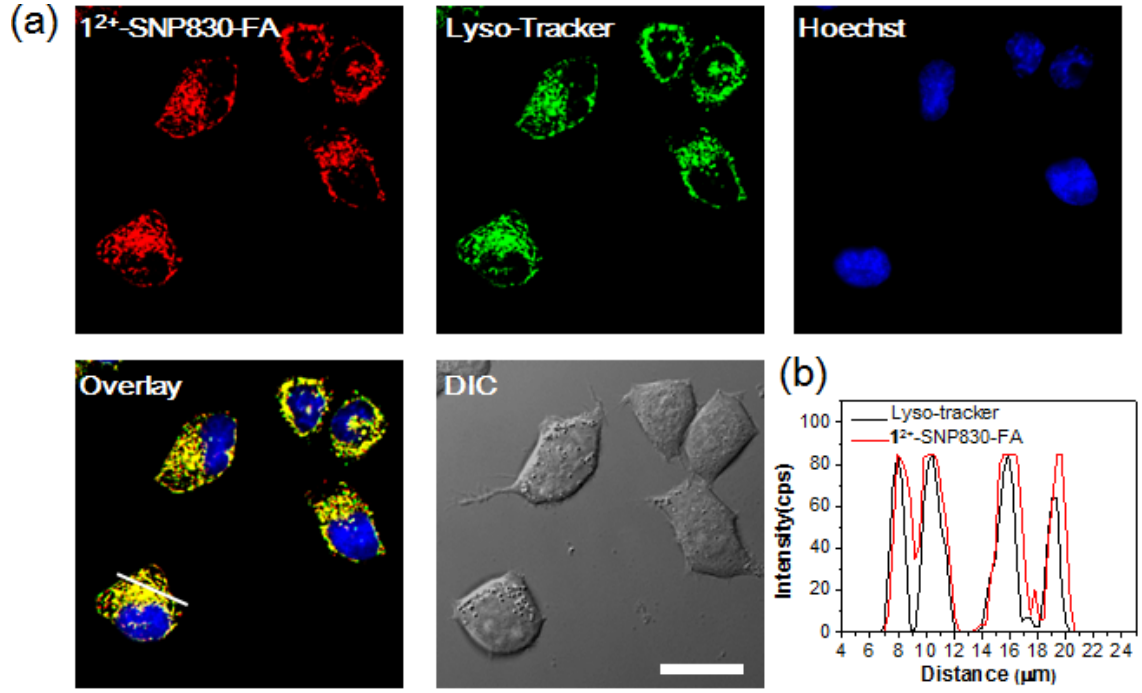

Figure S30. Detection of H_2S in KB cells with $\mathbf{1}^{2+}$-SNP830-FA. (a) Fluorescence images of KB cells following incubation with $\mathbf{1}^{2+}$-SNP830-FA and indicated reagents. KB cells were untreated (control) or pretreated with $ZnCl_2$ (300 μM, 10 min), L-Cys (200 μM, 1 h), PAG(50 mg/L, 0.5 h) + L-Cys (200 μM, 1 h), and then incubated with $\mathbf{1}^{2+}$-SNP830-FA (28 μg/mL PCPDTBT, 48 μg/mL $\mathbf{1}^{2+}(BF_4^-)_2$) for 1 h. For NaHS, KB cells were incubated with $\mathbf{1}^{2+}$-SNP830-FA for 1 h, washed, and then incubated with NaHS (1 mM) for 1 h. Scale bar: 20 μm. (b) Average intracellular fluorescence intensity of KB cells as shown in the images of (a). Values are mean ± SD from three repeated experiments. (** $P < 0.01$, *** $P < 0.001$).

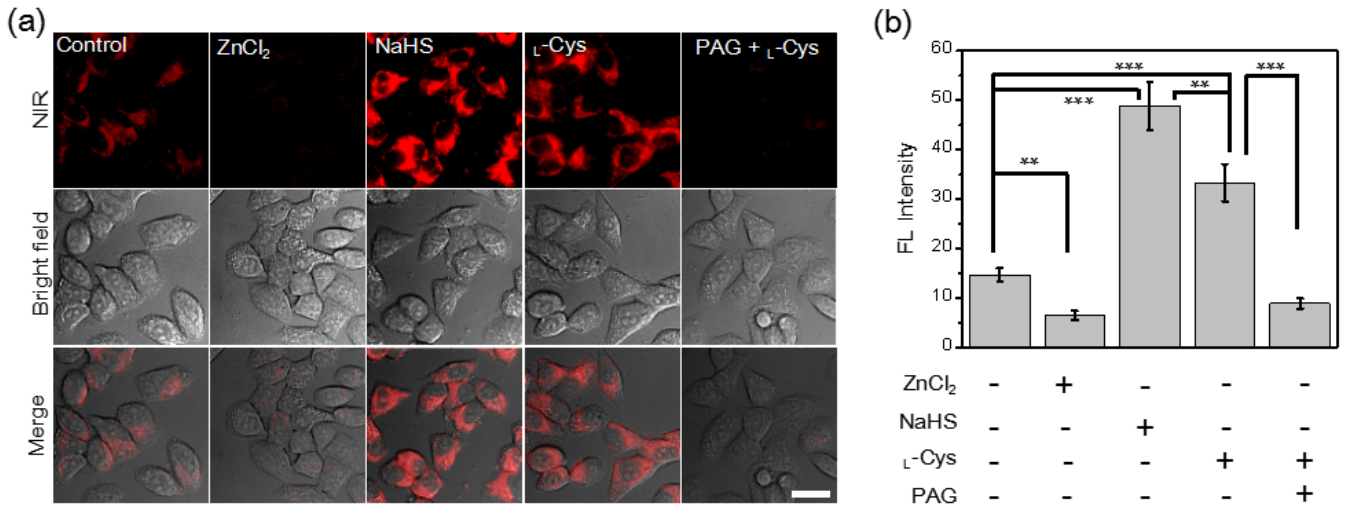

Figure S31. Differentiation of H_2S-rich tumor cells and H_2S-deficient normal cells using $\mathbf{1}^{2+}$-SNP830-FA. Fluorescence images of human colon tumor cells (HT29 and HCT116) and human embryonic kidney HEK293 cells upon incubation with $\mathbf{1}^{2+}$-SNP830-FA (28 μg/mL PCPDTBT, 48 μg/mL $\mathbf{1}^{2+}(BF_4^-)_2$ for 1 h. Scale bar: 20 μm (Exposure time: 1 s).

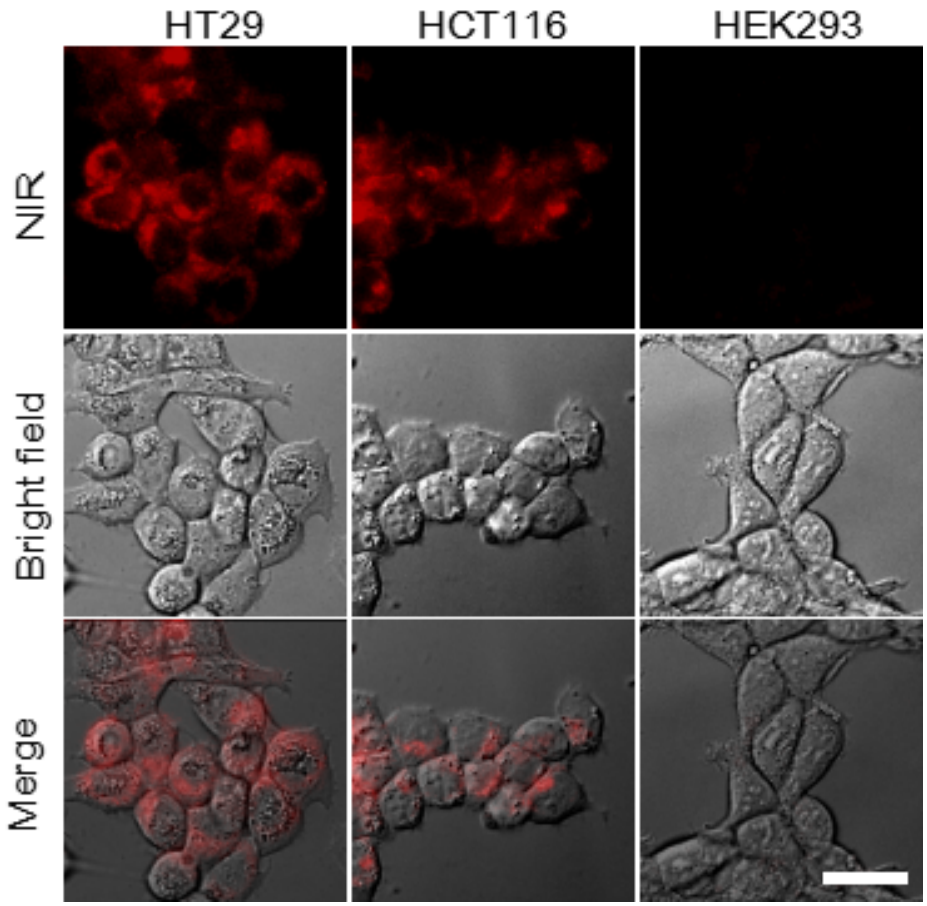

Figure S32. Fluorescence imaging of KB tumor tissue slices resected from mice 24 h after indicated treatments. KB tumor-bearing mice were i.v. injected with $\mathbf{1}^{2+}$-SNP830-FA or $\mathbf{1}^{2+}$-SNP830 (78.4 μg PCPDTBT, 134 μg $\mathbf{1}^{2+}(BF_4^-)_2$, 100 μL). After 3.5 h, L-Cys (1 mM) in 25 μL saline was directly injected into tumors to upregulate endogenous H_2S. After 24 h, the mice were sacrificed, and the tumors were dissected. The tumor tissues were then cut to obtain 10 μm-thickness slices. After staining with DAPI, the tumor tissue slices were imaged with the IX73 optical microscope equipped with DAPI and Cy5.5 filters. Scale bar: 20 μm.

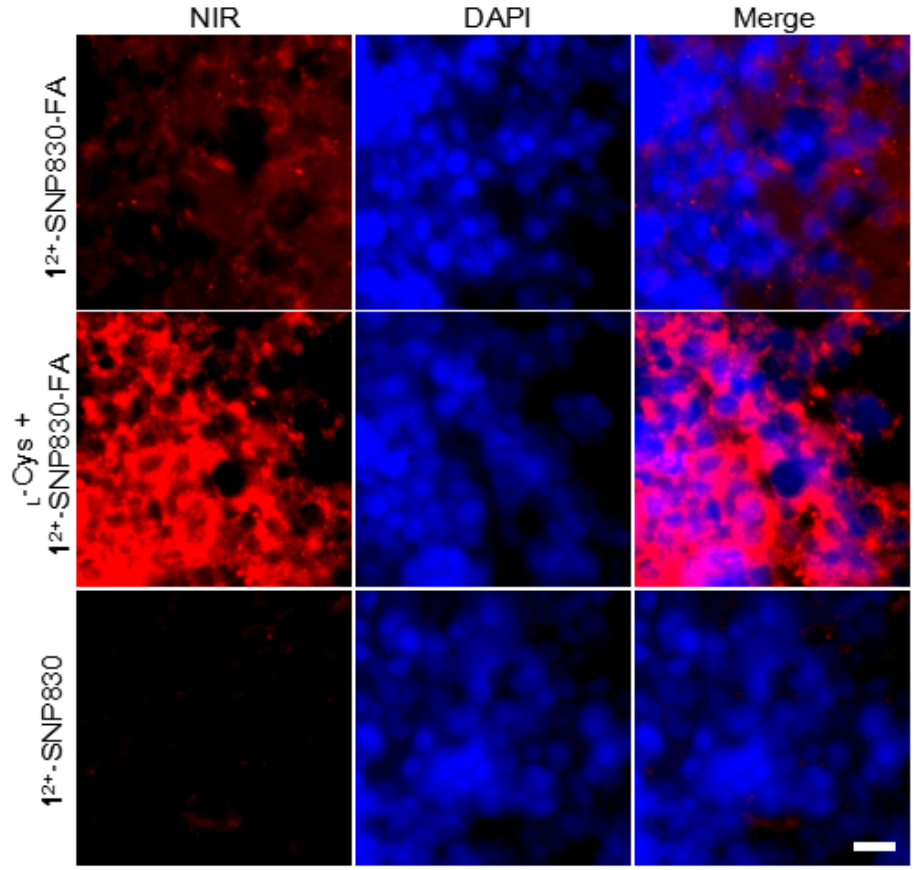

Figure S33. Characterization of tumor-targeting and H_2S-activatable PS ($\mathbf{1}^{2+}$-PSs-FA) *in vitro*. (a) Comparison of the absorption spectra of $\mathbf{1}^{2+}$ and fluorescence spectra of NIR775 and R6G shows good overlapping spectra between them. (b) The hydrodynamic diameter, (c) TEM, and (d) AFM of $\mathbf{1}^{2+}$-PSs-FA. e) Zeta potentials of $\mathbf{1}^{2+}$-PSs-FA and $\mathbf{1}^{2+}$-PSs in D.I. water show that $\mathbf{1}^{2+}$-PSs-FA is more negative compared to that of $\mathbf{1}^{2+}$-PSs due to the presence of FA on the surface. (f) Comparison of the absorption spectra of $\mathbf{1}^{2+}$-PSs-FA and $\mathbf{1}^{2+}$-PSs shows the presence of typical UV-Vis absorption of FA (~295 nm indicated by arrow) in $\mathbf{1}^{2+}$-PSs-FA. Scale bars: 200 nm.

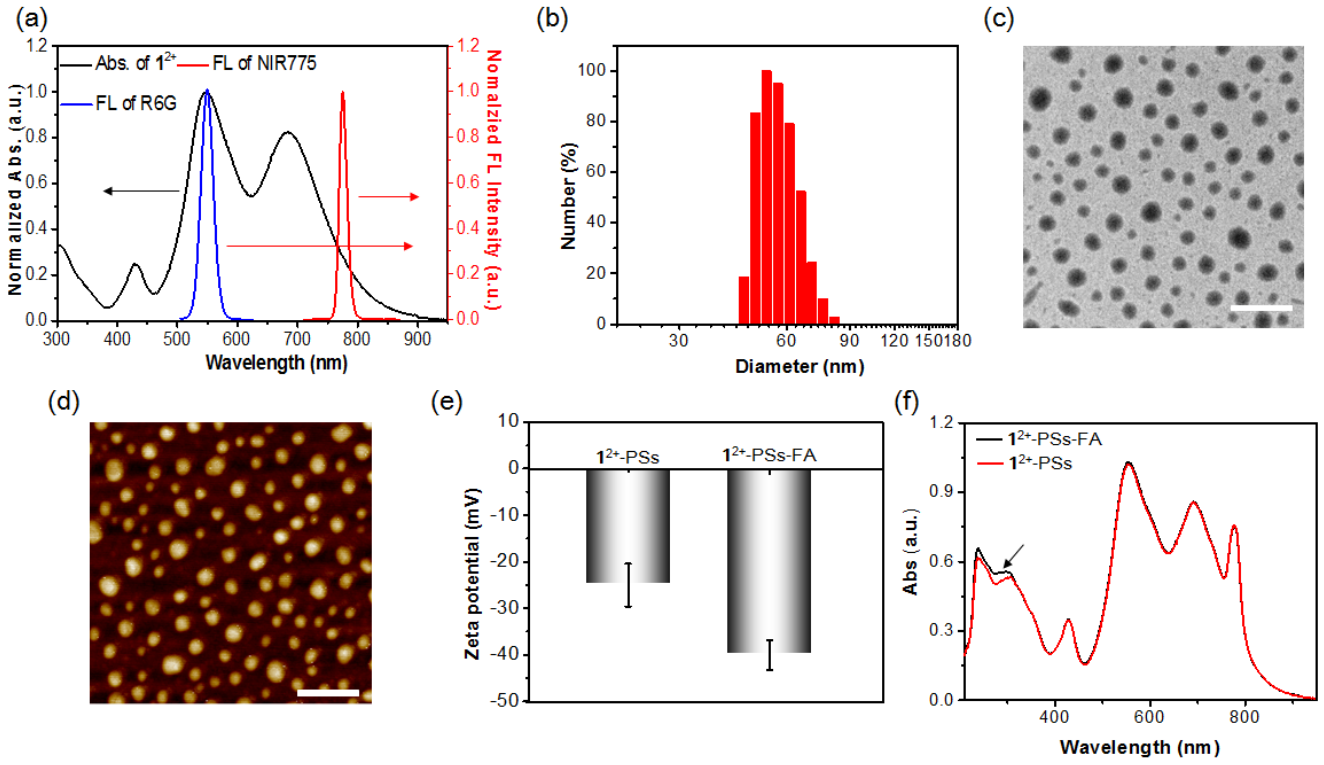

Figure S34. Evaluation of the activation of $\mathbf{1}^{2+}$-PSs-FA by H_2S. (a) Normalized absorption spectra of $\mathbf{1}^{2+}$-PSs-FA (5.5 μg/mL NIR775) upon incubation with NaHS (350 μM) in PBS buffer (pH 7.4) at r.t. for 0 to 600 s. (b) Fluorescence spectra of $\mathbf{1}^{2+}$-PSs-FA upon incubation with NaHS in PBS buffer (pH 7.4) at r.t. for 0 to 540 s. Fluorescence spectra were measured by synchronous fluorescence scanning (λ_{ex} = 700 to 900 nm, offset = 10 nm). (c) Fluorescence spectra and (d) fluorescence turn-on ratios (F/F_0)of $\mathbf{1}^{2+}$-PSs-FA (48 μg/mL $\mathbf{1}^{2+}(BF_4^-)_2$) following incubation with different biological agents, including (1) 350 μM NaHS; (2) 0 μM NaHS (control); (3) 1.25 mM L-Cys; (4) 10 mM GSH; (5) 1 mM DL-Homocystein (Hcy); (6) 1.25 mM 2-mercaptothanol (BME); (7) 1.25 mM VC; (8) 1.25 mM DTT; (9) 1 mM H_2O_2; (10) 1 mM ClO^-; (11) $O_2^{\cdot-}$ (100 μM xanthine +22 mU XO); (12) $^1O_2$ (1 mM H_2O_2 +1 mM ClO^-); (13) $ONOO^-$ (1 mM $NaNO_2$+1 mM H_2O_2); (14) tert-butylm hydroperoxide (t-BuOOH, 300 μM); (15) cumene hydroperoxide(CuOOH, 300 μM). Inset: Fluorescence images of the incubation solutions containing $\mathbf{1}^{2+}$-PSs-FA and different agents. Fluorescence spectra were measured by synchronous fluorescence scanning (λ_{ex} = 500 to 850 nm, offset = 5 nm). Fluorescence images were acquired with $\lambda_{ex}/\lambda_{em}$ = 740/790 nm.

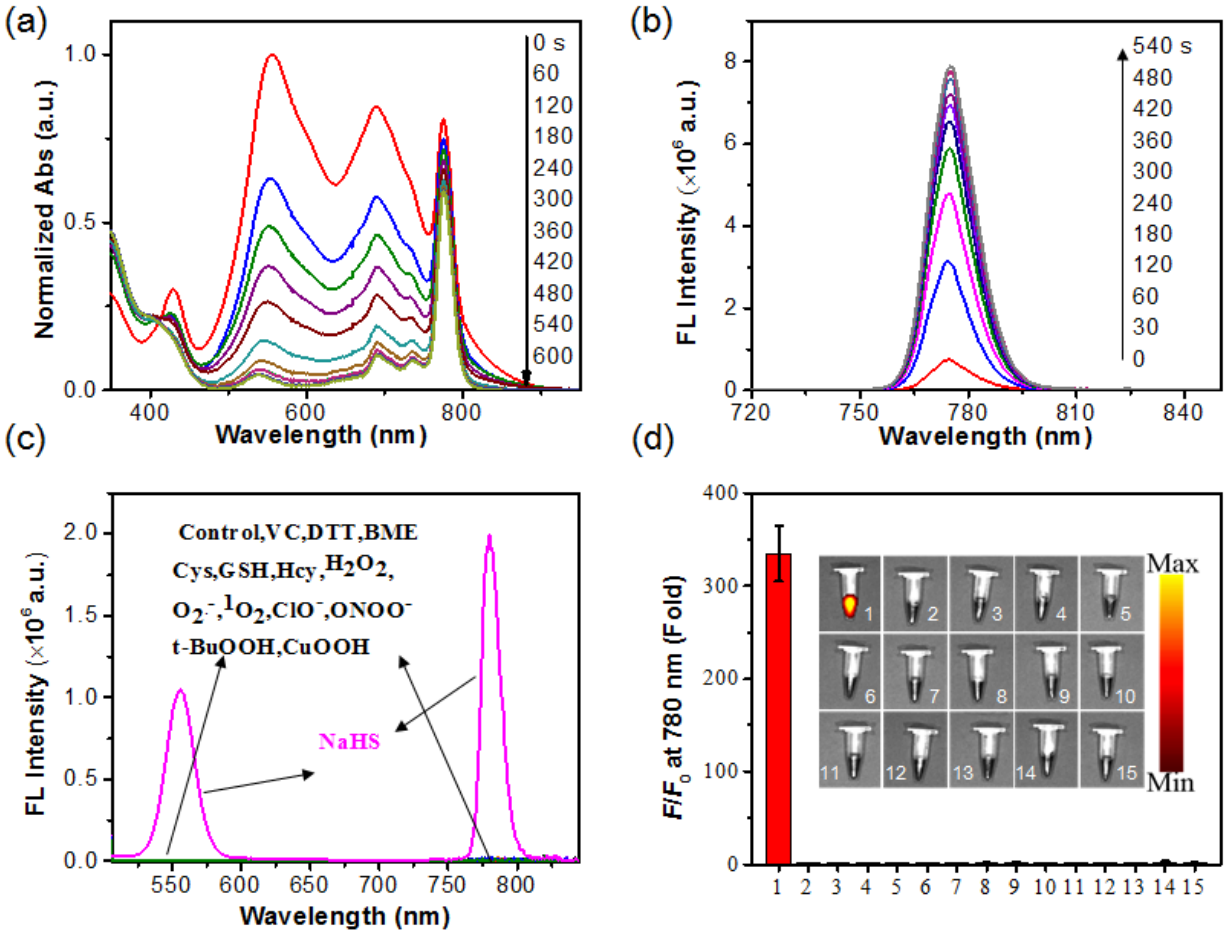

Figure S35. Determination of detection limit for H_2S. (a) Fluorescence spectra of $\mathbf{1}^{2+}$-PSs-FA (5.5 μg/mL NIR775) upon incubation with different concentration of NaHS in PBS buffer at r.t. for 10 min. The fluorescence spectra were measured by synchronous fluorescence scanning (λ_{ex} = 500 to 900 nm, offset = 5 nm). (b) Fluorescence spectra of $\mathbf{1}^{2+}$-PSs-FA (5.5 μg/mL NIR775) upon incubation with different concentration of NaHS in PBS buffer at r.t. for 10 min. (c) and (d) The linear relationship between the fluorescence intensity at 555 nm (R6G, c) and 780 nm (NIR775, d) versus the concentration of NaHS from 0.05 – 10 μM. The limit of detection (LOD) was calculated based on the blank + 3σ method (the concentration at which the fluorescence equals that of [blank + 3σ]) according to a linear regression fit of the data. The LOD at 555 nm and 780 nm was determined to be ~19 nM and ~39 nM, respectively. Values are mean ± SD (n = 3).

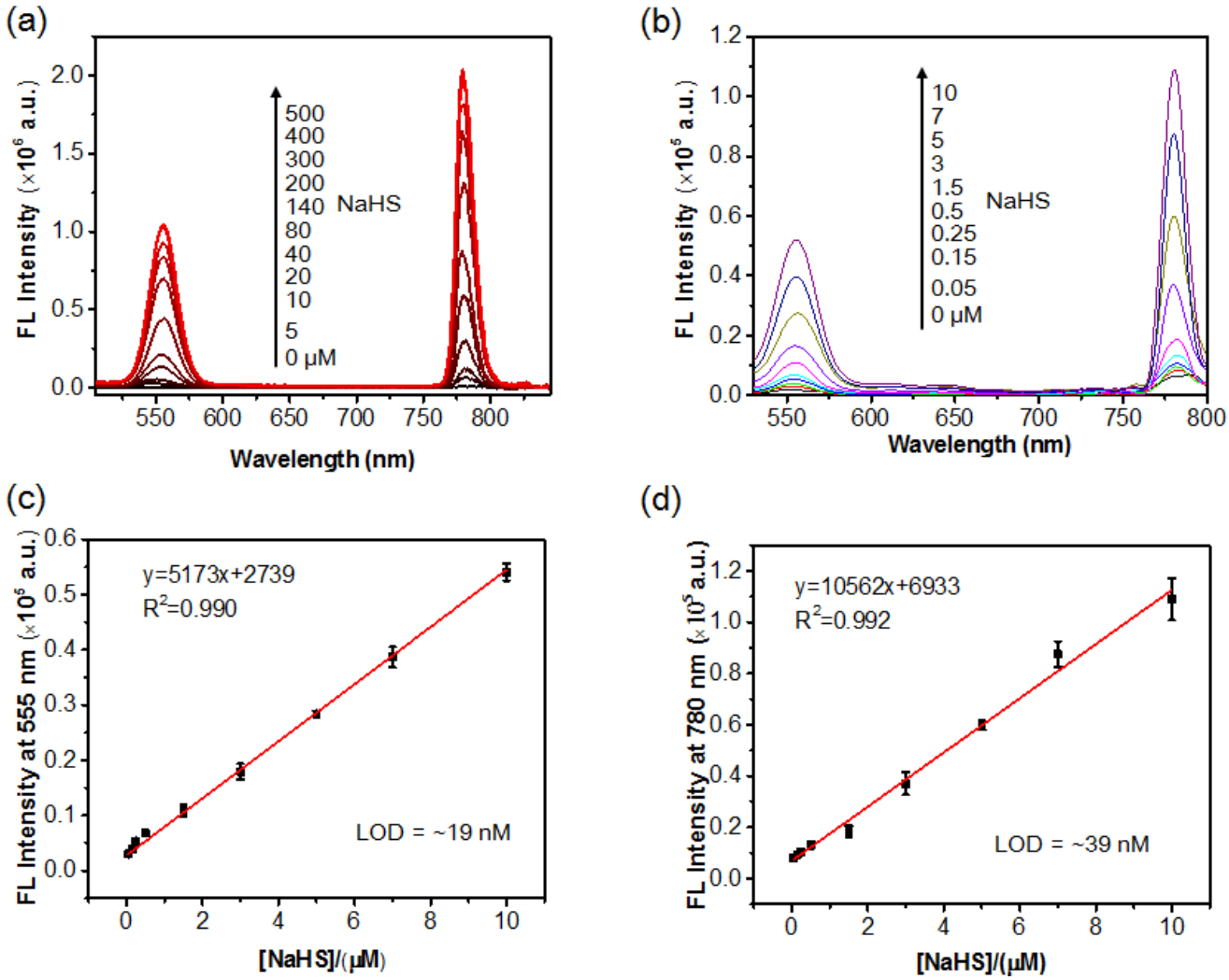

Figure S36. Comparison the irradiation effect between the 808 nm and 785 nm laser. (a,b) UV-Vis absorption spectra of activated $\mathbf{1}^{2+}$-PSs-FA (48/0.96/5.5 μg/mL $\mathbf{1}^{2+}(BF_4^-)_2$/R6G/NIR775 + 350 μM NaHS) following irradiation with an 808 nm (a) or a 785 nm laser (b) for 0, 5, 10, 15 and 20 min. (c) Normalized absorption intensity of activated $\mathbf{1}^{2+}$-PSs-FA at 775 nm following irradiation with indicated laser. (d) Measurement of fluorescence spectra of SOSG to compare the $^1O_2$ generation efficiency of activated $\mathbf{1}^{2+}$-PSs-FA upon irradiation with the 808 nm (a) or 785 nm laser for 60 s. $\lambda_{ex}/\lambda_{em}$ = 488/528 nm. The power density for both lasers is 1 W/cm^2. The results demonstrated that actvated $\mathbf{1}^{2+}$-PSs-FA was more resistant to photobleaching following irradiation with the 808 nm laser (808 ± 5 nm) compared to that with a 785 nm laser (785 ± 5 nm). Interestingly, the $^1O_2$ generation efficiency of activated $\mathbf{1}^{2+}$-PSs-FA irradiated with the 808 nm laser was found to be similar to that with the 785 nm laser, albeit the absorption is higher at 785 nm compared to 808 nm.

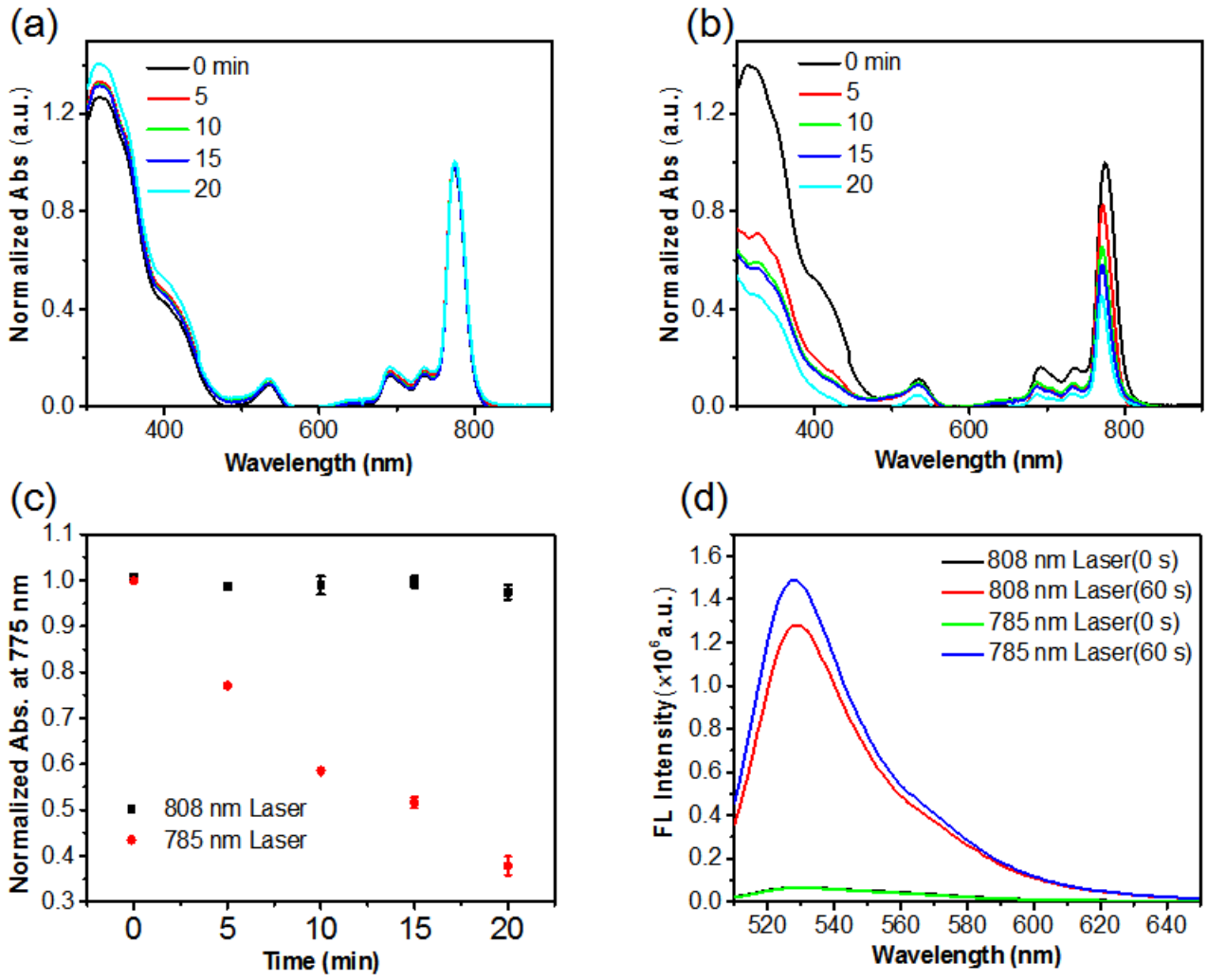

Figure S37. Measurement of $^1O_2$ generation using SOSG as a fluorescent indicator. (a) Fluorescence spectra of PBS solution containing SOSG (20.0 μM), (b) SOSG + $\mathbf{1}^{2+}$-PSs-FA (5.5 μg/mL NIR775), (c) SOSG + NaHS (350 μM) or (d) SOSG + $\mathbf{1}^{2+}$-PSs-FA (5.5 μg/mL NIR775) + NaHS (350 μM) upon irradiation with an 808 nm laser (1 W/cm^2) for 0, 10, 20, 30, 40, 50 and 60 s. The results showed that $\mathbf{1}^{2+}$-PSs-FA alone had little $^1O_2$ generation capacity upon 808 nm laser irradiation, while the activation with NaHS resulted in remarkable $^1O_2$ generation.

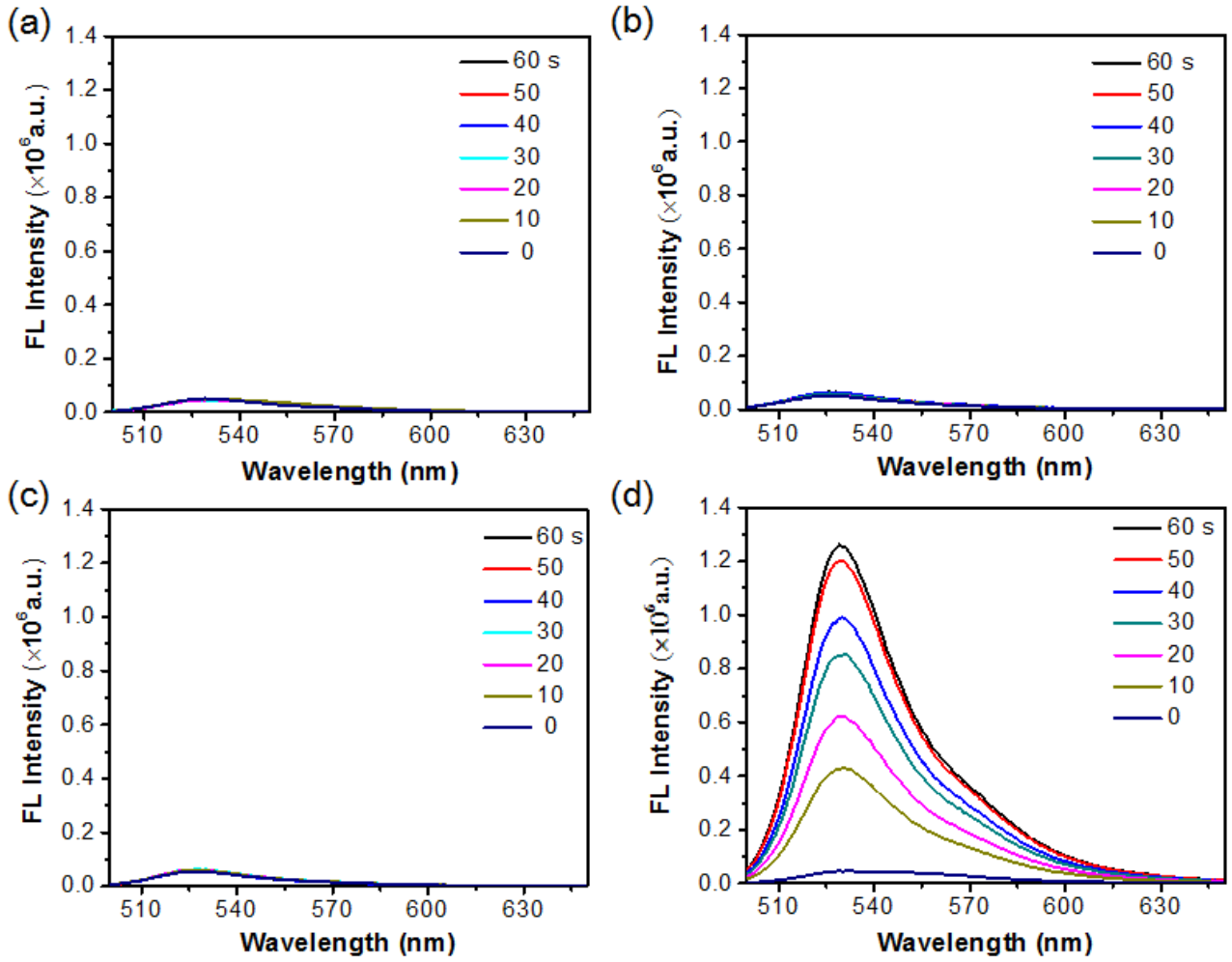

Figure S38. Effect of pH on the $^1O_2$ generation efficiency for $\mathbf{1}^{2+}$-PSs-FA upon H_2S activation. (a-c) Fluorescence spectra of aqueous solutions containing SOSG (20.0 μM), $\mathbf{1}^{2+}$-PSs-FA (5.5 μg/mL NIR775) and NaHS (350 μM) at pH 7.4 (a), 6.5 (b) and 5.0 (c) under irradiation with an 808 nm laser (1 W/cm^2) for different time. (d) Irradiation time-dependent enhancement of SOSG fluorescence (FL) intensity (528 nm) following treatment with condition a, b or c.

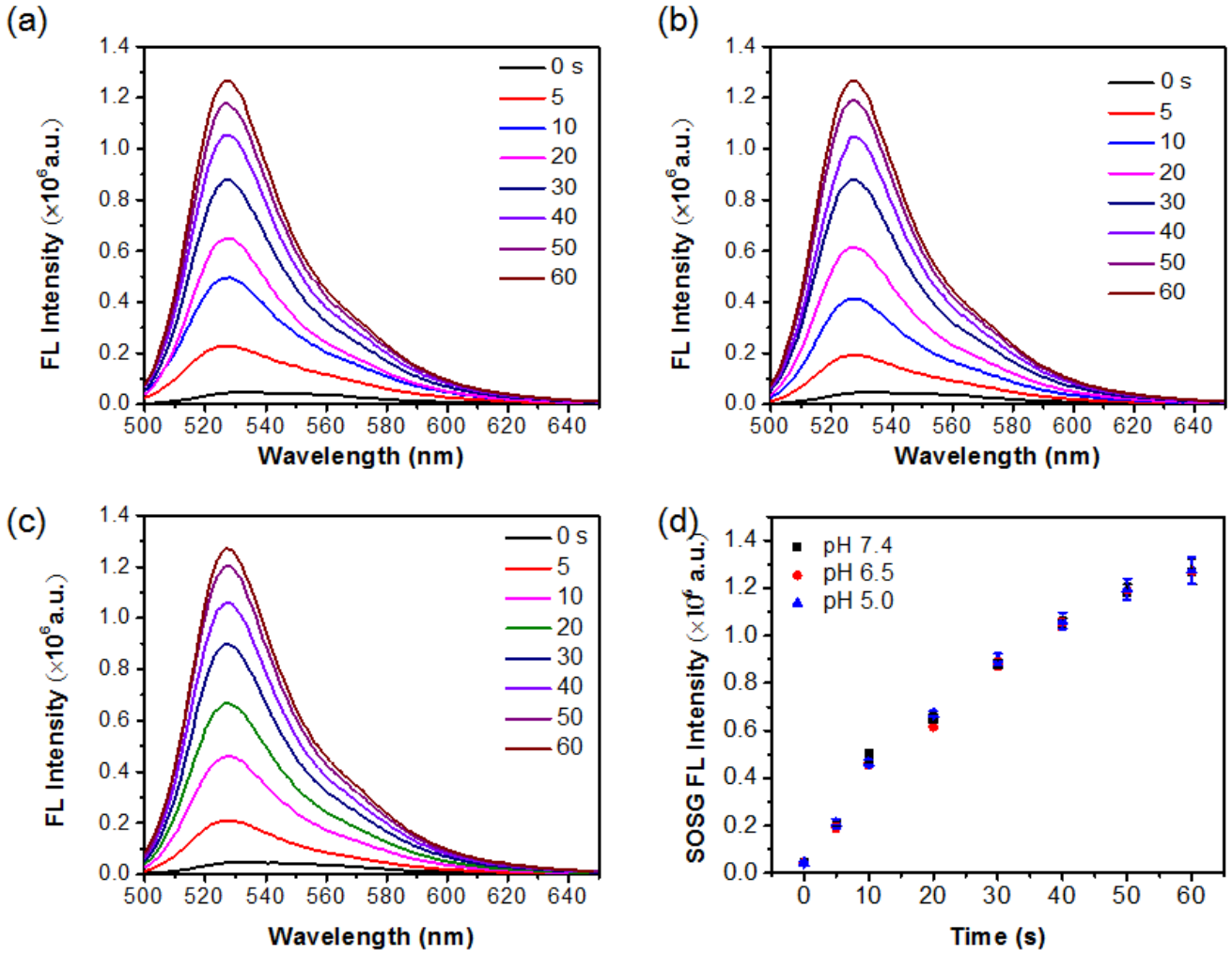

Figure S39. Investigation of cellular uptake and colocalization of $\mathbf{1}^{2+}$-PSs-FA in KB cells. (a) Fluorescence images of KB cells after incubation with $\mathbf{1}^{2+}$-PSs-FA, $\mathbf{1}^{2+}$-PSs or $\mathbf{1}^{2+}$-PSs-FA (5.5 μg/mL NIR775) together with 1 mM free FA for 1 h. Scale bar: 20 μm. (b) Investigation of the intracellular localization of $\mathbf{1}^{2+}$-PSs-FA (green) in KB cells co-stained with Lyso-tracker (red) and nucleus staining dye (Hoechst 33342, blue). KB cells were incubated with $\mathbf{1}^{2+}$-PSs-FA (5.5 μg/mL NIR775) for 1 h, washed, and then incubated with 1 μM Lyso-Tracker and 2.0 μM Hoechst for 20 min. Scale bar: 20 μm. The fluorescence imaging results in (a) demonstrated that the uptake of $\mathbf{1}^{2+}$-PSs-FA into KB cells was FR-dependent. Results in (b) revealed that $\mathbf{1}^{2+}$-PSs-FA accumulated mainly in the lysosomes.

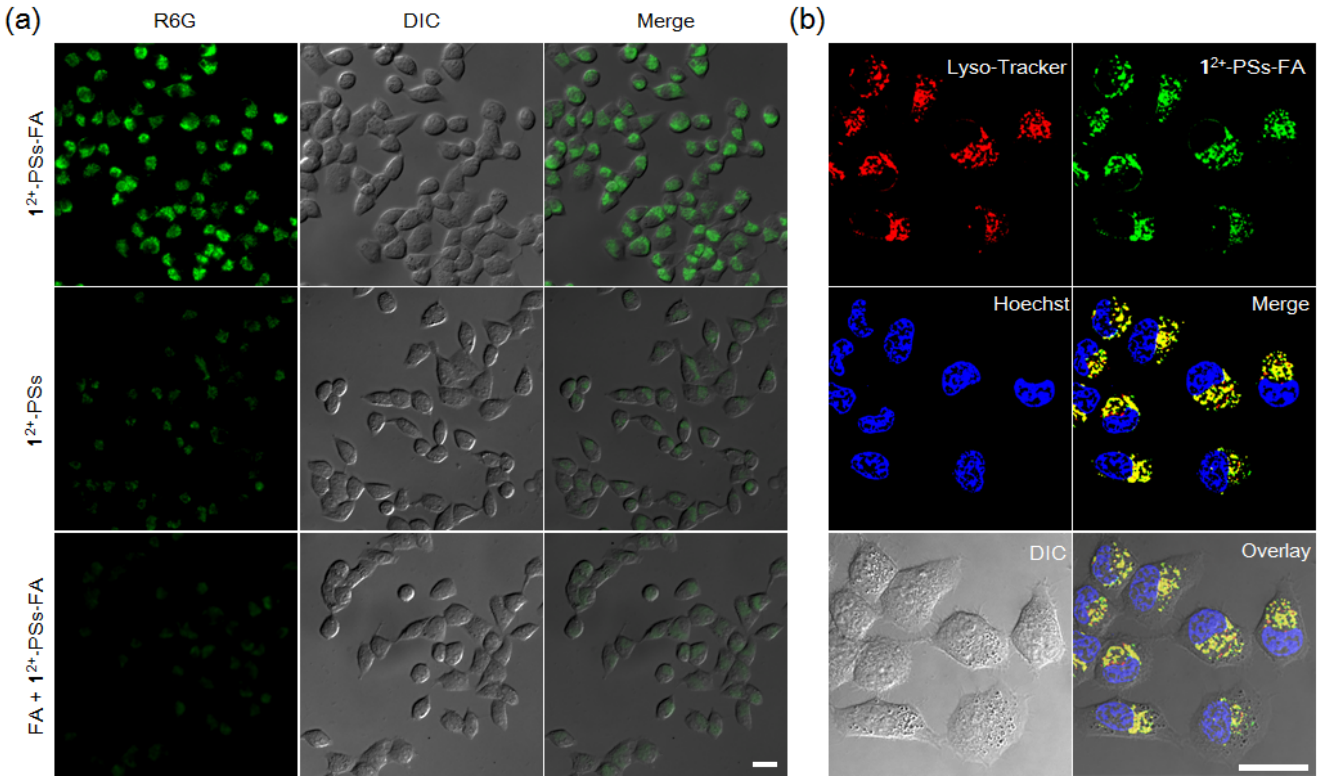

Figure S40. Visualization of H_2S in KB cells with $\mathbf{1}^{2+}$-PSs-FA. Fluorescence images of KB cells following incubation with $\mathbf{1}^{2+}$-PSs-FA and indicated reagents. KB cells were untreated (control) or pretreated with $ZnCl_2$ (300 μM, 10 min) or L-Cys (200 μM, 1 h), and then incubated with $\mathbf{1}^{2+}$-PSs-FA (5.5 μg/mL NIR775) for 1 h. For NaHS, KB cells were incubated with $\mathbf{1}^{2+}$-PSs-FA for 1 h, and then incubated with NaHS (1 mM) for another 1 h. All the cells were then stained with 2.0 μM Hoechst for 20 min. Scale bar: 50 μm.

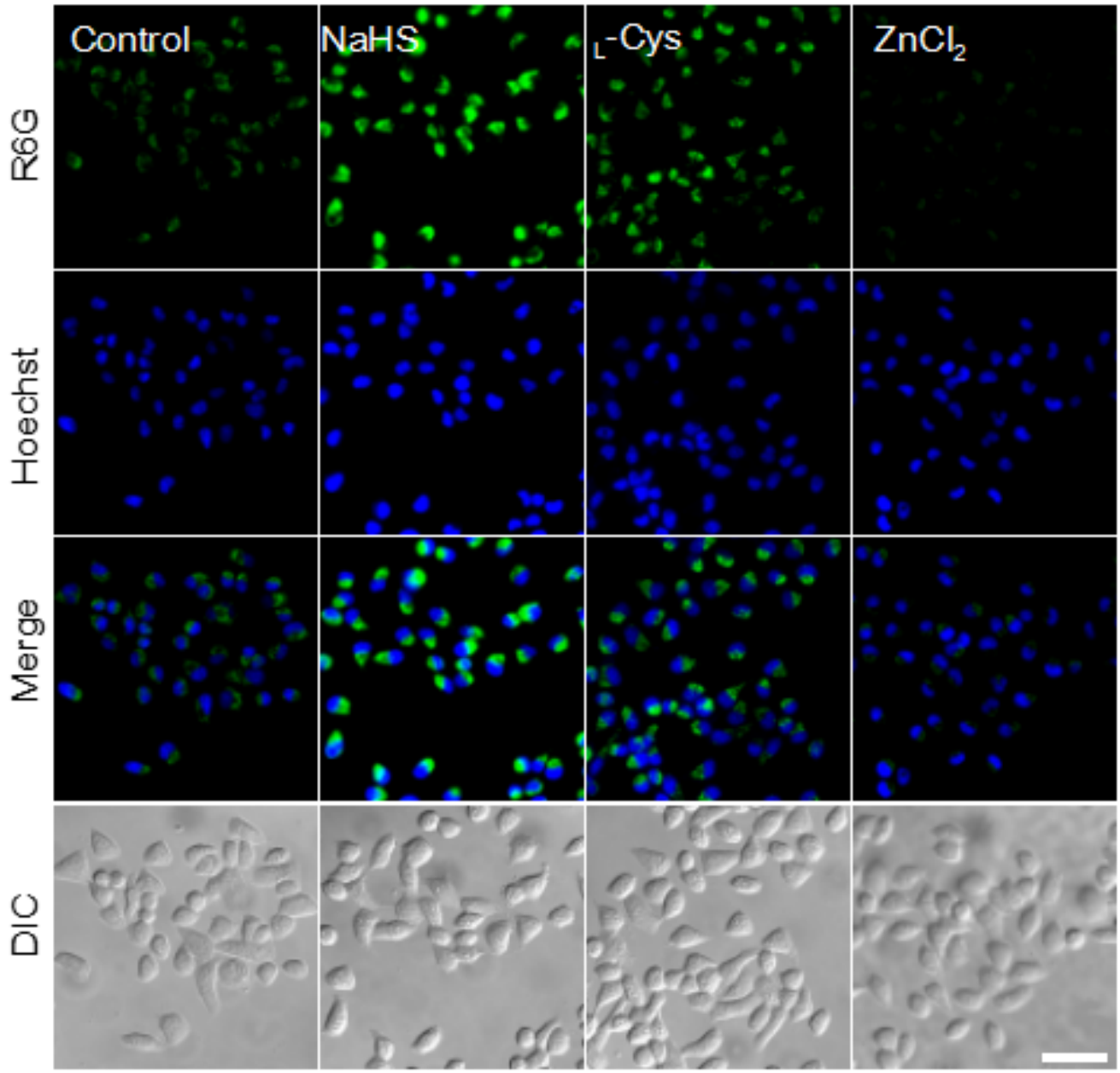

Figure S41. Evaluation of $^1O_2$ production in KB cells. Fluorescence images of DCFH-DA-loaded KB cells following indicated treatments. KB cells were untreated (control), or treated with $\mathbf{1}^{2+}$-PSs-FA (5.5 μg/mL NIR775) for 1 h ($\mathbf{1}^{2+}$-PSs-FA), and then treated with NaHS (1 mM) for another 1 h ($\mathbf{1}^{2+}$-PSs-FA + NaHS). For group $\mathbf{1}^{2+}$-PSs-FA + $_L$-Cys, KB cells were treated with $_L$-Cys (0.2 mM) for 1 h, and then incubated with $\mathbf{1}^{2+}$-PSs-FA (48 μg/mL $\mathbf{1}^{2+}(BF_4^-)_2$) for 1 h. For group $\mathbf{1}^{2+}$-PSs-FA + $ZnCl_2$, KB cells were treated with $ZnCl_2$ (0.3 mM) for 10 min, and then incubated with $\mathbf{1}^{2+}$-PSs-FA (5.5 μg/mL NIR775) for 1 h. After incubation, cells were then incubated with DCFH-DA (20 μM) for 20 min, following by irradiation with an 808 nm laser (1 W/cm^2) for 5 min. The fluorescence images from DCF (psuedo green) and R6G (psuedo red) were acquired with FITC and TRITC filter, respectively. Scale bars: 20 μm.

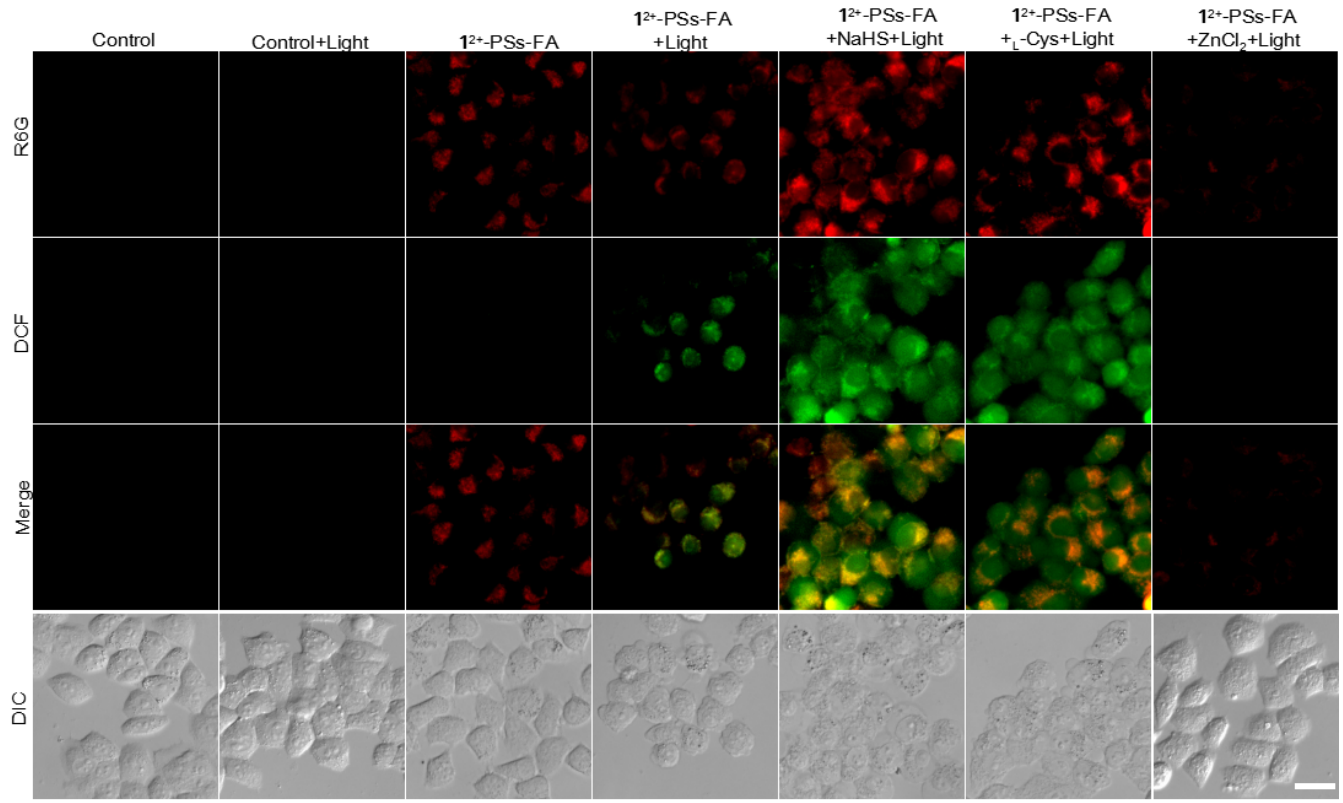

Figure S42. Flow cytometric analysis of KB cell apoptosis using Annexin V-FITC/ propidium iodide (PI) staining. KB cells were untreated (control), or treated with $\mathbf{1}^{2+}$-PSs-FA (5.5 μg/mL NIR775) for 1 h ($\mathbf{1}^{2+}$-PSs-FA), and then treated with NaHS (1 mM) for another 1 h ($\mathbf{1}^{2+}$-PSs-FA + NaHS). For group $\mathbf{1}^{2+}$-PSs-FA + $_{L}$-Cys, KB cells were treated with $_{L}$-Cys (0.2 mM) for 1 h, and then incubated with $\mathbf{1}^{2+}$-PSs-FA (48 μg/mL $\mathbf{1}^{2+}(BF_4^-)_2$) for 1 h. For group $\mathbf{1}^{2+}$-PSs-FA + $ZnCl_2$, KB cells were treated with $ZnCl_2$ (0.3 mM) for 10 min, and then incubated with $\mathbf{1}^{2+}$-PSs-FA (5.5 μg/mL NIR775) for 1 h. After incubation, cells were irradiated with an 808 nm laser (1 W/cm^2) for 5 min. Afterwards, the cells were trypsinized, and the cell pelletes were stained with Annexin V-FITC (5.0 μL) and propidium iodide (PI) (5.0 μL). After staining, the cell population was analyzed by Coulter FC-500 flow cytometer using FITC and PI channel. All experiments were detected using at least 10000 cells, and the data was processed using FlowJo software. The results showed that KB cells treated with $\mathbf{1}^{2+}$-PSs-FA or light irradiation only exhibited little apoptotic and necrotic cell populations. However, treatment of KB cells with $\mathbf{1}^{2+}$-PSs-FA and light irradiation can cause ~80% cell apoptosis and necrosis, which could increase to 94% when NaHS was added.

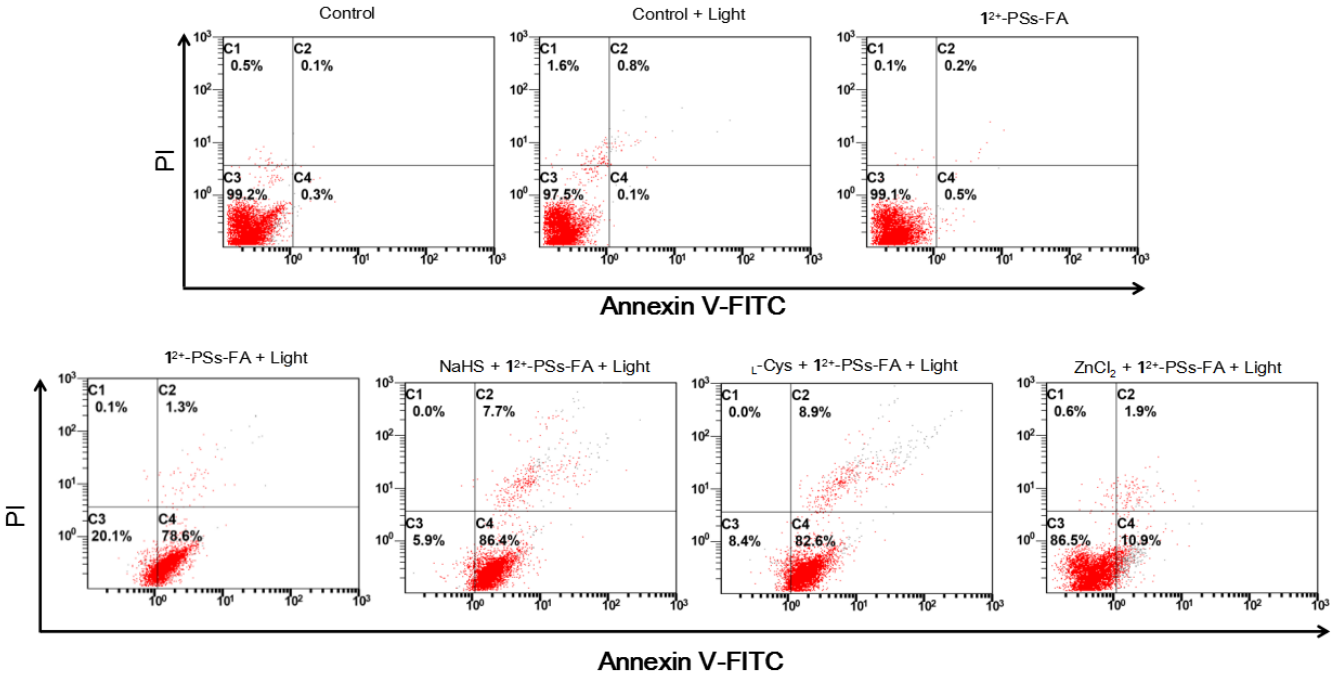

Figure S43. Investigation of lysosomal rupture in KB cells using AO staining. (a) Fluorescence images of KB cells following indicated treatments (with conditions shown in Fig. S38) and co-stained with 5.0 μM AO for 15 min. Then, the cells were irradiated under an 808 nm laser (1 W/cm^2) for 5 min. The fluorescence images of KB cells were acquired on a confocal fluorescence microscopy, with an excitation at 488 nm. The emission from 515-545 nm and 610-640 nm were acquired for green and red, respectively. Scale bar: 20 μm. (b) Fluorescence images of $\mathbf{1}^{2+}$-PSs-FA-loaded KB cells stained with AO. KB cells were incubated with $\mathbf{1}^{2+}$-PSs-FA (5.5 μg/mL NIR775) for 1 h, and then incubated with AO (5.0 μM) for 15 min. Then, half of the cells in the dish were irradiated with 808 nm laser (1 W/cm^2) for 5 min, and the half left were kept under dark. Red arrows showed he cell collapse after treatment with $\mathbf{1}^{2+}$-PSs-FA and light irradiation. The results showed that KB cells treated with $\mathbf{1}^{2+}$-PSs-FA and light irradiation have little red fluorescence from AO, indicating that the lysosomes in these cells were ruptured. Scale bar: 20 μm.

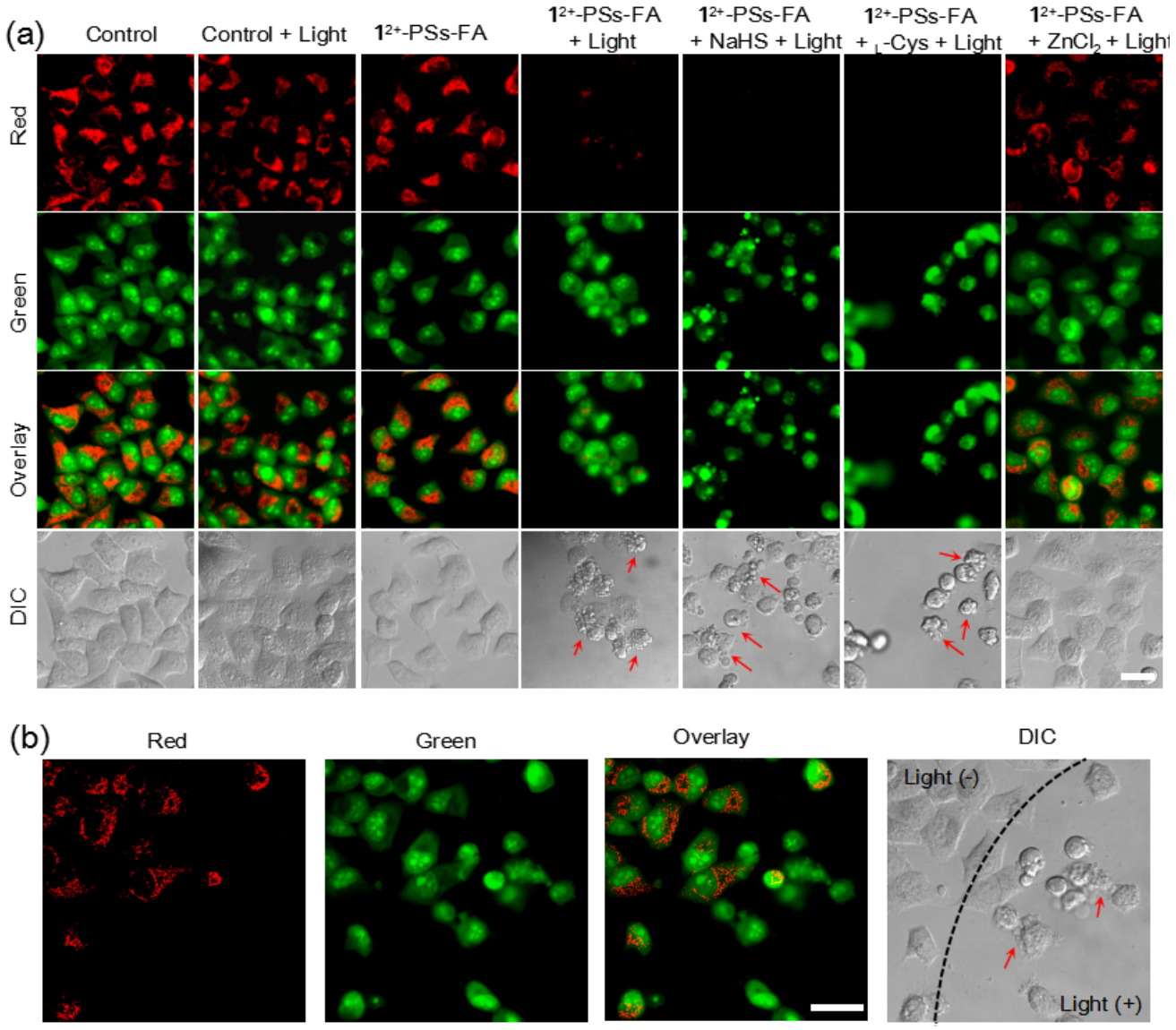

Figure S44. Investigation of KB cell death using AM/PI staining. Fluorescence images of KB cells following indicated treatments (with conditions shown in Fig. S38) and co-stained with calcein AM/PI. Scale bars: 100 μm.

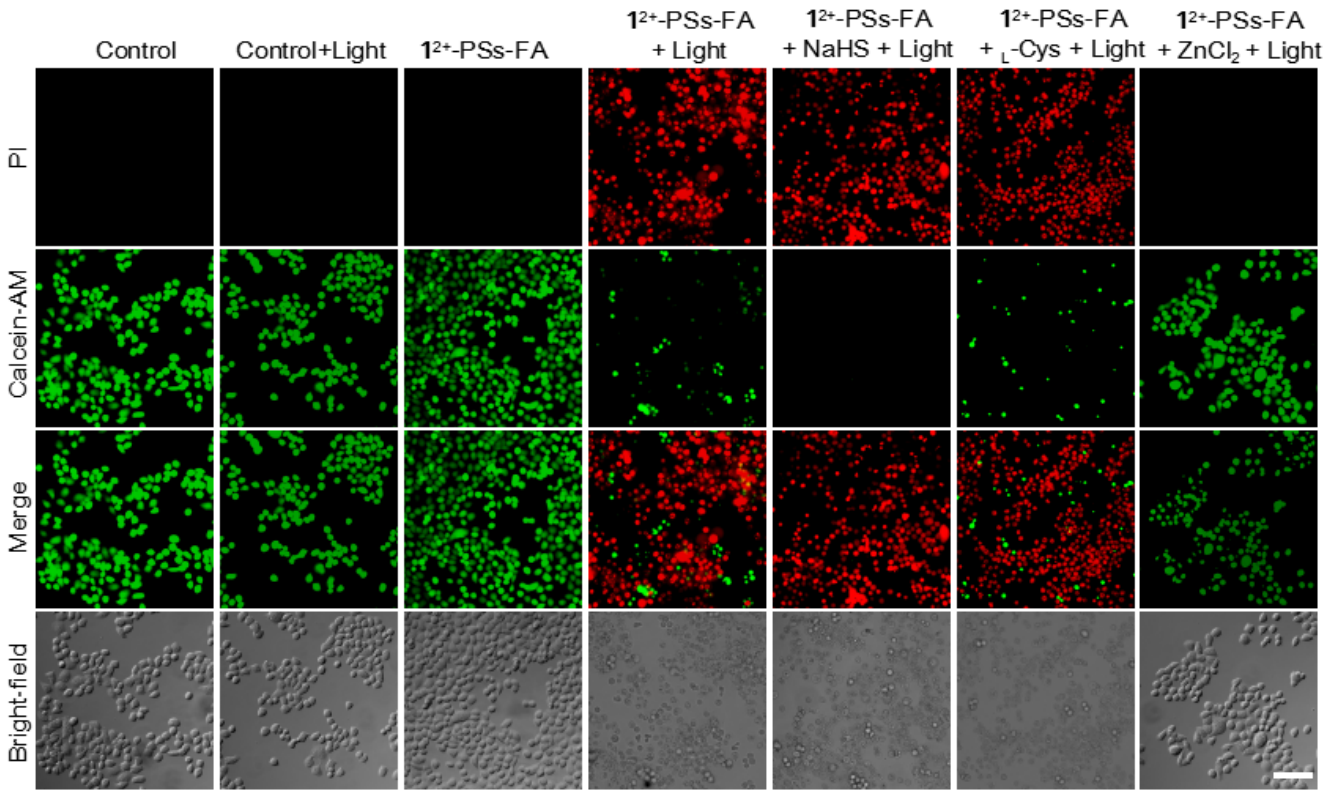

Figure S45. Fluorescence imaging of KB tumor tissue slices dissected from mice 12 h after indicated treatments. KB tumor-bearing mice were i.v. injected with $\mathbf{1}^{2+}$-PSs-FA or $\mathbf{1}^{2+}$-PSs (55 μg/mL NIR775, 200 μL). After 3.5 h, $_{L}$-Cys (1 mM) in 25 μL saline was directly injected into tumors to upregulate endogenous H_2S. After 12 h, the mice were sacrificed, and the tumors were dissected. The tumor tissues were then cut to obtain 10 μm-thickness slices. After staining with DAPI, the tumor tissue slices were imaged with the IX73 inverted fluorescent microscope equipped with DAPI and Cy3 filters. Scale bar: 20 μm.

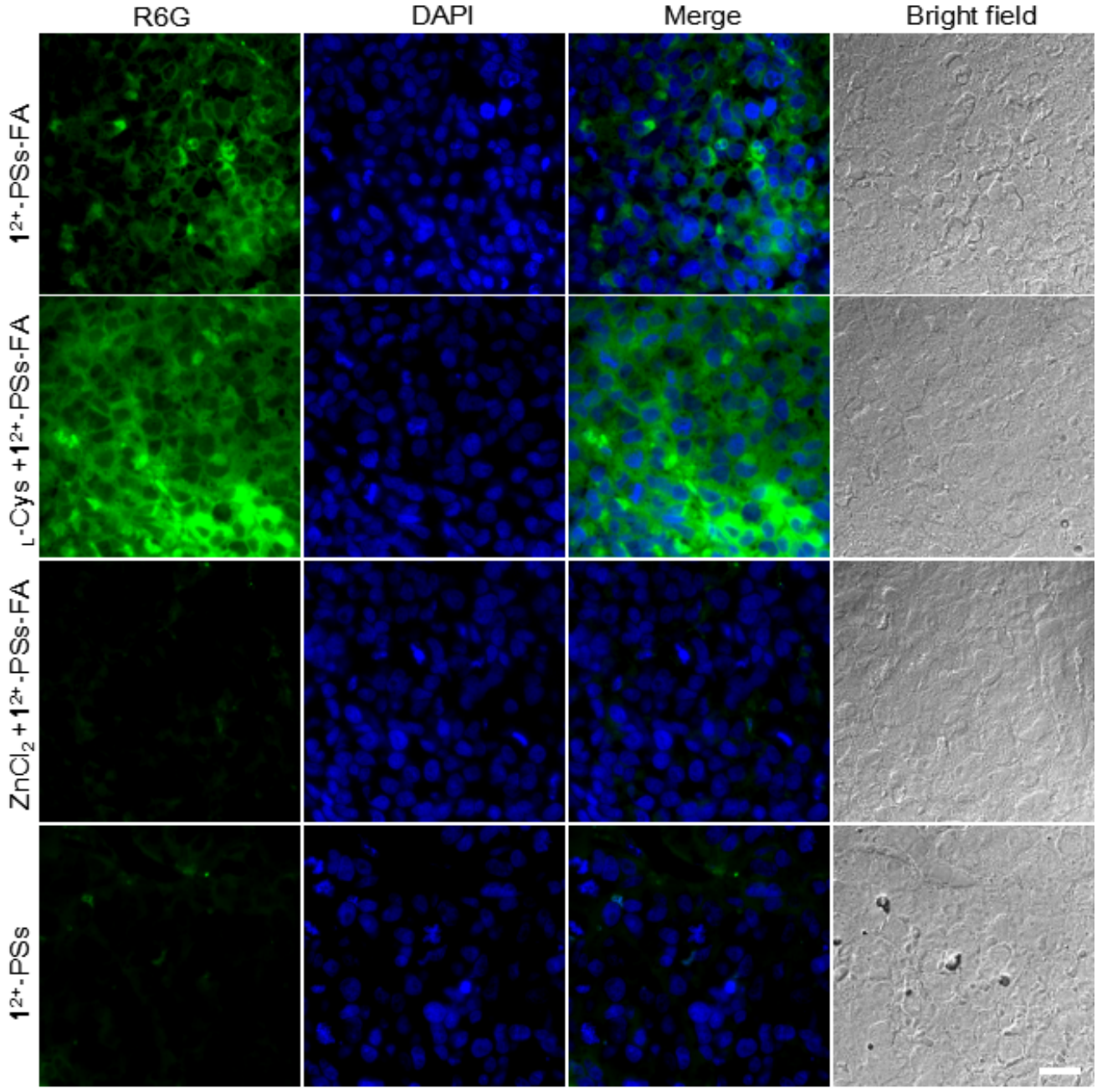

Figure S46. In vivo PDT of HCT116 tumors with $\mathbf{1}^{2+}$-PSs-FA. (a) Longitudinal fluorescence images and (b) average fluorescence intensity of HCT116 tumors in mice following i.v. injection of $\mathbf{1}^{2+}$-PSs-FA and $\mathbf{1}^{2+}$-PSs-FA plus $_{L}$-Cys. Mice were i.v. injected of $\mathbf{1}^{2+}$-PSs-FA (55 μg/mL NIR775, 200 μL). After 3.5 h, $_{L}$-Cys (1 mM) in saline (25 μL) or saline (25 μL) was injected into tumors. Fluorescence images were acquired ($\lambda_{ex}/\lambda_{em}$ = 740/790 nm). Values are mean ± SD (n = 3, * $P < 0.05$). (c) Relative tumor volume and (d) relative body weight of mice after different treatments (saline + light; $\mathbf{1}^{2+}$-PSs-FA + light; $_{L}$-Cys + $\mathbf{1}^{2+}$-PSs-FA + light). $\mathbf{1}^{2+}$-PSs-FA (55 μg/mL NIR775, 200 μL) or saline was i.v. injected into mice. After 12 h, mice were irradiated with the 808 nm laser (1 W/cm^2) for two consecutive exposures of 10 min each, with an interval of 10 min. Values are mean ± SD (n = 4, * $P < 0.05$, *** $P < 0.001$).

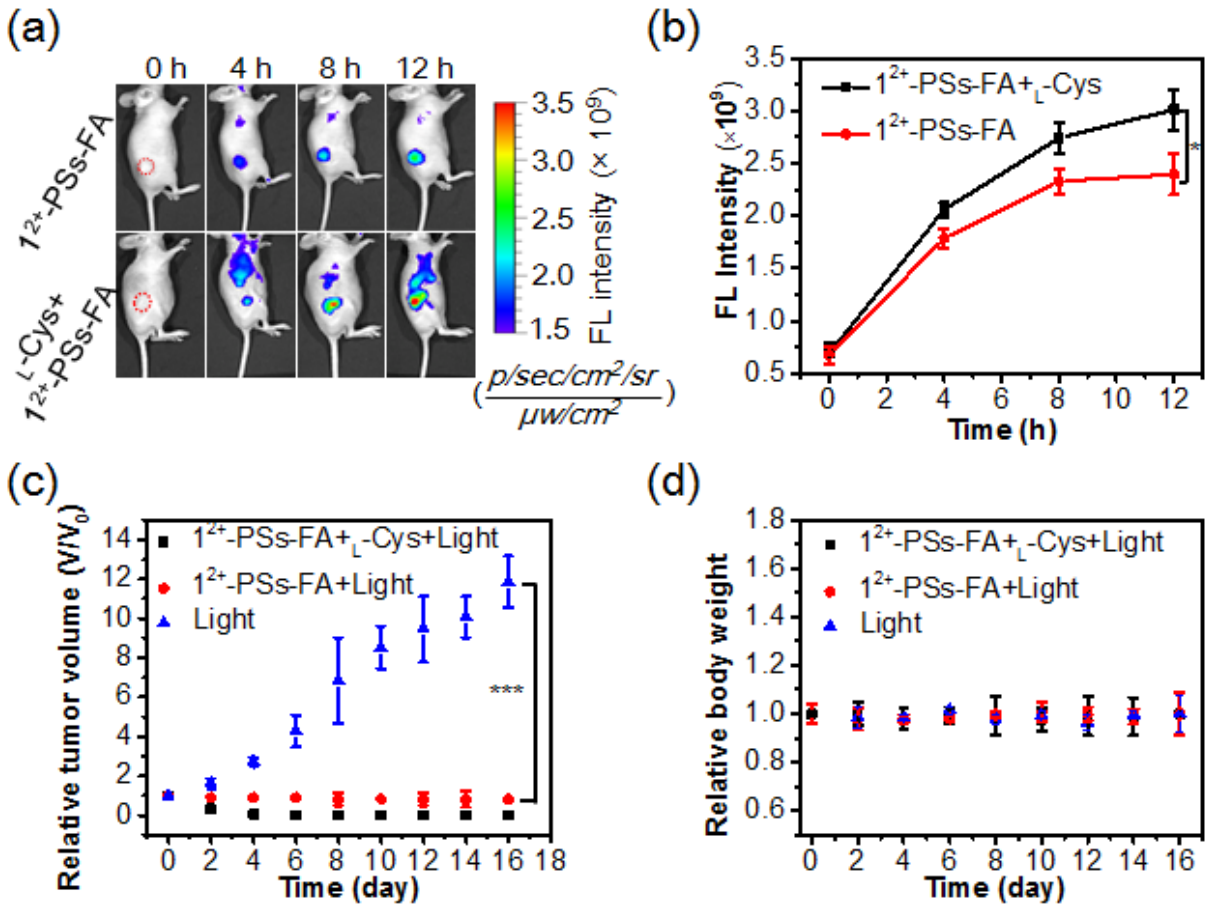

Figure S47. Histological examination of representative organs from mice following i.v. injection with $\mathbf{1}^{2+}$-PSs-FA. $\mathbf{1}^{2+}$-PSs-FA (55 μg/mL NIR775, 200 μL) were i.v. injected into healthy nude mice, and treated with indicated conditions. On day two, the mice were sacrificed. Healthy mice without injection of $\mathbf{1}^{2+}$-PSs-FA were used as control. Major organs including heart, liver, spleen, kidney and lung were excised and stained by H&E. Scale bar: 50 μm.

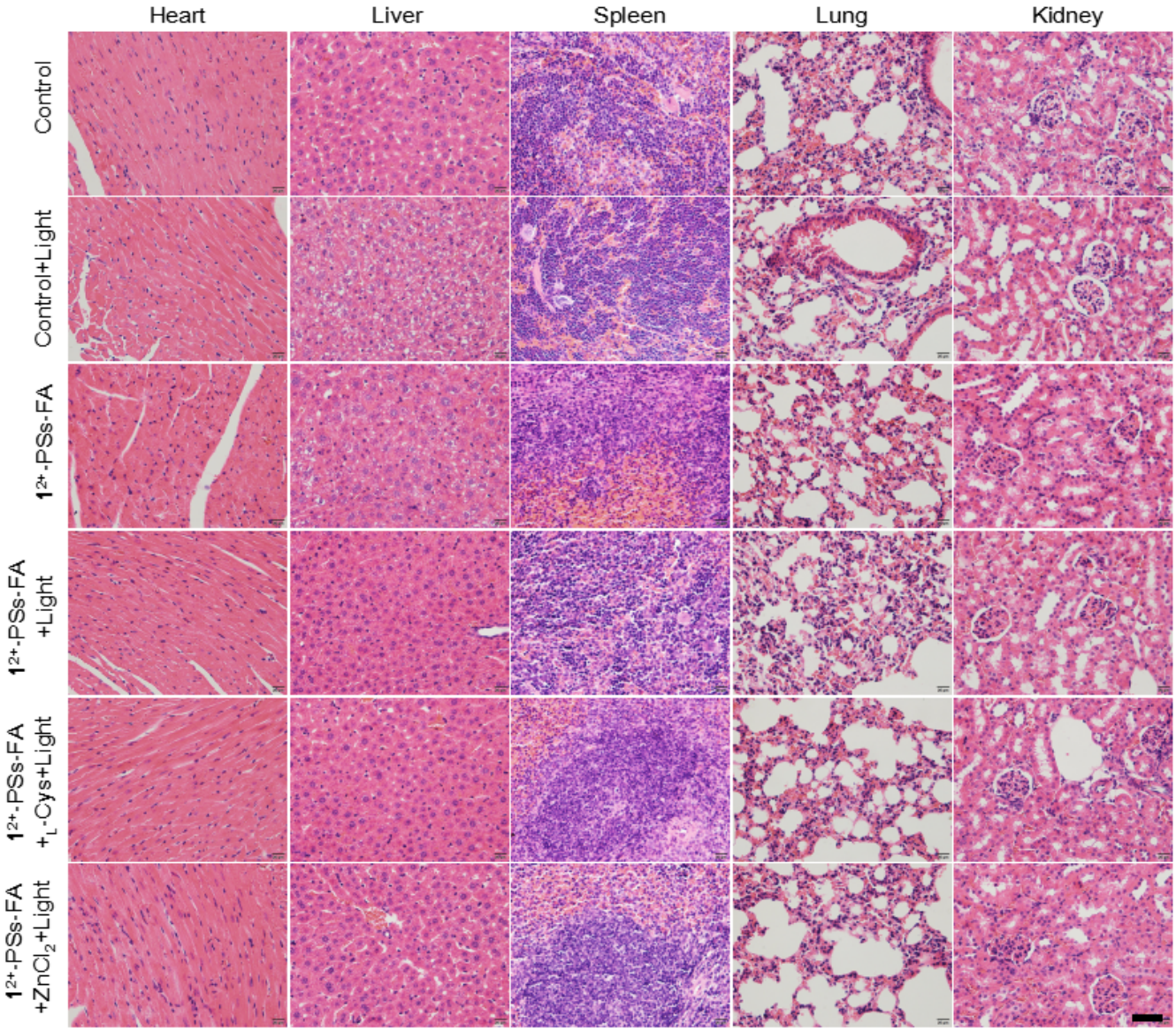

Figure S48. Fluorescence spectra of PBS buffer (green), $\mathbf{1}^{2+}$ (black) or $\mathbf{1}^{2+}$ (48 μg/mL $\mathbf{1}^{2+}(BF_4^-)_2$) following incubation with NaHS (350 μM) (red) for 10 min in PBS buffer. The fluorescence spectra were acquired with excitaion at 680 nm. The results showed both $\mathbf{1}^{2+}$ and **2** ($\mathbf{1}^{2+}$ following reduction with NaHS) were nearly nonfluorescent upon excitation at 680 nm.

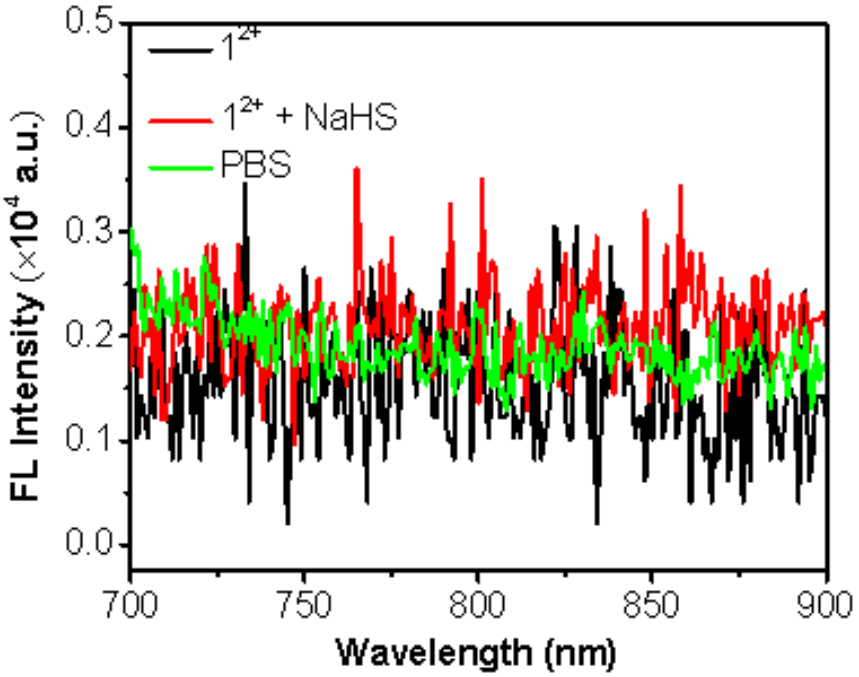

Table S1 Summary of the physicochemical properties of synthesized nanoparticles.

NPs	Size (nm) [a]	PDI [a]	Zeta potential (mV)	LE (%) [b]	LC (%) [c]
$\mathbf{1}^{2+}$-NPs	36.1 ± 1.87	0.214 ± 0.058	-26.81 ± 2.47	~100 [d]	4.14 [h]
$\mathbf{1}^{2+}$-SNP830	51.44 ± 2.32	0.232 ± 0.087	-28.28 ± 1.30	~100 [d]	4.04 [h]
				~100 [e]	2.36 [i]
$\mathbf{1}^{2+}$-SNP580	55.55 ± 3.11	0.215 ± 0.012	-28.57 ± 0.82	~100 [d]	4.04 [h]
				~100 [e	2.36 [i]
$\mathbf{1}^{2+}$-SNP700	45.89 ± 4.08	0.265 ± 0.076	-27.80 ± 1.03	~100 [d]	4.04 [h]
				~100 [e]	2.36 [i]
$\mathbf{1}^{2+}$-SNP830-FA	50.81 ± 2.06	0.251 ± 0.112	-32.06 ± 2.78	~100 [d]	4.04 [h]
				~100 [e]	2.36 [i]
$\mathbf{1}^{2+}$-PSs-FA	51.14 ± 2.71	0.248 ± 0.120	-33.40 ± 0.65	~100 [d]	4.12 [h]
				~100 [f]	0.076 [j]
				~100 [g]	0.48 [k]

[a] Size and polydispersity index (PDI) were determined by DLS analysis. Values are mean ± SD (n = 3) [b] Loading efficiency. [c] Loading capacity. [d] LE of EM**1**. [e] LE of semiconducting polymers. [f] LE of R6G. [h] LE of NIR775. [h] LC of EM**1**. [i] LC of semiconducting polymers. [j] LC of R6G. [k] LC of NIR775.

Table S2 Physicochemical characterization of $\mathbf{1}^{2+}$-SNP830 from eight independent preparations.

Number	Size [a]	PDI [a]	Zeta potential (mv) [a]	LE (%) [b]		Absorption (a.u.) [c]		F/F_0 at 830 nm [d]
				PCPDTBT	1^{2+}	A_0	A	
No.1	51.76 ± 2.29	0.253 ± 0.089	-28.60 ± 0.32	~100	~100	0.955	0.369	15.5
No.2	53.83 ± 0.76	0.232 ± 0.010	-28.59 ± 0.54	~100	~100	0.957	0.362	14.7
No.3	53.68 ± 1.04	0.213 ± 0.013	-29.53 ± 0.61	~100	~100	0.963	0.366	16.1
No.4	51.10 ± 0.17	0.204 ± 0.019	-28.13 ± 1.11	~100	~100	0.974	0.373	13.8
No.5	50.36 ± 1.67	0.243 ± 0.025	-27.09 ± 1.81	~100	~100	0.955	0.359	15.3
No.6	50.90 ± 0.61	0.201 ± 0.016	-28.55 ± 0.72	~100	~100	0.965	0.366	16.8
No.7	50.32 ± 0.98	0.257 ± 0.075	-28.66 ± 0.81	~100	~100	0.959	0.353	16.1
No.8	54.19 ± 0.68	0.229 ± 0.018	-28.26 ± 0.91	~100	~100	0.950	0.354	15.6

[a] Size and polydispersity index (PDI) were determined by DLS analysis. Values are mean ± SD (n = 3). [b] Loading efficiency. [c] A_0 and A indicates the absorbance of $\mathbf{1}^{2+}$-SNP830 (692 nm) before and after incubation with NaHS (350 μM). [d] F/F_0 indicate the fluorescence turn-on ratio of $\mathbf{1}^{2+}$-SNP830 following incubation with NaHS (350 μM).

Table S3 Summary of reported H_2S-activatable fluorescent probes.

Probe [a]	Fluorescence [nm]	Turn-on ratio (fold)	LOD [b]	Reaction Kinetics [c]	Biological System [d]	Detect endogenous H_2S?	Ref
SF2	525	9	5-10 μM	60 min (10 equiv. of H_2S in PBS containing 1 mM CTAB)	Culture cells	no	1
SF7-AM	525	20	500 nM	60 min (10 equiv. H_2S in HEPES)	Culture cells	yes	2
DNS-Az	535	40	1 μM	10 min (1 equiv. H_2S) in PBS containing 0.05% Tween-20	Mouse blood	no	3
Probe **1**	450	1150	0.78 nM	3 min (10 equiv. H_2S in PBS containing 1 mM CTAB)	Culture cells	yes	4
HSN2	542	60	1–5 μM	90 min (100 equiv. H_2S in PIPES)	Culture cells	no	5
CLSS-1	425	128	0.7 ± 0.3 μM	5 min (33 equiv. H_2S in PIPES)	Culture cells	yes	6
Probe **1**	670	65	3.05 μM	10 min (50 equiv. H_2S in PBS containing 50% DMSO)	Culture cells & Mouse (i.p.) [f]	no no	7
SHS-M2	420/545 [e]	3~4	0.4 μM	K_2 = 7.0 M^{-1} s^{-1}	Culture cells Tissue samples	yes	8
Cy–NO_2	789	12.7	N.D. [j]	60 min (35 equiv. H_2S in HEPES)	Culture cells	no	9
CouMC	510/652 [e]	~120	1 μM	30 s (10 equiv. H_2S in PBS containing 2 % DMSO)	Culture cells	no	10
Probe **1**	515	55–70	N.D. [j]	60 min (0.5 equiv. H_2S in PBS containing 10 % CH_3CN)	Culture cells	no	11
WSP4	531	20	266 nM	5 min (5 equiv. H_2S in PBS containing 50 % CH_3CN)	Culture cells	no	12
Probe **7**	765	20	80 nM	N.D. [j]	Culture cells Mouse (i.p.) [f]	no	13
CHC1-UCNPs	541	N.D. [j]	0.13 μM	≈120 s (with 60 μM H_2S in HEPES buffer)	Culture cells Mouse live tissue slices	yes	14
HS–Cy [c]	780/625	2500	5.0–10 nM	35 min (8 equiv. H_2S in HEPES containing 0.5% CH_3CN)	Culture cells	no	15
HSip-1	516	50	N.D. [j]	5 min (10 equiv. H_2S in HEPES)	Culture cells	no	16
MeRho-Az	516	1200	86 ± 7 nM	60 min (50 equiv. H_2S in PIPES containing 100 mM KCl)	Culture cells Zebrafish	yes	17
NanoBODIPY	511/589 [e]	9	7 nM	140 s (20 equiv. H_2S in PBS)	Culture cells	yes	18
Mito-HS	540	21	N.D. [j]	0.034 min^{-1}; 45 min (20 equiv. H_2S in PBS)	Culture cells Mouse tumor (i.t.) [h]	yes	19

NIR-HS	723	50	38 nM	30 min (10 equiv. H_2S in PBS containing 5% CH_3CN)	Culture cells Mouse (i.p.)[f]	yes no	20
NIR-Az	720	~46	<0.26 μM	over 30 min (20 equiv. H_2S in PBS buffer (10 mM, pH 7.4, 30% acetonitrile, v/v))	Culture cells Mouse (i.p.)[f]	no	21
Probe **3**	517	32	0.13 μM	10 min (80 equiv. H_2S in HEPES containing 0.5 % DMSO)	Culture cells	yes	22
Probe **1**	796	87	39.6 nM	14.9 $M^{-1}s^{-1}$: 25 min (60 equiv. H_2S in PBS containing 10% DMSO)	Culture cells & Mouse liver (i.v.)[g] Mouse tumor (i.t.)[h]	yes yes yes	23
MOF NP-1	610 & 660	N.D.[j]	N.D.[j]	1 min (10 equiv. H_2S) in PBS	Culture cells	no	24
RPC-1	445/580	N.D.[j]	192.1 nM	900 s (5 equiv. of H_2S in PBS buffer (pH 7.4, DMF 10% v/v))	Culture cells & Liver tissue slices	yes	25
BSOHS@Si300	717	15	53 nM	180 s (10 equiv. of H_2S in PBS buffer)	Culture cells Mouse tumor (i.t.)[h]	yes	26
NIR-II@Si	900	N.D.	37 nM	5 min (10 equiv of H_2S in PBS)	Culture cells Mouse tumor (i.t.)[h]	yes yes	27
Ru-MDB	612	86	45 nM	50 min (10 equiv. H_2S in PBS)	Culture cells Zebrafish	yes	28
YB	560	N.D.[j]	135.8 nM	20 min (10 equiv. H_2S) in PBS/DMSO solution (1:1 v/v)	no	no	29
Mito-VS	510	7	0.17 μM	30 min (10 equiv. H_2S in PBS)	Culture cells	yes	30
NIR-H_2S	830	58	270 nM	60 min (100 equiv. H_2S in PBS)	Culture cells & Mouse (i.p.)[f]	yes no	31
TPC-N_3	498	N.D.[j]	N.D.[j]	N.D.[j]	liver tissue slices	yes	32
$\mathbf{1}^{2+}$-SNP580	580	~25	0.14 μM				
$\mathbf{1}^{2+}$-SNP700	700	~60	79 nM	k_2 = ~91.6 M^{-1} s^{-1} 10 min (6.25 equiv. H_2S in PBS)	Culture cells Mouse liver (i.v.)[g] Mouse tumor (i.v.)[i]	yes yes yes	This work
$\mathbf{1}^{2+}$-SNP830	830	~15	0.70 μM				
$\mathbf{1}^{2+}$-PSs-FA	555 & 780[k]	~557 (555 nm) ~335 (780 nm)	19 nM; 39 nM				

[a] The name of each probe is the one shown in each ref. [b] LOD: limitation of detection. [c] Second-order reaction rate. If there is no value reported, we just list the time to achieve the maximum activation. We also list the buffer for the reaction. [d] The probe was used to detect H_2S in different biological samples. [e] Ratiometric fluorescent probe. [f] Probe was directly injected into intraperitoneal cavity to detect exogenous H_2S. [g] Probe was i.v. injected into mice to detect endogenous H_2S in liver. [h] Probe was directly injected into xenograft tumors to detect H_2S. [i] Probe was i.v. injected into mice to detect endogenous H_2S in tumors. [j] N.D.: Not Determined. [k] The probe simultaneously emits dual fluorescence at 555 and 780 nm.

Reference:

(1) Lippert, A. R.; New, E. J.; Chang, C. J. *J. Am. Chem. Soc.* **2011**, *133*, 10078-10080.

(2) Lin, V. S.; Lippert, A. R.; Chang, C. J. Proc. *Natl. Acad. Sci*. **2013**, *110*, 7131-7135.
(3) Peng, H.; Cheng, Y.; Dai, C.; King, A. L.; Predmore, B. L.; Lefer, D. J.; Wang, B. *Angew. Chem. Int. Ed*. **2011**, *50*, 9672-9675.
(4) Zhang, J.; Guo, W. *Chem. Commun.* **2014**, *50*, 4214-4217.
(5) Montoya, L. A.; Pluth, M. D. *Chem. Commun*. **2012**, *48*, 4767-4769.
(6) Bailey, T. S.; Pluth, M. D. *J. Am. Chem. Soc*. **2013**, *135*, 16697-16704.
(7) Sun, W.; Fan, J.; Hu, C.; Cao, J.; Zhang, H.; Xiong, X.; Wang, J.; Cui, S.; Sun, S.; Peng, X. *Chem. Commun*. **2013**, *49*, 3890-3892.
(8) Bae, S. K.; Heo, C. H.; Choi, D. J.; Sen, D.; Joe, E.-H.; Cho, B. R.; Kim, H. M. *J. Am. Chem. Soc*. **2013**, *135*, 9915-9923.
(9) Wang, R.; Yu, F.; Chen, L.; Chen, H.; Wang, L.; Zhang, W. *Chem. Commun*. **2012**, *48*, 11757-11759.
(10) Chen, Y.; Zhu, C.; Yang, Z.; Chen, J.; He, Y.; Jiao, Y.; He, W.; Qiu, L.; Cen, J.; Guo, Z. *Angew. Chem. Int. Ed*. **2013**, *125*, 1732-1735.
(11) Liu, C.; Pan, J.; Li, S.; Zhao, Y.; Wu, L. Y.; Berkman, C. E.; Whorton, A. R.; Xian, M. *Angew. Chem. Int. Ed*. **2011**, *123*, 10511-10513.
(12) Peng, B.; Chen, W.; Liu, C.; Rosser, E. W.; Pacheco, A.; Zhao, Y.; Aguilar, H. C.; Xian, M. *Chem. Eur. J*. **2014**, *20*, 1010-1016.
(13) Wu, H.; Krishnakumar, S.; Yu, J.; Yu, J.; Liang, D. Qi, H.; Lee, Z.W.; Deng, L.W.; Huang, D. *Chem. Asian. J.* **2014**, *9*, 3604-3611.
(14) Zhou, Y.; Chen, W.; Zhu, J.; Pei, W.; Wang, C.; Huang, L.; Yao, C.; Yan, Q.; Huang, W.; Loo, J. S. C.; Zhang, Q. *Small* **2014**, *10*, 4874-4885.
(15) Wang, X.; Sun, J.; Zhang, W.; Ma, X.; Lv, J.; Tang, B. *Chem. Sci.* **2013**, *4,* 2551-2556.
(16) Sasakura, K.; Hanaoka, K.; Shibuya, N.; Mikami, Y.; Kimura, Y.; Komatsu, T.; Ueno, T.; Terai, T.; Kimura, H.; Nagano, T. *J. Am. Chem. Soc*. **2011**, *133*, 18003-18005.
(17) Hammers, M. D.; Taormina, M. J.; Cerda, M. M.; Montoya, L. A.; Seidenkranz, D. T.; Parthasarathy, R.; Pluth, M. D. *J. Am. Chem. Soc*. **2015**, *137*, 10216-10223.
(18) Zhao, C.; Zhang, X.; Li, K.; Zhu, S.; Guo, Z.; Zhang, L.; Wang, F.; Fei, Q.; Luo, S.; Shi, P. Tian, H.; Zhu, W. H. *J. Am. Chem. Soc*. **2015**, *137*, 8490-8498.
(19) Wu, Z.; Liang, D.; Tang, X. *Anal. Chem.* **2016**, *88*, 9213-9218.
(20) Zhang, L.; Zheng, X. E.; Zou, F.; Shang, Y.; Meng, W.; Lai, E.; Xu, Z.; Liu, Y.; Zhao, J. *Sci. Rep*. **2016**, *6*, 18868.
(21) Park, C. S.; Ha, T. H.; Choi, S.; Nguyen, D. N.; Noh, S.; Kwon, O. S.; Lee, C.; Yoon, H. *Biosens. Bioelectron.* **2017**, *89*, 919-926.
(22) Reja, S. I.; Sharma, N.; Gupta, M.; Bajaj, P.; Bhalla, V.; Parihar, R. D.; Ohri, P.; Kaur, G.; Kumar, M. *Chem. Eur. J*. **2017**, *23*, 9872-9878.
(23) Zhang, K.; Zhang, J.; Xi, Z.; Li, L.-Y.; Gu, X.; Zhang, Q.-Z.; Yi, L. *Chem. Sci*. **2017**, *8*, 2776-2781.
(24) Ma, Y.; Li, X.; Li, A.; Yang, P.; Zhang, C.; Tang, B. *Angew. Chem. Int. Ed*. **2017**, *129*, 13940-13944.
(25) Jiao, X.; Xiao, Y.; Li, Y.; Liang, M.; Xie, X.; Wang, X.; Tang, B. *Anal. Chem.* **2018**, *90*, 7510-7516.
(26) Wang, F.; Xu, G.; Gu, X.; Wang, Z.; Shi, B.; Lu, C.; Gong, X.; Zhao, C. *Biomaterials* **2018**, *159*, 82-90.
(27) Xu, G.; Yan, Q.; Lv, X.; Zhu, Y.; Xin, K.; Shi, B.; Wang, R.; Chen, J.; Gao, W.; Shi, P. Fan, C. Zhao, C. Tian, H. *Angew. Chem. Int. Ed*. **2018**, *57*, 3626-3630.
(28) Du, Z.; Song, B.; Zhang, W.; Duan, C.; Wang, Y. L.; Liu, C.; Zhang, R.; Yuan, J. *Angew. Chem. Int. Ed*. **2018**, *57,* 3999-4004.
(29) Yu, B.; Chen, C.; Ru, J.; Luo, W.; Liu, W. *Talanta* **2018,** *188*, 370-377.
(30) Li, S.-J.; Li, Y.-F.; Liu, H.-W.; Zhou, D.-Y.; Jiang, W.-L.; Ou-Yang, J.; Li, C.-Y. *Anal. Chem.* **2018**, *90*, 9418−9425.
(31) Xiong, J.; Xia, L.; Huang, Q.; Huang, J.; Gu, Y.; Wang, P., *Talanta* **2018,** *184*, 109-114.
(32) Ren, T.-B.; Xu, W.; Zhang, Q.-L.; Zhang, X.-X.; Wen, S.-Y.; Yi, H.-B.; Yuan, L.; Zhang, X.-B. *Angew. Chem. Int. Ed.* **2018,** *57*, 7473-7477.

Materials and Instrumentation

Materials

All chemicals were purchased from Sigma-Aldrich unless otherwise stated and used without further purification. 1,2-Distearoyl-sn-glycero-3-phosphoethanolamine-N-[folate (polyethylene glycol)-2000] (DSPE-PEG2000-FA) and 1,2-distearoyl-sn-glycero-3-phosphoethanolamine-N-[methoxy (polyethylene glycol)-2000] (DSPE-PEG2000) were obtained from Avanti (Alabaster, AL, USA). (Poly[2-methoxy-5-92-ethylhexyloxy)-1,4-penylene-vinylene] (MEH-PPV) was purchased from Xi,an Polymer Light Technology Corp. Poly{3-(5-(9-hexyl-9-octyl-9H-fluoren-2-yl)thiophen-2-yl)-2,5-bis(2-hexyldecyl)-6-(thiophen-2-yl)pyrrolo[3,4-c]pyrrole-1,4(2H,5H)-dione} (PFDPP) was provided by the Kanyi Pu' group. Singlet oxygen sensor green (SOSG) and acridine orange (AO) were obtained from Invitrogen (Carlsbad, CA, USA). Annexin V-FITC/propidium iodide (PI) cell apoptosis kit and 3-(4,5-dimethylthiazol-2-yl)-2,5-diphenyltetrazolium bromide (MTT) kit were obtained from KeyGen Biotech. Co. Ltd. (Nanjing, China).

Instrumentation

HPLC analysis was performed on Thermo Fisher U3000 HPLC systems. Absorption spectra were recorded an Ocean Optics UV-Visible spectrometer. Fluorescence spectra were carried out on a HORIBA Jobin Yvon Fluoromax-4 fluorescence spectrometer. Fluorescence imaging assays were conducted on an Olympus IX73 fluorescent inverted microscope. Dynamic light scattering (DLS) analysis and Zeta potential analysis were measured using a 90 Plus/ BI-MAS equipment (Brookhaven, USA). TEM images were obtained on a JEM-1011 transmission electron microscope (JEOL, Ltd., Japan) with an accelerating voltage of 100 kV. Atomic force microscope (AFM) images were acquired in tapping mode on a Multimode V AFM with a NanoScope V Controller (Bruker Inc., Germany), and the diameter analysis was performed with NanoScope Analysis 1.5. The phosphorescence of $^1O_2$ at 1270 nm was measured using a FLS 920 time-resolved spectroscope (Edinberge, UK). MTT assay was performed on a microplate reader (Tcan). The fluorescence images in vivo were acquired with the IVIS Lumina XR III imaging system. PDT was conducted with an 808 nm laser (FC-808-10W-MM, Xilong Company, China). ^1H and ^{13}C NMR spectra were recorded on a BRUKER Ascend TM400 (^1H/400 MHz, ^{13}C/100 MHz) spectrometer. IR spectra were obtained on a JEOL JIR-WINSPEC100 FT/IR spectrophotometer. Mass spectra were recorded on a JMS-T100GCV spectrometer. Column chromatography was performed on a silica gel I-6-40 (YMC) with a particle size of 40-63 μm. Melting points were measured on a Yamato MELTING POINT APPARATUS MODEL MP-21 and uncorrected.

Synthesis of Electrochromic Dye, $\mathbf{1^{2+}(BF_4)_2}$

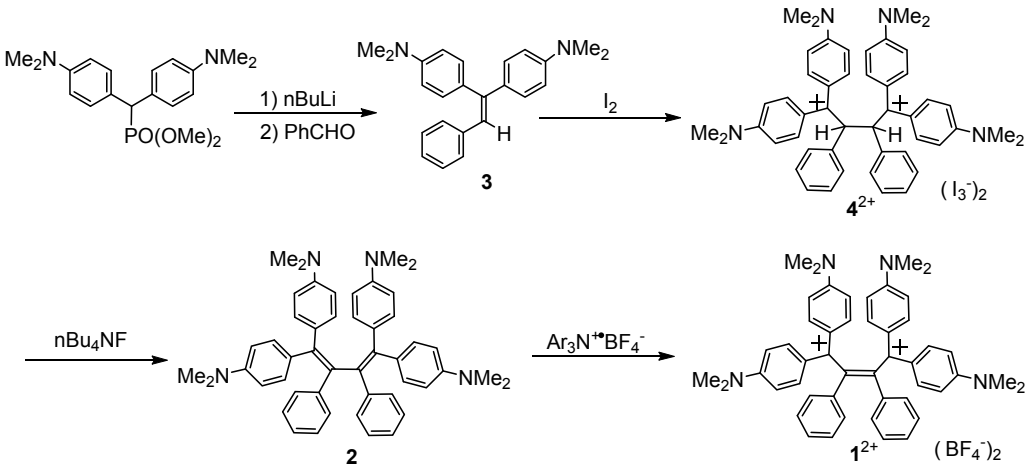

Scheme S1. Synthesis of $\mathbf{1}^{2+}(BF_4)_2$.

*Preparation of alkene **3***

To a solution of dimethyl bis(4-dimethylaminophenyl)methylphosphonate (4.33 g, 12.0 mmol) in dry THF (200 mL) was added dropwise nBuLi (1.56 M in hexane, 7.66 mL, 12.0 mmol) at –78 °C under Ar, and the mixture was sitrred at –78 °C for another 2 h. Then, benzaldehyde (1.23 mL, 12.0 mmol) was added to the reaction solution dropwise. The resulting mixture was allowed to warm to room temperature (r.t.) and then kept stirring overnight. Water (1 mL) was then added to quench the reaction, and the solvent was removed under vaccum. The residue was then suspended in water and extracted with $CHCl_3$. The organic layer was washed with brine, dried over Na_2SO_4 and the solvent was removed under vaccum. Alkene **3** (3.88 g) was obtained as yellow plates by recrystallization from hexane in 95% yield: m.p. 122-123 °C; ^{1}H NMR (400 MHz, $CDCl_3$) δ/ppm 7.26-7.23 (2H, m), 7.22-7.04 (7H, m), 6.74 (1H, s), 6.69-6.65 (4H, m), 2.98 (6H, s), 2.96 (6H, s); ^{13}C NMR (100 MHz, $CDCl_3$) δ/ppm 150.08, 149.72, 142.84, 138.77, 132.54, 131.46, 129.36, 128.79, 128.59, 127.90, 125.72, 123.93, 112.32, 112.04, 40.59, 40.55; MS (FD) m/z 342 (M^+). HRMS(FD) Calcd. For $C_{24}H_{26}N_2$: 342.2096. found: 342.2095.

Preparation of dication salt $\mathbf{4}^{2+}(I_3^-)_2$

To a solusion of alkene **3** (1.00 g , 2.92 mmol) in dry CH_2Cl_2 (100 mL) was added iodine (1.11 g, 4.29 mmmol) under Ar, and the mixture was stirred at r.t. overnight. Dry ether (50 mL) was then added into the reaction solution, and the resulting precipitates were filtered to give dicationic salt $\mathbf{4}^{2+}(I_3^-)_2$ (2.06 g) as a brown powder. in 97% yield: m.p. 189-198 °C (decomp.); ^{1}H-NMR (400 MHz, CD_3CN) δ/ppm 7.48-7.42 (4H, m), 7.34-7.29 (10H, m), 7.15-7.11 (4H, m), 6.83-6.81 (4H, m), 6.70-6.68 (4H, m), 6.04 (2H, s), 3.37 (12H, br. s), 3.17 (12H, br. s); ^{13}C NMR could not be measured due to low solubility of $\mathbf{4}^{2+}(I_3^-)_2$; IR (KBr) 1614, 1582, 1404, 1376, 1164 cm^{-1}; MS (FD) m/z 341 (M^{2+}); Anal. Calcd for $C_{48}H_{52}N_4I_6$: C, 39.86; H, 3.62; N, 3.87. Found: C, 39.62; H, 3.58; N, 3.82. ORTEP drawing obtained by X-ray analysis is provided (CCDC/164961).

*Preparation of diene **2***

To a solution of dication salt $\mathbf{4}^{2+}(I_3^-)_2$ (50 mg, 34.6 μmol) in dry MeCN (5 mL) was added drpowise nBu_4NF (1 M in THF, 350 μL, 350 μmol) at r.t. under Ar, and the mixture was kept stirring overnight. Water (1 mL) was then added to quench the reaction, and the solvent was removed under vaccum. The residue was suspended in 5%

$Na_2S_2O_3$ aq and extracted with benezene. The organic layer was washed with brine and dried over Na_2SO_4. Chromatographic separation on Al_2O_3 (benzene/hexane = 1/1) gave diene **2** (18 mg) as an intense yellow solid in 75% yield: m.p. 235-240 °C (decomp.); ^{1}H-NMR (400 MHz, $CDCl_3$) δ/ppm 7.22-7.20 (4H, m), 6.92-6.80 (14H, m), 6.44-6.40 (8H, m), 2.86 (12H, br. s), 2.84 (12H, br. s); ^{13}C NMR (100 MHz, $CDCl_3$) δ/ppm 149.06, 148.73, 143.30, 142.86, 138.11, 133.92, 133.02, 132.64, 131.51, 131.09, 126.96, 124.76, 111.38, 111.23, 40.72, 40.46; IR (KBr) 1603, 1518, 1442, 1352, 1190, 1164, 814 cm^{-1}; MS (FD) m/z 682 (M^+). Anal. Calcd for $C_{48}H_{50}N_4$: C, 84.42; H, 7.38; N, 8.20%. Found: C, 84.16; H, 7.60; N, 8.11%.

Preparation of butadiene dication salt $\mathbf{1}^{2+}(BF_4^-)_2$

To a solution of diene **2** (101 mg, 49 μmol) in dry CH_2Cl_2 (1.5 mL) was added $(4\text{-}BrC_6H_4)_3N^{\cdot+}BF_4^-$ (168 mg, 296 μmol) under Ar, and the mixture was stirred at r.t. for 1.5 h. Dry ether (20 mL) was added, and the precipitates were filtered to give dication salt $\mathbf{1}^{2+}(BF_4^-)_2$ (116 mg) as a dark violet powder in 92% yield: mp > 250 °C. ^{1}H-NMR (400 MHz, CD_3CN) δ/ppm 7.40-7.38 (8H, m), 7.26-7.22 (10H, m), 6.76-6.74 (8H, m), 3.19 (24H, s) (Chart-7); ^{13}C NMR (100 MHz, $CDCl_3$) δ/ppm 174.27, 156.05, 153.69, 143.14, 140.47, 131.35, 129.32, 128.75, 128.59, 113.54, 40.73 (Chart-8); IR (KBr) 1613, 1582, 1483, 1368, 1170, 1051, 943 cm^{-1}. MS (FD) m/z 341 (M^{2+}). Anal. Calcd (%) for $C_{48}H_{50}B_2F_8N_4 \cdot 1/2H_2O \cdot 1/2CH_2Cl_2$: C 64.15, H 5.77, N 6.17 %; found: C 64.40, H 5.63, N 6.19 %.

Preparation of $\mathbf{1}^{2+}$-NPs, $\mathbf{1}^{2+}$-SNP830-FA and $\mathbf{1}^{2+}$-PSs-FA

All the micellar nanoparticles were prepared using amphiphilic polymers-assisted nanoprecipitation method. Typically, to prepare $\mathbf{1}^{2+}$-NPs, $\mathbf{1}^{2+}(BF_4^-)_2$ (0.43 mg) and DSPE-PEG2000 (10 mg) were dissolved in THF (1 mL) to prepare a clear solution. To prepare $\mathbf{1}^{2+}$-SNP830-FA, $\mathbf{1}^{2+}(BF_4^-)_2$ (0.43 mg), PCPDTBT (0.25 mg), DSPE-PEG2000 (9.9 mg) and DSPE-PEG2000-FA (0.1 mg) were dissolved in THF (1 mL) to prepare a clear solution. To prepare $\mathbf{1}^{2+}$-PSs-FA, $\mathbf{1}^{2+}(BF_4^-)_2$ (0.43 mg), R6G (8.6 μg), NIR775 (50 μg), DSPE-PEG2000 (9.9 mg) and DSPE-PEG2000-FA (0.1 mg) were dissolved in THF (1 mL) to prepare a clear solution. These solutions were rapidly injected into D.I. water (9 mL) under continuous sonication. After addition, the mixture was kept sonication for 10 min. Then, THF was removed with N_2 bubbling at 65 °C. The resulting deep color aqueous solution was washed with D.I. water for three times, using a 10 K centrifugal filter (Millipore) under centrifugation at 3,500 r.p.m. for 15 min. After concentration, the stock solution of each nanoprobe was obtained, and stored at 4 °C under dark. The amount of $\mathbf{1}^{2+}(BF_4^-)_2$ and PCPDTBT (or R6G and NIR775) were determined by indirectly measuring the UV-Vis absorption spectra of filtrate, showing that nearly all $\mathbf{1}^{2+}(BF_4^-)_2$ and semiconducting polymers (or NIR775, R6G) were encapsulated into nanoparticles. The loading efficiency (LE%) and loading capacity (LC%) were then calculated using the following equations:

LE(%) = (Weight of EM $\mathbf{1}^{2+}$ loaded / Weight of EM $\mathbf{1}^{2+}$ added) × 100%

LC(%) = (Weight of EM $\mathbf{1}^{2+}$ loaded / Weight of nanoparticles) × 100%

Invesitigation of the Reaction of $\mathbf{1}^{2+}(BF_4^-)_2$ or $\mathbf{1}^{2+}$-NPs with Different Reducing Agents

To investigate the reaction of $\mathbf{1}^{2+}(BF_4^-)_2$ and reductants, $\mathbf{1}^{2+}(BF_4^-)_2$ was dissolved in DMSO to prepare the stock solution, which was then diluted in PBS buffer (pH 7.4) to prepare different concentration of $\mathbf{1}^{2+}(BF_4^-)_2$ for the measurement. Briefly,8 μg $\mathbf{1}^{2+}(BF_4^-)_2$ were incubated with indicated biological reductants (e.g., Cys, Hcy, VC, 1

mM; GSH, DTT, 5 mM; NaHS, 100 μM) in 1.0 mL PBS buffer (pH 7.4) at 37 ºC overnight. The reactions were then analyzed by HPLC, and resulting UV-Vis absorption spectra were recorded with an Ocean Optics spectrometer.

To investigate the reaction of $\mathbf{1}^{2+}$-NPs and reductants, $\mathbf{1}^{2+}$-NPs were dissolved in D.I. H_2O to prepare the stock solution, which was then diluted in PBS buffer (pH 7.4) to prepare different concentration of $\mathbf{1}^{2+}$-NPs for the measurement. Typically, $\mathbf{1}^{2+}$-NPs (1.6 μg $\mathbf{1}^{2+}(BF_4^-)_2$) in 200 μL PBS buffer (pH 7.4) were put in a black 96-well plate, to which different reductants (e.g., Cys, Hcy, VC, 1 mM; GSH, DTT, 5 mM; NaHS, 300 μM) were added. The intensities of absorption at 555 nm for $\mathbf{1}^{2+}$-NPs were recorded every 20 s in a Spark^{TM} 10_M Multimode Microplate Reader, and last for 10 min.

General Procedure for the Fluorescence Measurement

To measure the fluorescence of $\mathbf{1}^{2+}$-SNPs in response to H_2S, the stock solution of $\mathbf{1}^{2+}$-SNPs was diluted in PBS buffer (pH 7.4) to prepare different concentration of $\mathbf{1}^{2+}$-SNPs. Typically, various solutions of $\mathbf{1}^{2+}$-SNPs (28 μg semiconducting polymers, 48 μg $\mathbf{1}^{2+}(BF_4^-)_2$) in 1.0 mL PBS buffer (pH 7.4) were incubated with varying concentrations of NaHS at r.t. for different time, and the fluorescence spectra in the reaction solutions were recorded on a HORIBA Jobin Yvon Fluoromax-4 fluorometer, with excitation at 460 nm for SPN580, 580 nm for SPN700, 650 nm for SPN830, respectively. To measure the fluorescence of $\mathbf{1}^{2+}$-PSs-FA in response to H_2S, the fluorescence spectra from 505 to 905 nm with excitation from 500 to 900 nm were recorded by fluorescence synchronous scanning, with offset of 5 nm.

To test the sensitivity of $\mathbf{1}^{2+}$-SNPs for H_2S, varying concentrations of NaHS (0-500 μM) were added into the solutions of $\mathbf{1}^{2+}$-SNPs (28 μg semiconducting polymers, 48 μg $\mathbf{1}^{2+}(BF_4^-)_2$) in PBS buffer (pH 7.4), and incubated at 37 ^oC for 10 min. The resulting fluorescence spectra were acquired a HORIBA Jobin Yvon Fluoromax-4 fluorometer, with excitation at 460 nm for SPN580, 580 nm for SPN700, 650 nm for SPN830, respectively. The fluorescence enhancement (F/F_0) at 580 nm for $\mathbf{1}^{2+}$-SNP580, 700 nm for $\mathbf{1}^{2+}$-SNP700, and 830 nm for $\mathbf{1}^{2+}$-SNP830 was obtained, and plot with the concentration of NaHS. The detection limit were determined by [blank + 3σ] method. The detection limit of each probe was calculated to be the concentration at which the resulting fluorescence intensity equals that of [blank + 3σ] according to a linear regression fit of each plot, where σ is the standard deviation of probe blank's signal.

To measure the selectivity of $\mathbf{1}^{2+}$-SNP830 toward H_2S, $\mathbf{1}^{2+}$-SNP830 (28 μg PCPTBT, 48 μg $\mathbf{1}^{2+}(BF_4^-)_2$) were added with different biologically relevant reductant (1: 350 μM NaHS; 2: 1.25 mM $_L$-Cys; 3: 10 mM GSH; 4: 1 mM Hcy; 5: 1.25 mM VC; 6: 1.25 mM DTT; 7: 10 μg/mL BSA) or ROS (8: 1 mM H_2O_2; 9: 1 mM ClO^-; 10: $O_2^{\cdot-}$ (100 μM xanthine + 22 mU XO); 11: $^1O_2$ (1 mM H_2O_2 + 1 mM ClO^-); 12: $ONOO^-$ (1 mM $NaNO_2$ +1 mM H_2O_2); 13: 300 μM ^{t}-BuOOH; 14: 300 μM CuOOH.) 15: NADPH (100 μM); 16: Fe^{2+} (100 μM); 17: Cu^+ (100 μM); 18: NO (Diethylamine NONOate, 100 μM); 19: CO (CORM-3, 100 μM). The solutions were kept at 37 ºC for 10 min, and the fluorescence spectra of the solutions were acquired with excitation at 650 nm.

To investigate the effect of pH, $\mathbf{1}^{2+}$-SNP830 (28 μg PCPTBT, 48 μg $\mathbf{1}^{2+}(BF_4^-)_2$) in PBS buffer with different pH values (4.0, 5.0, 6.0, 6.8, 7.4, 8.0 and 9.0) were incubated with 350 μM NaHS at r.t. for 10 min. The fluorescence spectra of the solutions were measured acquired with excitation at 650 nm.

General Procedure for the Measurement of Reaction Kinetics

To evaluate the reaction kinetics between EM $\mathbf{1}^{2+}$ and H_2S, $\mathbf{1}^{2+}(BF_4^-)_2$ (8 μg/mL) in 200 μL PBS buffer (pH 7.4) were put in a black 96-well plate. NaHS (0, 1, 5, 10, 20, 30, 40, 50, 70 and 100 μM) was then added into the wells, and the reactions were conducted at r.t.. The absorption intensities of $\mathbf{1}^{2+}$ at 546 nm were recorded every 20 s in a Spark^{TM} 10_M Multimode Microplate Reader, and last for 10 min. The pseudo-first-order rate (k_{obs}) was determined by fitting the absorption intensities at 546 nm with single exponential function:

$$y = y_0 + A \times \exp(R_0 \times t)$$

where $k_{obs} = -R_0$.

Plot of the calculated k_{obs} versus H_2S concentrations (40-100 μM), and the secondary reaction rate k_2 value was obtained from the slope of the plot.

To evaluate the apparant reaction kinetics between $\mathbf{1}^{2+}$-NPs and H_2S, $\mathbf{1}^{2+}$-NPs containing 8 μg/mL $\mathbf{1}^{2+}(BF_4^-)_2$ in 200 μL PBS buffer (pH 7.4) were put in a black 96-well plate. NaHS (0, 10, 20, 30, 60, 150, 200 and 300 μM) was then added into the wells, and the reactions were conducted at r.t.. The absorption intensities of $\mathbf{1}^{2+}$-NPs at 555 nm were recorded every 20 s, and last for 10 min. The secondary reaction rate k_2 value was obtained using the similar methods for EM $\mathbf{1}^{2+}$.

To evaluate the apparant reaction kinetics between $\mathbf{1}^{2+}$-SNP830 and H_2S, $\mathbf{1}^{2+}$-SNP830 (4.5 μg/mL PCPDTBT, 8 μg/mL $\mathbf{1}^{2+}(BF_4^-)_2$) in 200 μL PBS buffer (pH 7.4) were put in a black 96-well plate, to which different concentration of NaHS (0, 10, 30, 50, 100, 150, 200 and 400 μM) was added. The fluorescence intensities at 830 nm in each well (λ_{ex} = 650 nm) were recorded every 10 s, and last for 10 min. The pseudo-first-order rate (k_{obs}) was determined by fitting the fluorescence intensities with single exponential function, and the secondary reaction rate k_2 value was obtained from the linear plot of the k_{obs} versus H_2S concentration.

Measurement of H_2S Concentration in Human Plasma

The concentration of H_2S in human plasma was measured using exogenous NaHS as internal standard. Brieftly, human plasma (200 μL) was added with 1 μL $ZnCl_2$ (200 mM) to scavenge endogenous H_2S (0 μM H_2S^-), 1 μL D.I. H_2O (x μM HS^-), or 1 μL of varying concentrations of NaHS (1 mM: x + 5 μM HS^-, 2 mM: x + 10 μM HS^-, 4 mM: x + 20 μM HS^-, 6 mM: x + 30 μM HS^-, 8 mM: x + 40 μM HS^-, 10 mM: x + 50 μM HS^-). 1^{2+}-SNP830 (final concentration 28 μg/mL PCPDTBT, 48 μg/mL $\mathbf{1}^{2+}(BF_4^-)_2$) was added to above HS^- After incubation at 37 ºC for 10 min, the fluorescence spectra in each solution was collected with excitation at 650 nm. The fluorescence intensity at 830 nm in each solution was obtained, and linearly plot against the concentration of added NaHS (5, 10, 20, 30, 40, 50 μM). The slope was then obtained from the linear plot, which could be used to calculate the concentration of H_2S (x μM HS^-) in plasma with the measured fluorescence intensity in the solution.

General Procedure for the Measurement of $^1O_2$ Generation Capacity *in vitro*

The $^1O_2$ production capacity of $\mathbf{1}^{2+}$-PSs-FA *in vitro* was evaluated using two independent methods. First, singlet oxygen sensor green (SOSG, 20 μM) was used as the fluorescent $^1O_2$ indicator. Typically, $\mathbf{1}^{2+}$-PSs-FA (48/0.96/5.5 μg/mL $\mathbf{1}^{2+}(BF_4^-)_2$/R6G/NIR775) was incubated with or without NaHS (350 μM) in PBS buffer (pH 7.4) at r.t. for 10 min. Then, SOSG (20 μM) was added, and the solutions were irradiated with an 808 nm laser (1 W/cm^2) for 0, 10, 20, 30, 40, 50, 60 s. The fluorescence spectra of SOSG were acquired with excitation at 488 nm. The $^1O_2$

generation efficiency was evaluated by comparing the fluorescence intensity of SOSG at 528 nm. Second, we directly measured the $^1O_2$ emission at 1270 nm to identify the $^1O_2$ generation. Briefly, a solution of **1**$^{2+}$-PSs-FA(48/0.96/5.5 μg/mL **1**$^{2+}$(BF_4^-)$_2$/R6G/NIR775), **1**$^{2+}$-PSs-FA with NaHS (350 μM), or **1**$^{2+}$-PSs-FA in the presence of NaHS (350 μM) and NaN_3 (30 mM) in D_2O was irradiated with a 530-nm excitation laser, and the phosphorescence of $^1O_2$ in each solution was immediately acquired with a FLS 920 time-resolved spectroscope equipped with a NIR detector. The $^1O_2$ generation capacity was evaluated by comparing the phosphorescence intensity of $^1O_2$ at 1270 nm.

Cell Culture

RAW264.7 macrophages and human embryonic kidney HEK293 cells were cultured in DMEM (Dulbecco's Modified Eagle Medium) medium. Human carcinoma KB cells were cultured in Roswell Park Memorial Institute 1640 medium (RPMI-1640). Human colon HCT116 and HT29 cancer cells were grown in McCoy's 5a medium. All the mediums were supplemented with 10% (v/v) fetal bovine serum (FBS), 100 units per mL penicillin, and 100 units per mL streptomycin. All cells were cultured at 37 °C in a humidified atmosphere (5% CO_2).

Fluorescence Imaging of H_2S in RAW264.7 Cells

RAW264.7 cells (~ 5×10^4) were seeded onto glass-bottom dish (In Vitro Scientific, D35-20-1-N), and grew overnight. Cells were then incubated with **1**$^{2+}$-SNP830 (28/48 μg/mL PCPDTBT/**1**$^{2+}$(BF_4^-)$_2$) at 37 °C for 3 h. Then, the medium was removed, and washed with cold PBS buffer once, following by incubation with or without NaHS (1 mM) for another 1 h. The medium was removed, washed with PBS buffer for three times. Alternately, to elevate the endogenous H_2S production, untreated RAW264.7 cells were incubated with varying concentration of $_L$-Cys (0, 0.1, 0.2 and 0.5 mM) for different time (0, 0.5, 1 and 2 h); to scavenge the endogenous H_2S, cells were incubated with $ZnCl_2$ (0.3 mM) for 10 min; to inhibit the CSE activity and reduce H_2S production, cells were incubated with PAG (50 mg/L) for 0.5 h, and then incubated with $_L$-Cys (0.2 mM) for 1 h; to upregulate the CSE expression and enlarge H_2S production, cells were incubated with LPS (1.0 μg/mL) for 6 h, and then treated with $_L$-Cys (0.2 mM) for 1 h; to inhibit the CSE activity in LPS-stimulated cells, cells were treated with LPS (1.0 μg/mL) for 6 h, and then incubated with PAG (50 mg/L) for 0.5 h, followed by $_L$-Cys (0.2 mM) for 1 h. After treatment, cells were incubated with **1**$^{2+}$-SNP830 (28/48 μg/mL PCPDTBT/**1**$^{2+}$(BF_4^-)$_2$) for 3 h. Then, the medium was removed, washed with cold PBS for three times. After adding fresh medium, the fluorescence images with ~10-25 cells in view were acquired on an Olympus IX73 fluorescent inverted microscope, with the excitation filter at 630−670 nm, and the emission filter above 690 nm. Each experiment was repeated for three times. The cell images were then analyzed using the ImageJ software (NIH). The region-of-interest (ROI) measurement was applied to the fluorescence regions in each cell to quantify the average fluorescence intensity, and repeated in another two cell images acquired from the other two repeated experiments. The mean fluorescence intensities and standard deviations were calculated for the comparison of different H_2S concentration in cells.

Colocalization Analysis

To examine the intracellular location of **1**$^{2+}$-SNPs, RAW264.7 cells were incubated with **1**$^{2+}$-SNP830 (28 μg/mL PCPDTBT, 48 μg /mL **1**$^{2+}$(BF_4^-)$_2$) for 3 h. and then costained with 2.0 μM Hoechst 33342 and 1.0 μM Lyso-tracker

(Lyso-Tracker™ Red DND-99) for another 20 min. The medium was then removed, washed with cold PBS for three times, and the fluorescence images were acquired using the IX73 optical microscope (Olympus, Japan) equiped with DAPI, Cy3 and Cy5 filters. Each experiment was repeated for three times.

Western Blotting Analysis of CSE Expression in RAW264.7 Cells

RAW264.7 cells were incubated with different concentration of LPS (0, 0.2, 0.5, 1.0 μg/mL) for 6 h, and then washed with PBS (×1). Cells were scraped off the plate in the presence of lysis buffer. The cells were incubated on ice for 30 min, and the lysate was obtained by centrifugation at 13,000×g at 4˚C for 15 min. Aliquots of proteins were separated by SDS-PAGE (10%) and subsequently transferred to nitrocellulose membranes by electroblotting. The membrane was blocked in 5% skim milk powder in 0.1% Tris buffered saline/Tween 20 (TBST, 20 mM Tris-HCl, pH 7.4, 137 mM NaCl, and 0.1% Tween) at room temperature for 2 h, and then incubated with antibody raised against CSE overnight at 4 ºC. After three washes with TBST, the membrane was incubated with a secondary antibody horseradish peroxidase (HRP)-conjugated Goat Anti-Rabbit IgG for 2 h at room temperature. The film were developed with the ECL System. The proteins were visualized using G:BOX chemiXR5. The resulting band intensities were quantified using an Gel-Pro32.

To conduct the WB analysis of mouse liver homogenates, mice were i.p. injected with different doses of LPS (0, 5, 10, 20 mg/kg) for 6 h to induce inflammation. The mice were then euthanized, and the livers were resected. Liver tissue samples were homogenized, and applied for WB analysis according to the above mentioned procedures. Each experiment was repeated for three times.

Quantitative Real-Time Polymerase Chain Reaction Analysis of miRNA in RAW264.7 Cells

RAW264.7 cells were incubated with different concentration of LPS (0, 0.2, 0.5, 1.0 μg/mL) for 6 h, and then washed with PBS(×1). Cells were collected and homogenized in 1 mL Trizol by centrifugation at 13,000×g at 4˚C for 15 min. RNA extraction and reverse transcription were performed according to the manufacturer's instructions. The cDNA fragment coding for targeted genes were amplified by RT-PCR using the selective primers. The primers used are the following: CSE (sense primer, 5′-CATGGA TGA AGT GTA TGG AGG C-3′; antisense primer, 5′-CGG CAG CAG AGG TAA CAATCG-3′).

Fluorescence Imaging of Intracellular $^1O_2$ Levels

KB cells (~ 5×10^4) in glass-bottom dishes were untreated or treated with $_L$-Cys (0.2 mM), or $ZnCl_2$ (300 μM) for 10 min. Then, the medium was removed, and the cells were washed with PBS buffer, followed by incubation with $\mathbf{1}^{2+}$-PSs-FA (48/0.96/5.5 μg/mL $\mathbf{1}^{2+}(BF_4^-)_2$/R6G/NIR775) for 1 h. After removal of the medium, some cells were further treated with NaHS (1 mM) for 1 h to increase H_2S levels. KB cells without any treatment were used as the control. After incubation, the medium was removed, washed with PBS buffer once, and DCFH-DA (20.0 μM) in 0.5 mL medium was added into the cells. After incubation for 20 min, the cells were irradiated with or without an 808 nm laser (1 W/cm^2) for 5 min. Then, the cells were washed with PBS buffer for three times, and the fluorescence images from DCF and R6G were acquired on a fluorescent inverted microscope equipped with FITC and TRITC filters, respectively. Each experiment was repeated for three times. The cell images from DCF were then analyzed using the ImageJ software (NIH). The region-of-interest (ROI) measurement was applied to fluorescence regions

in each cell to quantify the average fluorescence intensity, and repeated in another two cell images acquired from the other two repeated experiments. The mean fluorescence intensities and standard deviations were calculated for the comparison of different $^1O_2$ levels in cells.

Cytotoxicity Studies

RAW 264.7, KB, HCT116, HT29 and HEK293 cells were seeded in transparent 96-well plates (1×10^4 cells/well), and allowed to grow at 37 °C for 24 h. The cells were then incubated with various concentrations of $\mathbf{1}^{2+}$-SNP830, $\mathbf{1}^{2+}$-SNP580, $\mathbf{1}^{2+}$-SNP830-FA or $\mathbf{1}^{2+}$-PSs-FA for 24 h. For PDT-induced cytotoxicity, KB cells were incubated with $\mathbf{1}^{2+}$-PSs-FA at different concentrations for 1 h. Then, the medium was removed, and washed with cold PBS buffer for three times. Fresh RPMI-1640 medium (100 μL) was added to wells, and KB cells in each well were irradiated under an 808 nm laser (1 W/cm^2) for 5 min. After irradiation, the cells were kept growing for another 24 h. 3-(4,5-Dimethylthiazol-2-yl)-2,5-diphenyltetrazolium bromide (MTT) in PBS buffer (50 μL, 1 mg /mL) was added into each well, and the cells were incubated at 37 °C for 4 h. Then, the culture medium was removed carefully, and DMSO (100 μL) was added into each well. The absorbance (OD) at 490 nm in each well was acquired on a microplate reader (Tcan). Each experiment was repeated for three times.

Flow Cytometric Analysis

~200K KB cells were seeded into 6-well plates and incubated at 37 °C for 24 h. KB cells were treated with $_L$-Cys (0.2 mM) for 1 h or $ZnCl_2$ (300 μM) for 10 min. The medium was then removed, washed with fresh medium. KB cells were then incubated with $\mathbf{1}^{2+}$-PSs-FA (5.5 μg/mL NIR775) for 1 h. After removal of the medium, cells were washed with cold PBS once, and then incubated with or without NaHS (1 mM) for another 1 h. Blank KB cells were used as control. After incubation, the medium was removed, washed with PBS (pH 7.4) for three times, and fresh culture medium was added. The cells were then irradiated with or without an 808 nm laser (1 W/cm^2) for 5 min. Afterwards, the cells were washed with PBS (pH 7.4) for three times, trypsinized, and the cell pelletes were collected. After washed with PBS (pH 7.4) for another three times. The cell pelletes were stained with 5.0 μL Annexin V-FITC and 5.0 μL propidium iodide (PI) at r.t for 15 min. After staining, the cells were washed with cold PBS for three times, and the cell population was analyzed by Coulter FC-500 flow cytometer using FITC and PI channel. All experiments were conducted using at least 10000 cells, and the data was processed using FlowJo software.

Confocal Fluorescence Imaging with AO Staining

To evaluate the disruption of lysosome, KB cells were stained with acridine orange (AO). Briefly, KB cells (~200K) were seeded into 35.0 mm confocal dishes (Glass Bottom Dish) and incubated at 37.0 °C for 24 h. Cells were treated with $_L$-Cys (200 μM) for 1 h or $ZnCl_2$ (300 μM) for 10 min. The medium was then removed,washed with fresh medium. Cells were then incubated with $\mathbf{1}^{2+}$-PSs-FA (5.5 μg/mL NIR775) for 1 h. After removal of the medium, cells were washed with cold PBS once, and then incubated with or without NaHS (1 mM) for another 1 h. Blank KB cells were used as control. After washed with PBS buffer for three times, 5.0 μM AO was added and incubated at 37 °C for another 15 min. Then, the medium was removed, washed with PBS (pH 7.4) three times, fresh RPMI-1640 medium was added,. The cells were irradiated with or without an 808 nm laser (1 W/cm^2) for 5

min. The fluorescence images of KB cells were acquired with a confocal fluorescence microscopy with 515-545 nm for green, and 610-640 nm for red signal.

Animals and Tumor Models

BALB/c female mice at 5-6 weeks old were purchased from the Model Animal Research Center (MARC) of Nanjing University (Nanjing, China) and used according to the regulations of the Institutional Animal Care and Use Committee (IACUC) of Nanjing University. To induce liver inflammation, mice were i.p. injected with LPS. To establish tumors, KB cells (2.0×10^6 cells) suspended in 50 μL of 50 v/v% mixture of matrigel in supplemented RPMI-1640 (10 % fetal bovine serum, 100 U/mL penicillin, and 100 μg/mL streptomycin) were injected subcutaneously into the selected positions of nude mice. The length (L) and width (W) of each tumor were measured with a caliper, and the tumor volume was calculated with the formula of $V = (L \times W^2)/2$. Tumors with a single aspect of ~7-9 mm were formed after 10-15 days before used for fluorescence imaging and PDT.

Fluorescence Imaging of Exogenous H_2S In vivo

To image exogenous H_2S in vivo, female nude mice (6-8 weeks) were i.p. injected with $\mathbf{1}^{2+}$-SNP830 (78 μg PCPDTBT and 134 μg $\mathbf{1}^{2+}(BF_4^-)_2$ in 100 μL saline), followed by injection of 200 μL NaHS (1 mM) or saline into the i.p. cavity. The fluorescence images were acquired at indicated time point on an IVIS Lumina XR III imaging system using a 780 nm excitation filter and an 845 nm emission filter. Each experiment was conducted in three mice. The fluroescence intensities in the peritoneal cavity were quantified by the region-of-interests (ROIs) measurment using Living Image Software (4.5.2, PerkinElmer, MA, U.S.A).

Fluorescence Imaging of Hepatic H_2S in Mice

To non-invasively image H_2S in livers, nude mice (~8 weeks old) were i.p. injected with saline (100 μL), $_L$-Cys (1 mM, 100 μL) or PAG (1 mg/mL, 100 μL). After 30 min, $\mathbf{1}^{2+}$-SNP830 (78/134 μg PCPDTBT/$\mathbf{1}^{2+}(BF_4^-)_2$ in 100 μL saline) was i.v. injected into the mice. To monitor LPS-stimulated H_2S production in livers, mice were i.p. injected with varying dose of LPS (0, 5, 10 and 20 mg/kg). After 6 h, saline (100 μL) or PAG (1 mg/mL, 100 μL) was i.p. injected into mice, followed by i.p. injection with $_L$-Cys (1 mM, 100 μL) 30 min later. After another 30 min, $\mathbf{1}^{2+}$-SNP830 (78 μg PCPDTBT and 134μg $\mathbf{1}^{2+}(BF_4^-)_2$ in 100 μL saline) was i.v. injected into mice. The whole body fluorescence images at indicated time point were acquired on an IVIS Lumina XR III imaging system, using a 780 nm excitation filter and an 845 nm emission filter. Each experiment was conducted in three mice. The liver fluroescence intensities were quantified by the ROIs measurment using Living Image Software (4.5.2, PerkinElmer, MA, U.S.A).

Fluorescence Imaging of Tumor H_2S In vivo

To image H_2S in KB tumors, mice bearing subcutanous KB tumors were i.v. injected with $\mathbf{1}^{2+}$-SNP830-FA or $\mathbf{1}^{2+}$-SNP830 (78 μg PCPDTBT and 134 μg $\mathbf{1}^{2+}(BF_4^-)_2$ in 100 μL saline). After 3.5 h, saline (25 μL) or $_L$-Cys (1 mM, 25 μL) was injected into tumors. The fluorescence images were acquired at indicated time point on an IVIS Lumina XR III imaging system using a 780 nm excitation filter and an 845 nm emission filter. Each experiment was conducted in three mice. ROIs were drawn over the tumor and the thigh of the mouse to quantify the fluorescence

intensities using Living Image Software (4.5.2, PerkinElmer, MA, U.S.A). The tumor-to-background ratios (TBR) were calculated by dividing the fluorescence intensities in tumor to that in thigh.

Fluorescence Imaging of Main Organs *Ex vivo*

Healthy nude mice or KB tumor-bearing mice were i.p. injected with $_L$-Cys (1 mM, 100 μL) or saline (100 μL). After 30 min, $\mathbf{1}^{2+}$-SNP830 (78.4 μg/mL PCPDTBT, 100 μL) or $\mathbf{1}^{2+}$-PSs-FA (55 μg/mL NIR775, 200 μL) was i.v. injected into mice. Mice were sacrificed after 6 h (for $\mathbf{1}^{2+}$-SNP830) or 12 h (for $\mathbf{1}^{2+}$-PSs-FA). Main organs, including liver, kidneys, intestines, heart, brain, lung, stomach, uterus and spleen were resected. The fluorescence images of these organs were acquired with the IVIS Lumina XR III imaging system using a 780 nm excitation filter and an 845 nm emission filter for $\mathbf{1}^{2+}$-SNP830, and a 740 nm excitation filter and an 790 nm emission filter for $\mathbf{1}^{2+}$-PSs-FA. Each experiment was conducted in three mice.

Fluorescence Imaging of Tissue Slices

For fluorescence imaging of liver tissue slices, mice were euthanized and the livers were dissected at 6 h post i.v. injection of $\mathbf{1}^{2+}$-SNP830 (78 μg PCPDTBT and 134 μg $\mathbf{1}^{2+}(BF_4^-)_2$ in 100 μL saline). For fluorescence imaging of tumor tissue slices, KB tumor-bearing mice were sacrificed and the tumor were resected at 24 h post i.v. injection of $\mathbf{1}^{2+}$-SNP830-FA or $\mathbf{1}^{2+}$-SNP830-FA (78 μg PCPDTBT and 134 μg $\mathbf{1}^{2+}(BF_4^-)_2$ in 100 μL saline). The isolated liver and tumors tissues were cut using a vibrating-blade microtome to obtain 10 μm-thickness slices. After staining with DAPI, the images of liver tissue slices were acquired with the IX73 fluorescent inverted microscope equipped with DAPI and C y5.5 filters.

In vivo Imaging and PDT of Tumors

KB tumor-bearing mice with tumor volume of 80-110 mm^3 were randomly divided into six groups: 1 (saline only), 2 (saline + light), 3 ($\mathbf{1}^{2+}$-PSs-FA), 4 ($\mathbf{1}^{2+}$-PSs-FA + $ZnCl_2$ + light), 5 ($\mathbf{1}^{2+}$-PSs-FA + light), 6 ($\mathbf{1}^{2+}$-PSs-FA + $_L$-Cys + light). Saline (200 μL) or $\mathbf{1}^{2+}$-PSs-FA (55 μg/mL NIR775, 200 μL) was i.v. injected into mice. For groups 4 and 6, $ZnCl_2$ (1 mM, 25 μL) and $_L$-Cys (1 mM, 25 μL) were injected into tumors at 3.5 h post injection of $\mathbf{1}^{2+}$-PSs-FA, respectively. After 12 h, whole body fluorescence images of mice were acquired with a 740 nm excitation filter and a 790 nm emission filter. Each experiment was conducted in three mice. ROIs were drawn over the tumor of the mouse to quantify the fluorescence intensities using Living Image Software (4.5.2, PerkinElmer, MA, U.S.A).

Guided by the fluorescence imaging results, the tumors in groups 2, 4, 5 and 6 were irradiated with an 808 nm laser (1 W/cm^2) for 10 min. After irradiation, the mice were kept under dark for 10 min, and the tumors were irradiated for another 10 min. The tumor volumes and body weights of mice were measured in every two days, and up to 16 days. The relative tumor volumes were calculated for each mouse as V/V_0 (V_0 was the tumor volume when the treatment was initiated), and the relative body weight was normalized to that of initial treatment. On day 16, all the mice were sacrificed, and the tumors were excised and photographed. Each experiment was conducted in four mice.

Immunohistochemistry Studies

KB tumor-bearing mice were treated according to the conditions shown in PDT experiment. Two days post treatment, the mice were sacrificed, and the tumors were excised from mice. The tumor tissues were fixed in 4%

formalin and then embedded in paraffin before 10-μm sectioning. Histology samples were stained by H&E or TUNEL using a standard protocol. White light images were acquired using an IX73 optical microscope equipped with a color cameral.

Statistical Analysis

Results are expressed as the mean ± standard deviation unless otherwise stated. Statistical comparison between two groups were determined by Student's *t* test. $P < 0.05$ was considered statistically significant. All statistical calculations were performed using GraphPad Prism 6 (GraphPad Software Inc., CA, USA).

^{1}H NMR of **3**

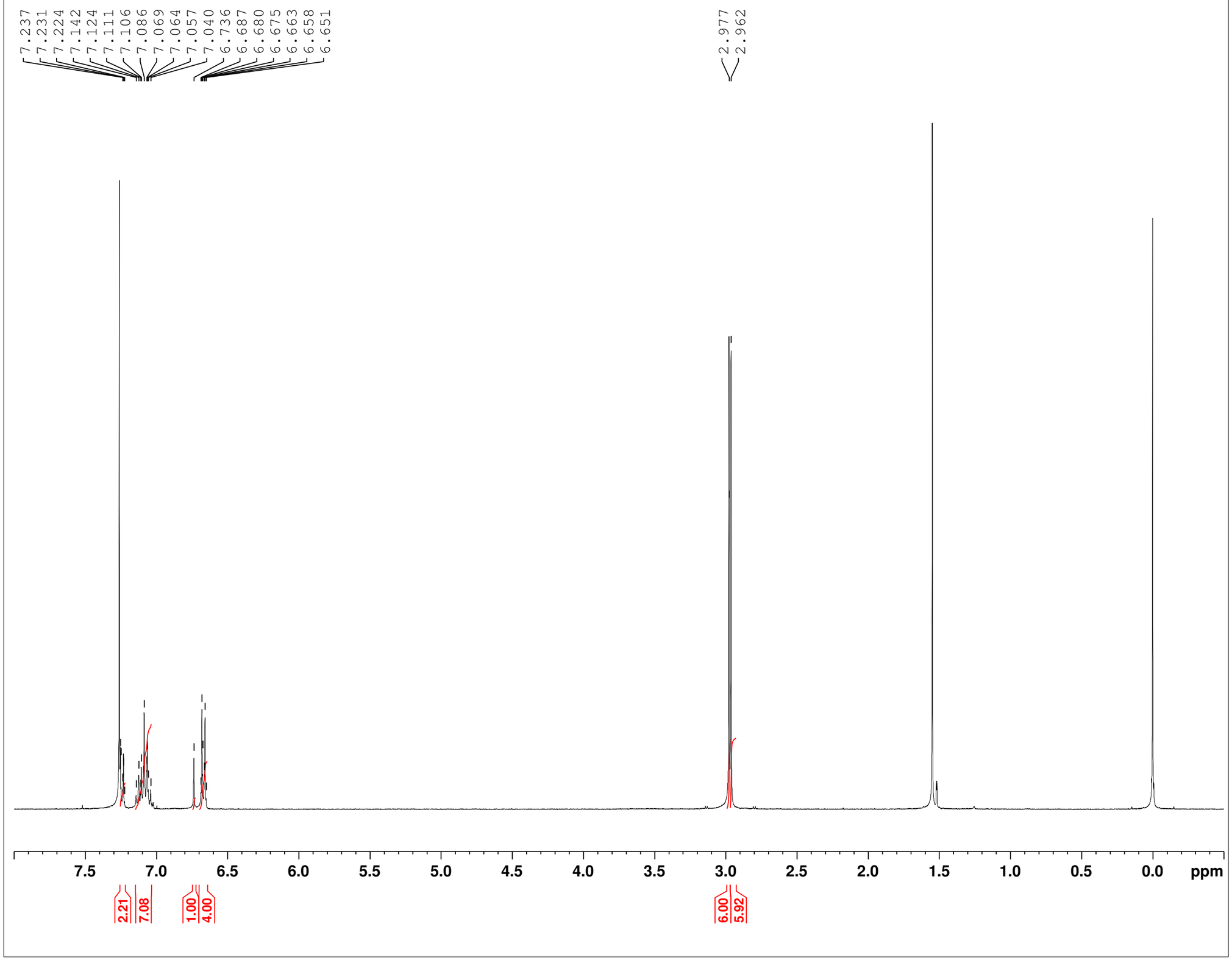


```
Current Data Parameters
NAME      KS106-1-1 kakunin
EXPNO                   10
PROCNO                   1

F2 - Acquisition Parameters
Date_           20180530
Time              16.40
INSTRUM           spect
PROBHD   5 mm PADUL 13C
PULPROG             zg30
TD                65536
SOLVENT           CDCl3
NS                   16
DS                    2
SWH             8012.820 Hz
FIDRES          0.122266 Hz
AQ              4.0894465 sec
RG                174.44
DW                62.400 usec
DE                 6.50 usec
TE                295.1 K
D1           1.00000000 sec
TD0                   1

======== CHANNEL f1 ========
SFO1         400.1324710 MHz
NUC1                 1H
P1                10.00 usec
PLW1         24.39999962 W

F2 - Processing parameters
SI                  65536
SF           400.1300094 MHz
WDW                   EM
SSB       0
LB                0.30 Hz
GB        0
PC                1.00
```

^{13}C NMR of **3**

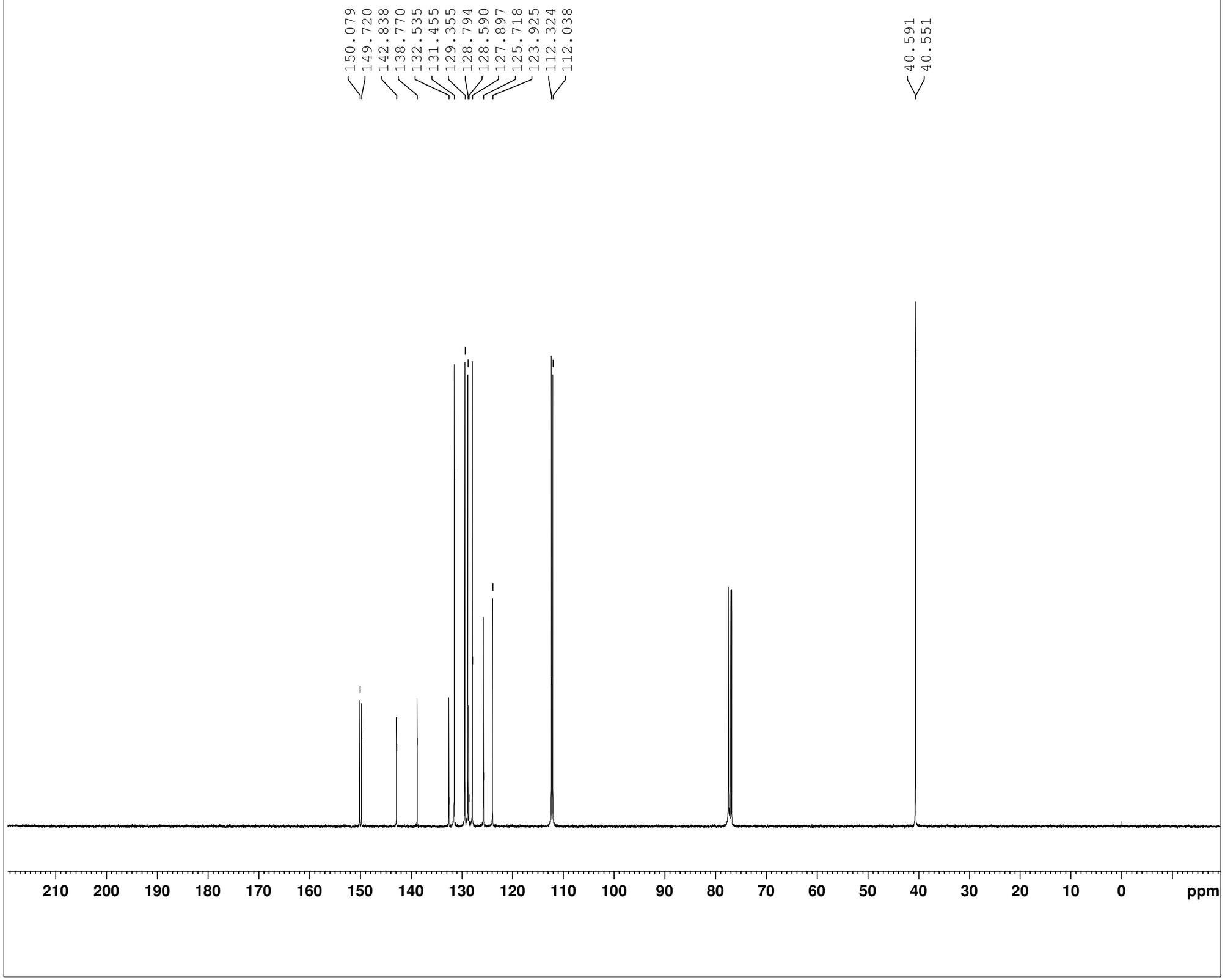


```
Current Data Parameters
NAME                  KS106
EXPNO                    20
PROCNO                    1

F2 - Acquisition Parameters
Date_              20180531
Time                  9.30
INSTRUM              spect
PROBHD    5 mm PADUL 13C
PULPROG              zgpg30
TD                    65536
SOLVENT               CDCl3
NS                     1024
DS                        4
SWH              24038.461 Hz
FIDRES            0.366798 Hz
AQ               1.3631488 sec
RG                    30.31
DW                   20.800 usec
DE                    6.50 usec
TE                   297.8 K
D1             2.00000000 sec
D11            0.03000000 sec
TD0                       1

======== CHANNEL f1 ========
SFO1           100.6228293 MHz
NUC1                  13C
P1                   10.00 usec
PLW1           46.59999847 W

======== CHANNEL f2 ========
SFO2           400.1316005 MHz
NUC2                  1H
CPDPRG[2           waltz16
PCPD2                90.00 usec
PLW2           24.39999962 W
PLW12           0.30123001 W
PLW13           0.24400000 W

F2 - Processing parameters
SI                    32768
SF             100.6127690 MHz
WDW                     EM
SSB       0
LB                    1.00 Hz
GB        0
PC                    1.40
```

HRMS of 3

Data: common/Jun14:a00120-
Sample: 2701 Sugimoto / KS106
Experiment Date/Time: 2018/06/14 13:31:22
Average(MS[1] Time:0.35)

Instrument Configuration: FDプローブ,JMS-T100GCV
Ionization Mode: FD+
Acquired m/z Range: 20.00..800.00
Detector Volt: 2300[V]

MS Tune Method Name: FD
Agilent7890A Method Name: -

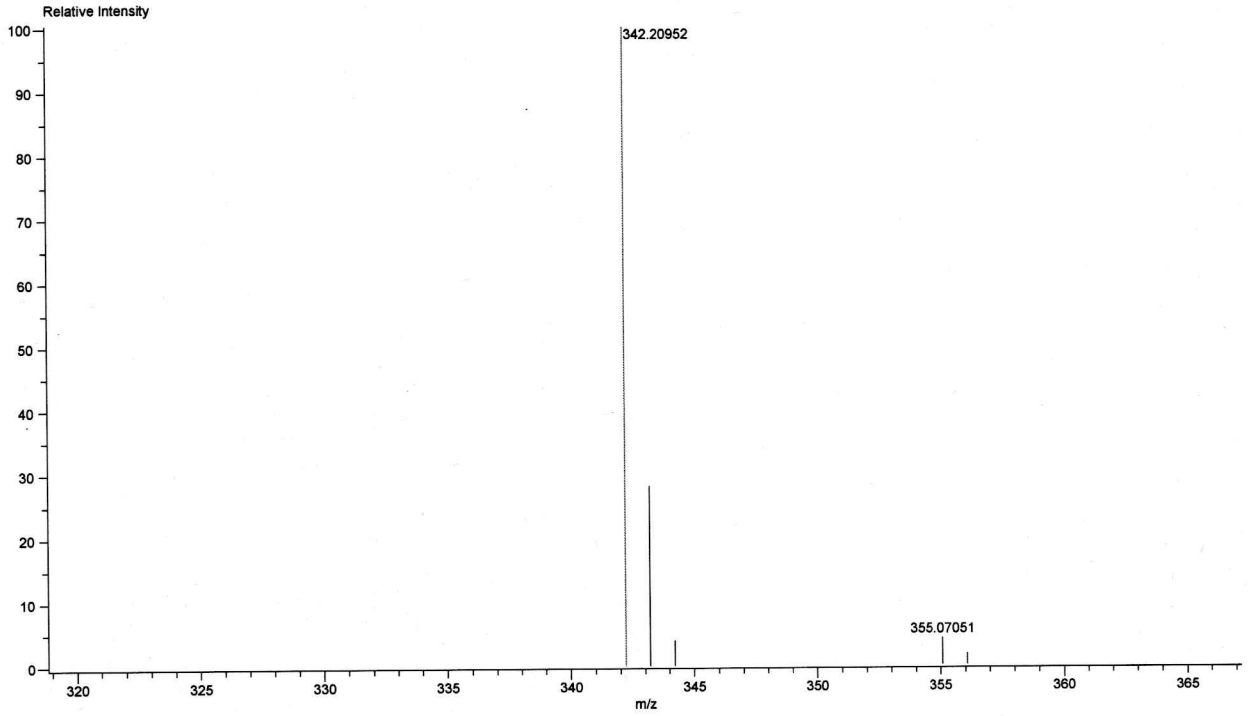

Data:a00120-
Sample Name:2701 Sugimoto / KS106
Description:
Ionization Mode:FD+
History:Determine m/z[Peak Detect[Centroid,10,Area];Correct Base[];Smooth[3]];Smooth[5];Average(MS[1] 0.35)

Charge number:1
Tolerance:5.00(mmu)
Element:^{12}C:0 .. 150, ^{1}H:0 .. 200, ^{14}N:0 .. 4

Mass	Calc. Mass	Mass Difference (mmu)	Mass Difference (ppm)	Possible Formula	Unsaturation Number
342.20952	342.20960	-0.08	-0.22	$^{12}C_{24}{}^{1}H_{26}{}^{14}N_2$	13.0

Acquired:2018/06/14 13:31:22
Operator:Administrator
Mass Calibration data:800_0.1minl_53
Created:2018/06/14 13:35:02
Created by:Administrator

Unsaturation Number:-1.5 .. 100.0 (Fraction:Both)

^{1}H NMR of **4**

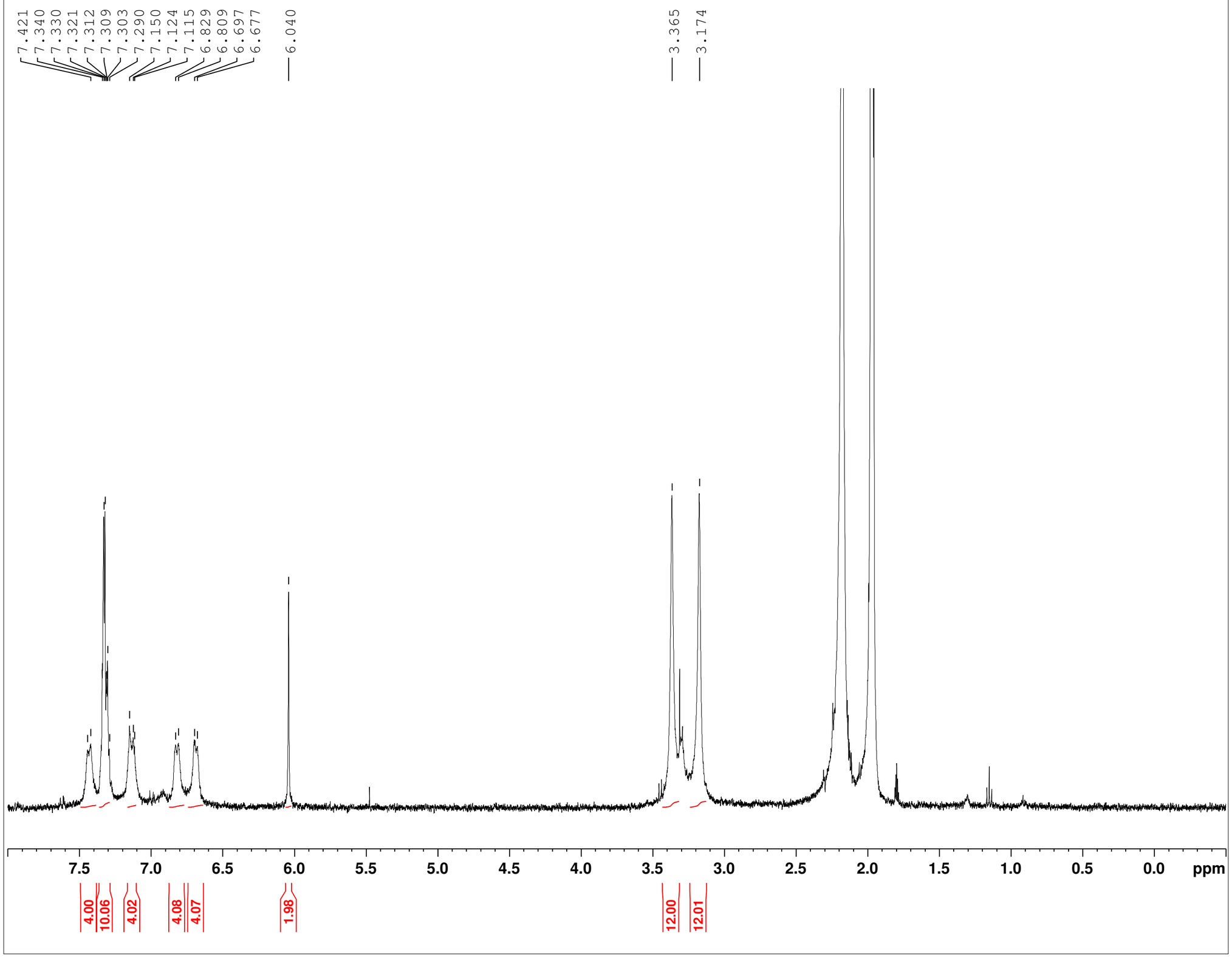


```
Current Data Parameters
NAME                  KS250
EXPNO                    10
PROCNO                    1

F2 - Acquisition Parameters
Date_              20180606
Time                  14.48
INSTRUM               spect
PROBHD   5 mm PADUL 13C
PULPROG                zg30
TD                    65536
SOLVENT               CD3CN
NS                       16
DS                        2
SWH                8012.820 Hz
FIDRES             0.122266 Hz
AQ                 4.0894465 sec
RG                    195.02
DW                    62.400 usec
DE                     6.50 usec
TE                    294.8 K
D1              1.00000000 sec
TD0                       1

======== CHANNEL f1 ========
SFO1           400.1324710 MHz
NUC1                     1H
P1                    10.00 usec
PLW1           24.39999962 W

F2 - Processing parameters
SI                    65536
SF           400.1300000 MHz
WDW                      EM
SSB          0
LB                    0.30 Hz
GB           0
PC                    1.00
```

$C_{48}H_{52}N_4I_6$, M 1446.39, monoclinic, $P2_1/n$, a = 10.054(2), b = 17.393(3), c = 28.880(5) Å, β = 92.970(9)°, U = 5043(1) Å^3, D_c (Z = 4) = 1.905 g cm^{-1}, μ(Mo-Kα) = 37.43 cm^{-1}, T = 123 K. The final R value is 0.062 for 4842 independent reflections with $I > 3\sigma I$ and 263 parameters. The molecular geometry of the dication is shown in the left, and the crystal packing including triiodide ions is shown below.

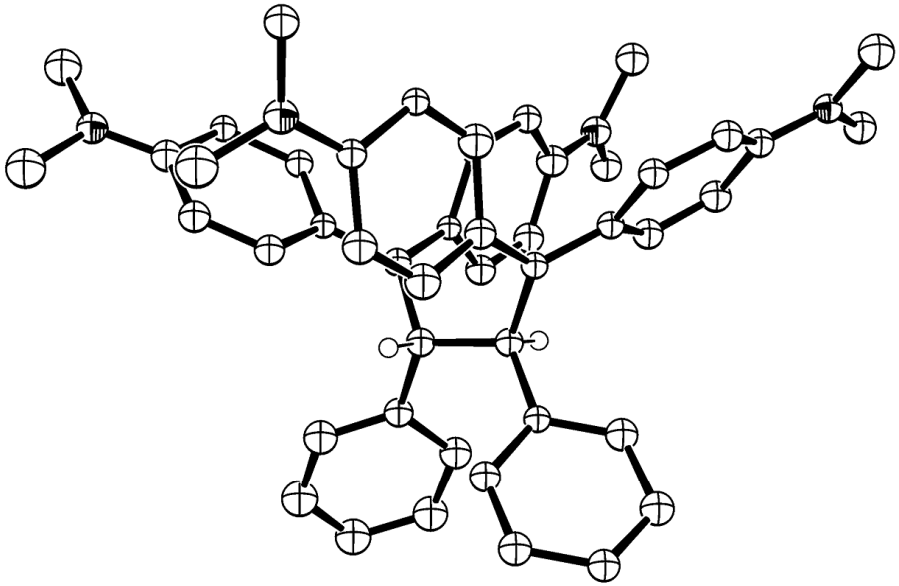

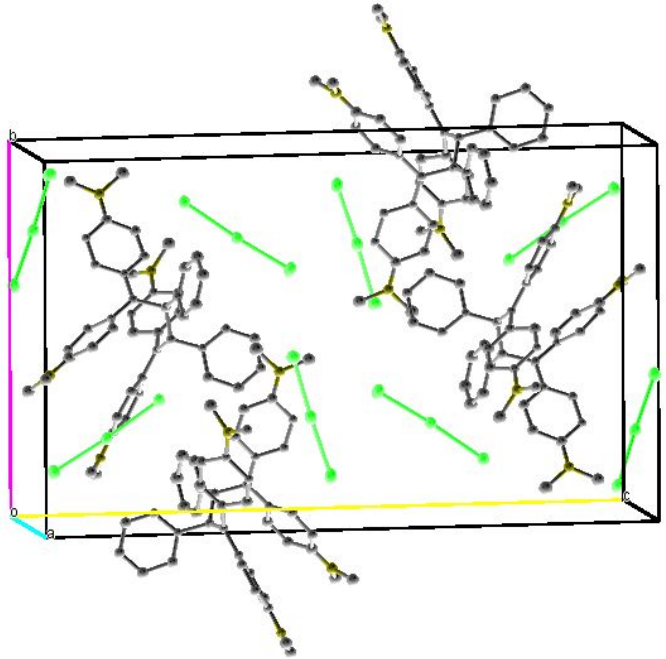

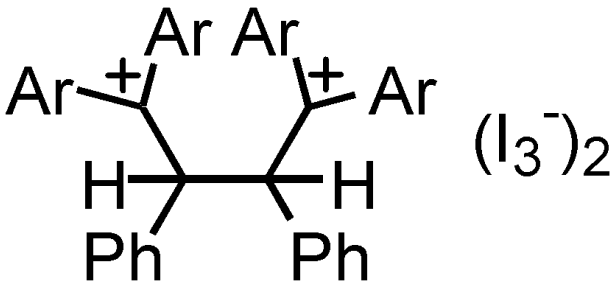

^{1}H-NMR of **2**

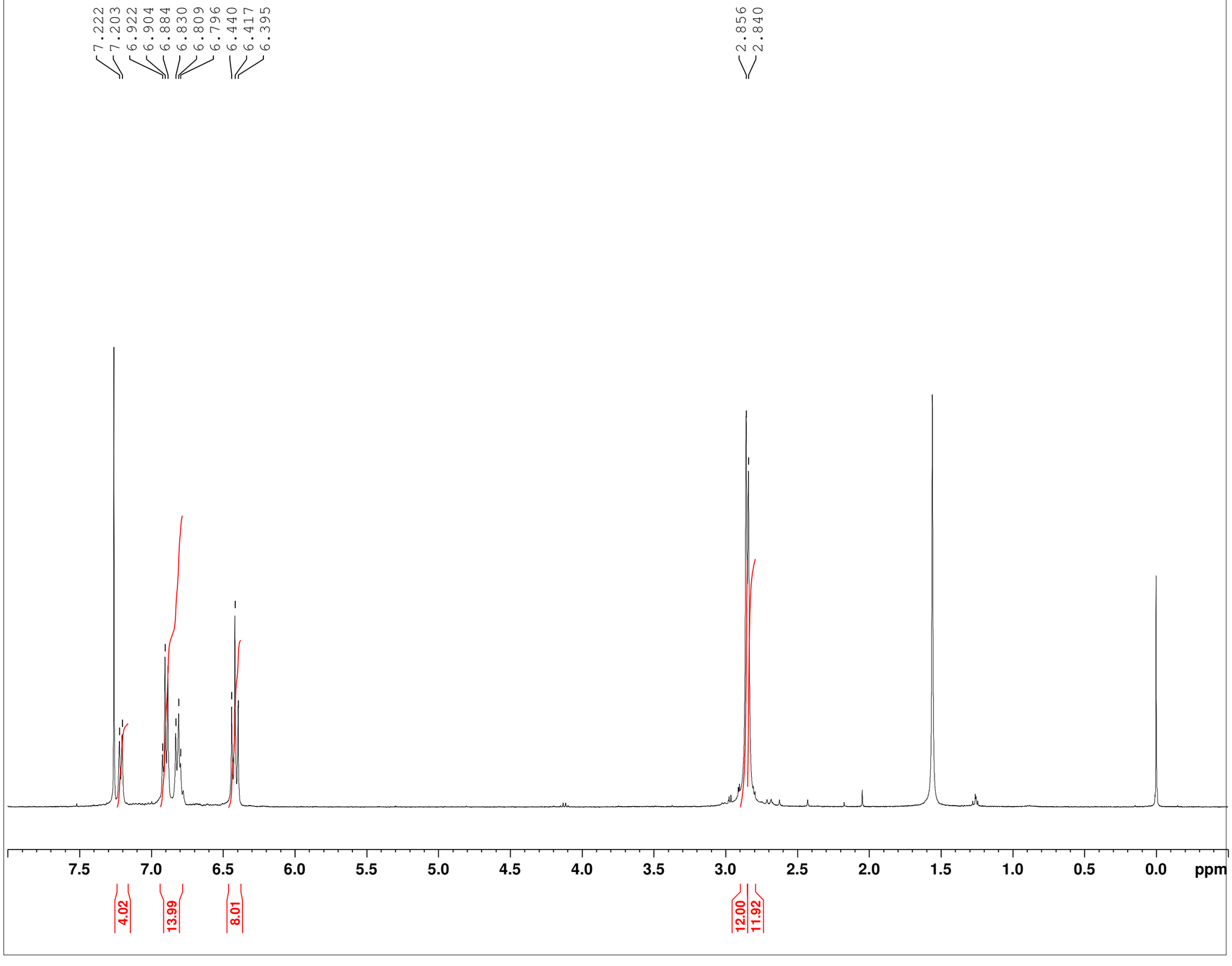


```
Current Data Parameters
NAME          KS109-2 PU
EXPNO                 10
PROCNO                 1

F2 - Acquisition Parameters
Date_           20180718
Time               11.17
INSTRUM            spect
PROBHD   5 mm PADUL 13C
PULPROG             zg30
TD                 65536
SOLVENT            CDCl3
NS                    16
DS                     2
SWH             8012.820 Hz
FIDRES          0.122266 Hz
AQ              4.0894465 sec
RG                 195.02
DW                62.400 usec
DE                 6.50 usec
TE                295.0 K
D1             1.00000000 sec
TD0                    1

======== CHANNEL f1 ========
SFO1         400.1324710 MHz
NUC1                   1H
P1                 10.00 usec
PLW1         24.39999962 W

F2 - Processing parameters
SI                  65536
SF          400.1300097 MHz
WDW                    EM
SSB       0
LB                 0.30 Hz
GB        0
PC                 1.00
```

^{13}C-NMR of **2**

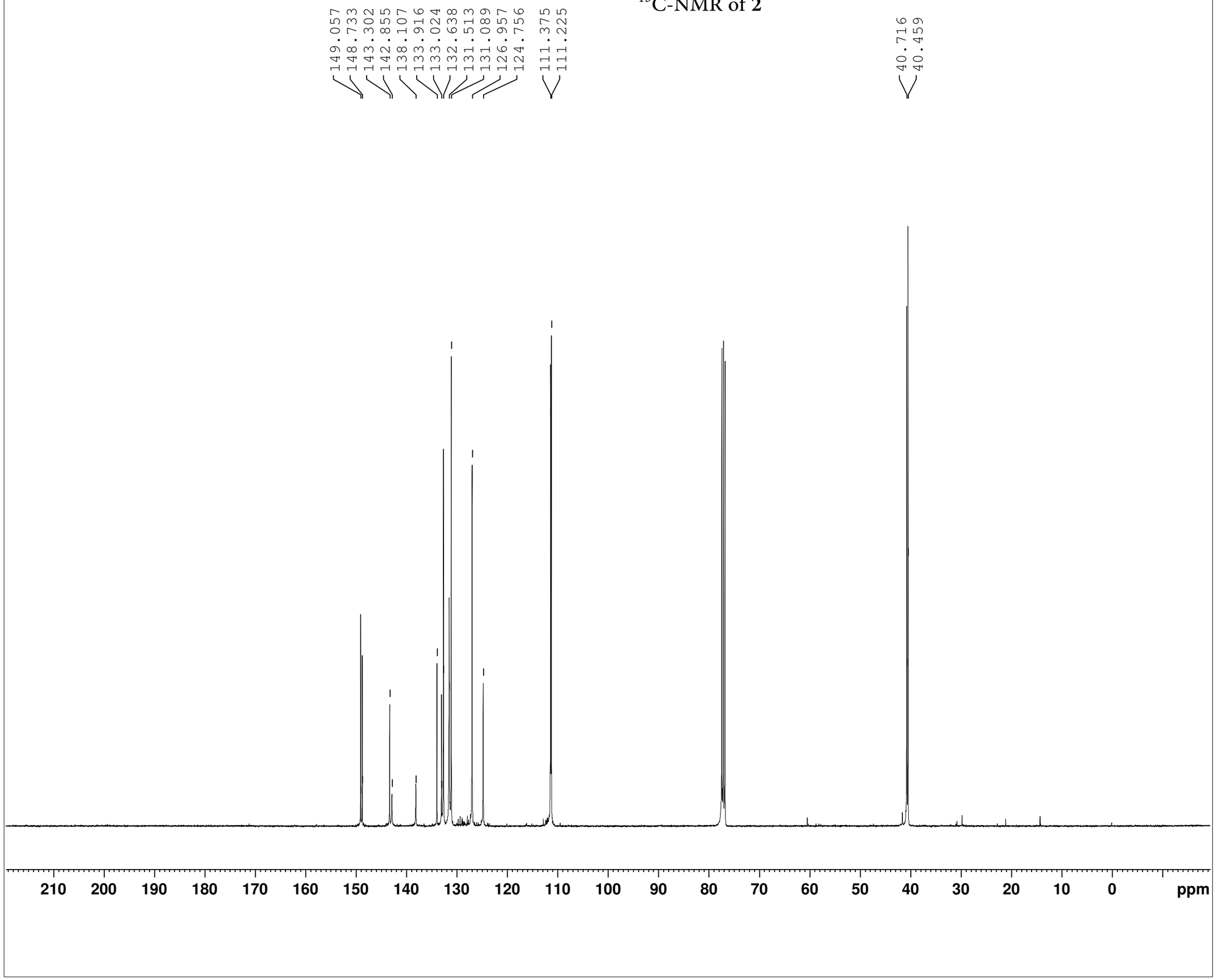


```
Current Data Parameters
NAME      KS109-2 PU 13C
EXPNO                 10
PROCNO                 1

F2 - Acquisition Parameters
Date_           20180719
Time                7.55
INSTRUM            spect
PROBHD   5 mm PADUL 13C
PULPROG           zgpg30
TD                 65536
SOLVENT            CDCl3
NS                 10240
DS                     4
SWH           24038.461 Hz
FIDRES         0.366798 Hz
AQ            1.3631488 sec
RG                 30.31
DW                20.800 usec
DE                 6.50 usec
TE                296.2 K
D1           2.00000000 sec
D11          0.03000000 sec
TD0                    1

======== CHANNEL f1 ========
SFO1         100.6228293 MHz
NUC1                13C
P1                10.00 usec
PLW1         46.59999847 W

======== CHANNEL f2 ========
SFO2         400.1316005 MHz
NUC2                1H
CPDPRG[2         waltz16
PCPD2              90.00 usec
PLW2         24.39999962 W
PLW12         0.30123001 W
PLW13         0.24400000 W

F2 - Processing parameters
SI                 32768
SF           100.6127690 MHz
WDW                  EM
SSB       0
LB                 1.00 Hz
GB        0
PC                 1.40
```

^{1}H-NMR of $\mathbf{1}^{2+}(BF_{4-})_2$

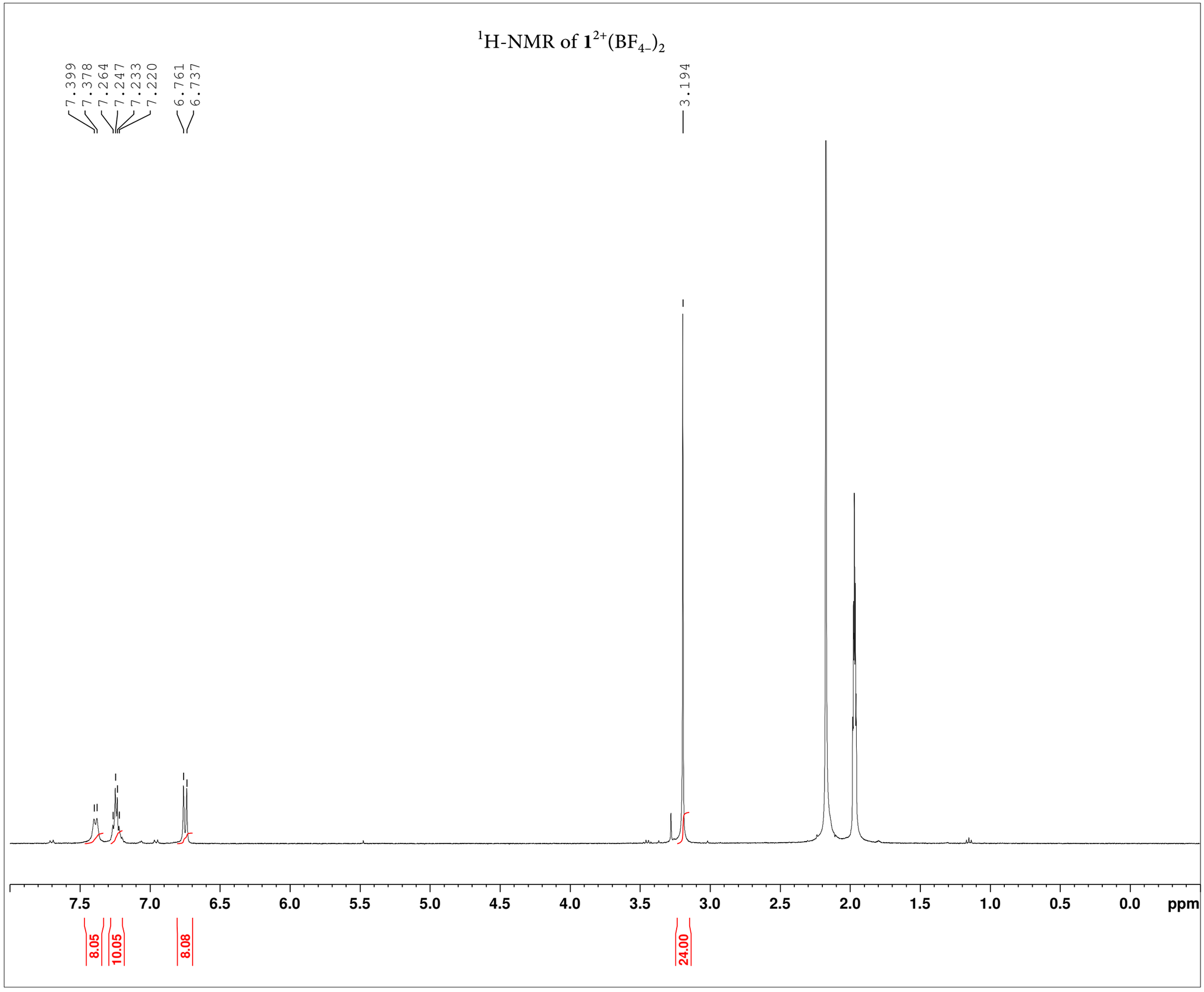


```
Current Data Parameters
NAME                  NK004
EXPNO                    30
PROCNO                    1

F2 - Acquisition Parameters
Date_              20180712
Time                  11.25
INSTRUM               spect
PROBHD    5 mm PADUL 13C
PULPROG                zg30
TD                    65536
SOLVENT               CD3CN
NS                       16
DS                        2
SWH                8012.820 Hz
FIDRES             0.122266 Hz
AQ                 4.0894465 sec
RG                    174.44
DW                    62.400 usec
DE                     6.50 usec
TE                    295.6 K
D1              1.00000000 sec
TD0                       1

======== CHANNEL f1 ========
SFO1           400.1324710 MHz
NUC1                    1H
P1                   10.00 usec
PLW1           24.39999962 W

F2 - Processing parameters
SI                    65536
SF             400.1300000 MHz
WDW                     EM
SSB          0
LB                    0.30 Hz
GB           0
PC                    1.00
```

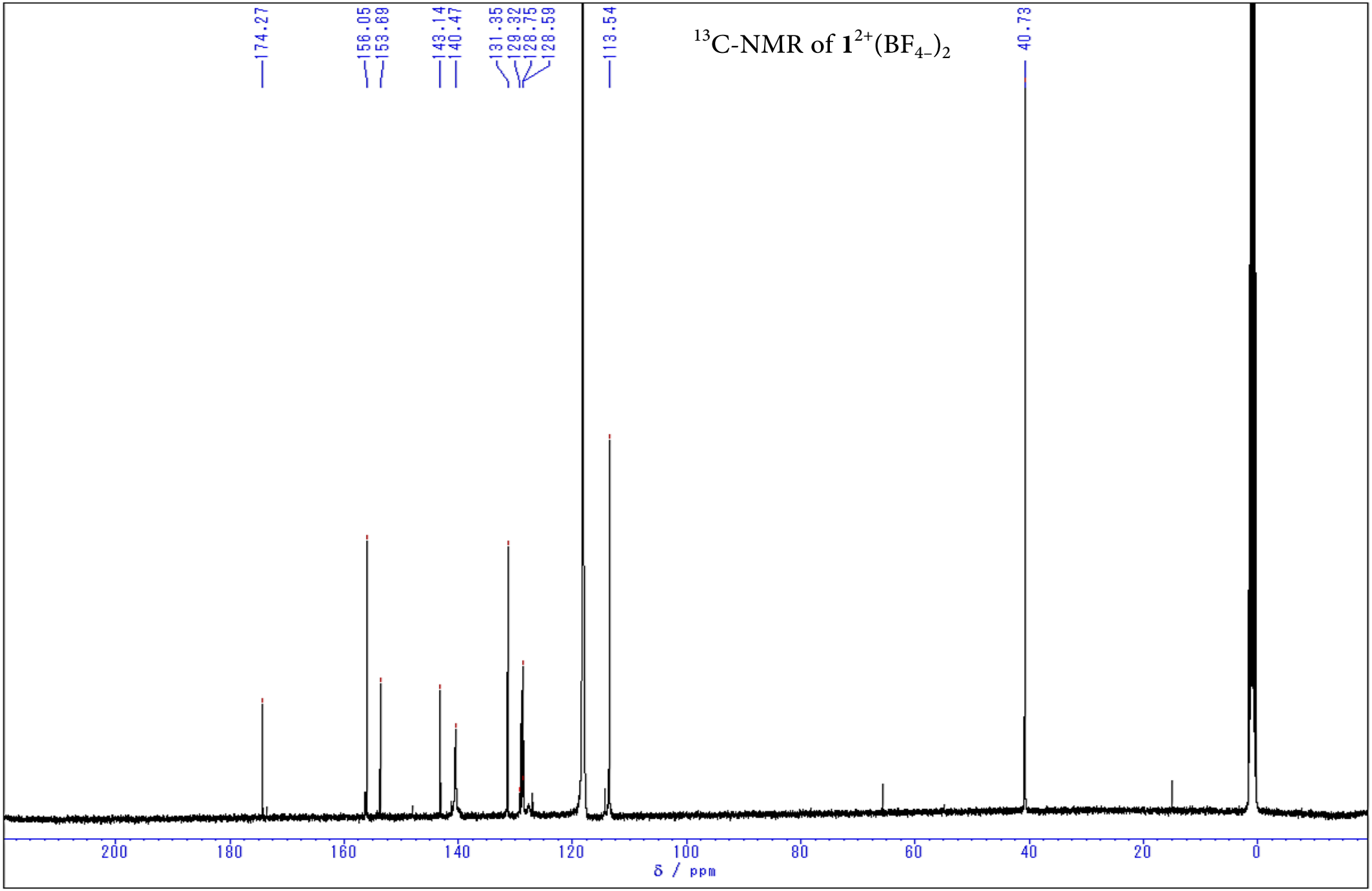
174.27
156.05
153.69
143.14
140.47
131.35
129.32
128.75
128.59
113.54
40.73
^{13}C-NMR of $\mathbf{1}^{2+}(BF_{4-})_2$
200
180
160
140
120
100
80
60
40
20
0
δ / ppm